Microfluidic Selection of Aptamers towards Applications in Precision Medicine

Timothy R. Olsen

Submitted in partial fulfillment of the
requirements for the degree of
Doctor of Philosophy
in the Graduate School of Arts and Sciences

COLUMBIA UNIVERSITY

2018

ABSTRACT

Microfluidic Selection of Aptamers towards Applications in Precision Medicine

Timothy R. Olsen

Precision medicine represents a shift in medicine where large datasets are gathered for massive patient groups to draw correlations between disease cohorts. An individual patient can then be compared to these large datasets to determine the best treatment strategy. While electronic health records and next generation sequencing techniques have enabled much of the early applications for precision medicine, the human genome only represents a fraction of the information present and important to a person's health. A person's proteome (peptides and proteins) and glycome (glycans and glycosylation patterns) contain biomarkers that indicate health and disease; however, tools to detect and analyze such biomarkers remain scarce. Thus, precision medicine databases are lacking a major source of phenotypic data due to the absence of available methods to explore these domains, despite the potential of such data to allow further stratification of patients and individualized therapeutic strategies.

Available methods to detect non-nucleic acid biomarkers are currently not well suited to address the needs of precision medicine. Mass spectrometry techniques, while capable of generating high throughput data, lack standardization, require extensive preparative steps, and have many sources of errors. Immunoassays rely on antibodies which are time consuming and expensive to produce for newly discovered biomarkers. Aptamers, analogous to antibodies but composed of nucleotides and isolated through *in vitro* methods, have potential to identify non-nucleic acid biomarkers but methods to isolate aptamers remain labor and resource intensive and time consuming.

Recently, microfluidic technology has been applied to the aptamer discovery process to reduce the aptamer development time, while consuming smaller amounts of reagents. Methods have been demonstrated that employ capillary electrophoresis, magnetic mixers, and integrated functional chambers to select aptamers. However, these methods are not yet able to fully integrate the entire aptamer discovery process on a single chip and must rely on off-chip processes to identify aptamers.

In this thesis, new approaches for aptamer selection are developed that aim to integrate the entire process for aptamer discovery on a single chip. These approaches are capable of performing efficient aptamer selection and polymerase chain reaction based amplification while utilizing highly efficient bead-

based reactions. The approaches use pressure driven flow, electrokinetic flow or a combination of both to transfer aptamer candidates through multiple rounds of affinity selection and PCR amplification within a single microfluidic device. As such, the approaches are capable of isolating aptamer candidates within a day while consuming <500 µg of a target molecule.

The utility of the aptamer discovery approach is then demonstrated with examples in precision medicine over a broad spectrum (small molecule to protein) of molecular targets. Seeking to demonstrate the potential of the device to generate probes capable of accessing the human glycome (an emerging source of precision medicine biomarkers), aptamers are isolated against gangliosides GM1, GM3, and GD3, and a glycosylated peptide. Finally, personalized, patient specific aptamers are isolated against a multiple myeloma patient serum sample. The aptamers have high affinity only for the patient derived antibody.

Table of Contents

List of Figures

List of Tables

List of Abbreviations

a.u.	Arbitrary units
ASO-PCR	Allele-specific oligonucleotide PCR
BM	Bone Marrow
CR	Complete response
DNA	Deoxyribonucleic acid
dsDN	Double-stranded DNA
EGFR	Epidermal growth factor receptor
ELISA	Enzyme-linked immunosorbent assay
FLC	Free light chain
fM	Femtomolar
GalNac	*N*-Acetylgalactosamine
GM1	Ganglioside GM1, monosialotetrahexosylganglioside
GM3	Ganglioside GM3, monosialodihexosylganglioside
GD3	Ganglioside GD3
IFE	Immunofixation electrophoresis
IgA	Immunoglobulin A
IgD	Immunoglobulin D
IgE	Immunoglobulin E
IgG	Immunoglobulin G
IgM	Immunoglobulin M
ITC	Isothermal titration calorimetry
KD	Binding dissociation constant
L	Liter
LCMM	Light chain multiple myeloma
LOD	Limit of detection
mg	milligram
M-Ig	Monoclonal immunoglobulin
MM	Multiple myeloma
MRD	Minimal residual disease
NGS	Next generation sequencing
nM	Nanomolar

PBS	Phosphate buffered saline
PBSM	Phosphate buffered saline with magnesium chloride
PCR	Polymerase chain reaction
PDMS	(Poly)dimethylsiloxane
qPCR	Quantitative, real-time PCR
RNA	Ribonucleic acid
SELEX	Systematic evolution of ligands by exponential enrichment
SPEP	Serum protein electrophoresis
SPR	Surface plasmon resonance
ssDN	Single-stranded DNA
µM	Micromolar
κ	Type of immunoglobulin light chain
λ	Type of immunoglobulin light chain

Acknowledgements

This thesis is the result of the colleagues, friends and family that have supported me throughout these years. I am eternally thankful for all these people and the positive contributions they have made in my life. I would like to thank my advisor Dr. Qiao Lin for his support and encouragement to pursue my interests. I would also like to thank our collaborator Dr. Milan Stojanovic for his constant enthusiasm, patience, and willingness to always look at results – especially when things were in an incomplete or contradictory state. I am also deeply grateful for our other collaborator, Dr. Tilla Worgall, for her relentless instruction on the clinical realities of scientific research, as well as for her contagious, inexhaustible and inspiring energy. I would like to offer my thanks to the TL1 training fellowship program and Dr. Siqin Ye and Dr. Wendy Chung who direct it. This program provided invaluable medical context. I am sincerely thankful for all of the students that came before me and gave me the experience needed to be independent. In particular, Dr. Jinho Kim, Dr. Jing Zhu, Dr. Jaeyoung Yang, and Dr. JP Hilton were lab mates that taught me microfabrication and how to apply microfluidics. I will always be in debt to the post-doctoral associates and research associates at the medical center. Dr. Claudia Tapia-Alveal, Dr. Kyung-Ae Yang, Dr. Steven Taylor, Dr. Stevan Pecic, and Dr. Nenad Milosavic were always generous with their time, taught me everything about the SELEX process, and were extremely helpful in explaining and directing me how to do even the most simple assays. I would like to thank my classmates Zhixing Zhang, Junyi Shang, and Dr. Yuan Jia for being open to sharing ideas and positively contributing to the lab culture. All research activities were made possible by the generous allocation of funds from the National Science Foundation and National Institutes of Health. Finally I would like to offer my sincere gratitude to the Central Park Conservancy and NYC Parks. Running through countless miles of their trails was the most effective way for me to organize the thoughts presented in this thesis.

Dedication

This thesis is dedicated to Shiyang Wang. In many ways, I pursued this doctorate so that we could share a life together in New York City. We have both learned a lot along the way. This thesis would not be possible without your steady support and constant motivation.

Chapter 1: Introduction

1.1. Precision Medicine

Precision medicine involves precisely adapting therapies to subclasses of disease by incorporating individualized genetic, biomarker, phenotypic, or psychosocial characteristics of a patient [1]. Precision medicine looks to address the reductionist nature of traditional medicine which generally disregards underlying mechanisms of symptoms, and may define multiple unique diseases into one disease with shared symptoms [2]. Essentially precision medicine seeks to stratify individuals into smaller groups and apply treatments which have been demonstrated to be effective in those groups [3, 4]. It is in opposition to traditional medicine which has sought to find a single treatment that helps the most people (one size fits all), rather effective treatments for targeted population groups are desired.

The goal of precision medicine is to enable clinical decisions based on an individual's variations in genes, proteins, environment and lifestyle. This information allows clinicians to tailor disease treatment and prevention strategies for subgroups of disease with similar symptoms. Thus, there is increased emphasis on the identification of new biomarkers which can be used to reveal these underlying mechanisms affecting a patient's health.

While the concept of tailored treatments has been around for millennia, the ability to interpret large datasets is new [5]. Diagnosis and treatment traditionally relied on physical exams, signs and symptoms, experience and personal expertise. Now technological advances are allowing the generation of massive data networks from large patient cohorts which can be mined to find the underlying mechanisms of healthy and disease conditions [6] (**Figure 1.1**). A confluence of biological, computational, computer, and engineering has enabled these large datasets to be generated and analyzed. Thus, precision medicine is not a new concept, rather it is a shift in the way information is collected and organized which alters the way research is conducted and patients are treated.

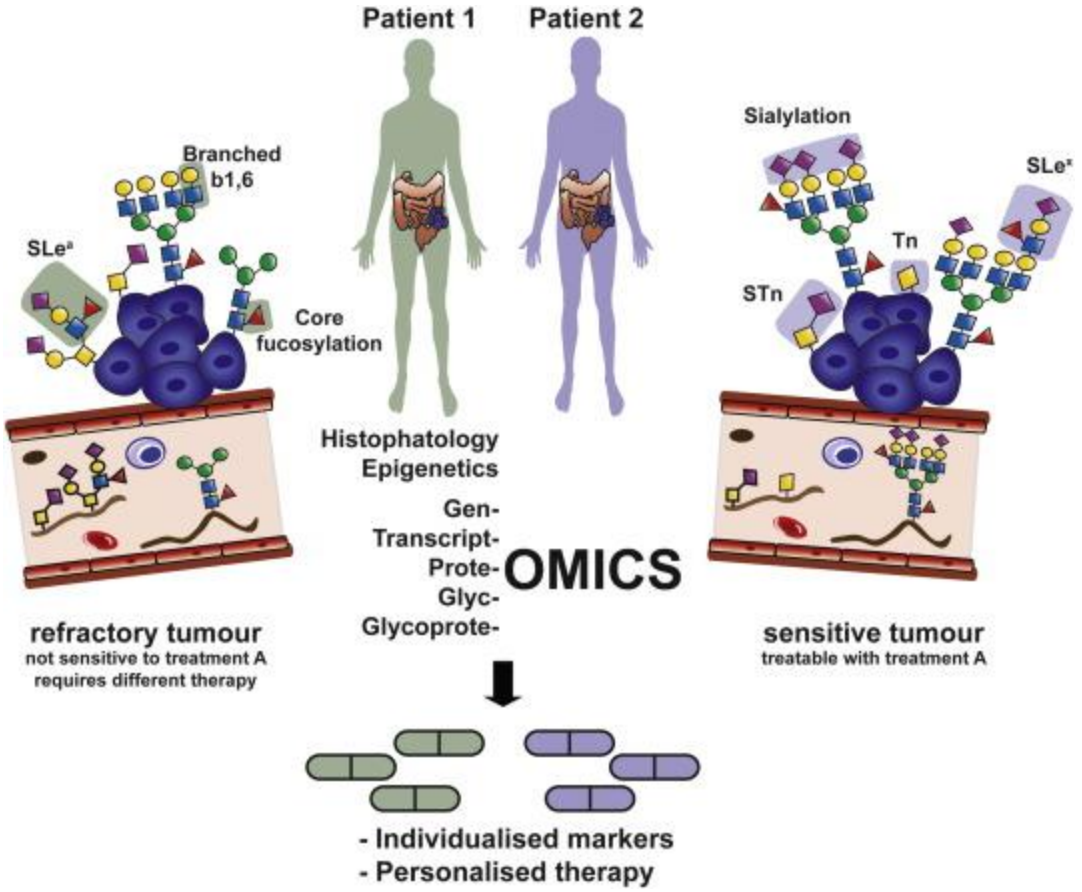

Figure 1.1: Precision medicine research strategy. “Omics” information is gathered to group patients and develop personalized therapies [7].

1.1.1. Examples of Precision Medicine

While precision medicine has been applied to the study and treatment of many diseases, a few examples on precision medicine in cystic fibrosis, cancer, and the glycome will serve to illustrate the applications and promise of this emerging and exciting paradigm of medicine.

1.1.1.1. Cystic Fibrosis

The genetic make-up of a person contributes to a patient’s health and has been found to be useful in making optimal treatment decisions [8]. One case where this is strongly observed is in cystic fibrosis. Of the over 1,900 cystic fibrosis related mutations, it has been found that 80% of U.S. patients have the F508del mutation [9]. As a result, therapies that modulate the function of protein related to this mutation have been developed [10]. Additional therapies (lumacaftor/ivacaftor) have been released for individuals

that contain two copies of this mutation. Therefore, clinicians today can request genetic tests for cystic fibrosis patients and tailor the treatment based on the presence of a genomic biomarker from the test.

1.1.1.2. Adenocarcinoma

The application of precision medicine to cancer has also attracted considerable interest, especially in lung cancer treatment. Lung cancer was previously divided into small cell carcinoma, non-small cell squamous cell carcinoma, non-small cell adenocarcinoma and large cell carcinoma subtypes which were identified by histology. The application of high-throughput sequencing techniques has now found more than 15 genes related to oncogenesis of lung cancer (**Figure 1.2**) [11]. Of these, a mutation to the epidermal growth factor receptor (EGFR) gene within positive non-small cell lung adenocarcinoma is now its own taxon within adenocarcinoma and has a unique treatment strategy relying on tyrosine kinase inhibitors [12]. Additional treatment strategies for the other mutations still attract interest and have potential to become their own adenocarcinoma subtypes if companion therapeutics emerge [13].

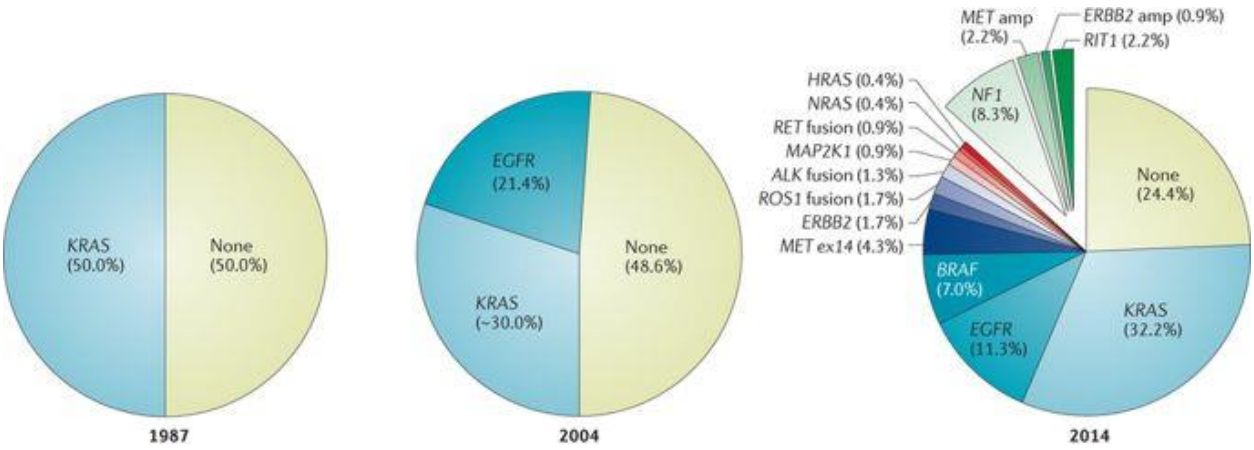

Figure 1.2: A time history of the identification of genomic biomarkers for lung cancer [14].

1.1.1.3. Glycome

While considered still in its infancy, the study of a patient's glycome, particularly the IgG glycome, has been used to make personalized therapy decisions. Galactosylation levels of IgG have been shown to be useful indicators of rheumatoid arthritis, and osteoarthritis [7, 15-19]. Furthermore, N-glycome profiling has been used on cardiac surgery patients and it has been found that the glycosylation patterns of patients before and after surgery could be used to cluster patients and predict the severity of the inflammatory

response resultant from surgery. Thus, the glycosylation patterns could be used to inform individual surgery maintenance strategies [16].

1.1.2. Tools for Identifying Precision Medicine Biomarkers

Precision medicine relies on the identification of biomarkers to stratify patients. Here an overview on the available techniques to identify genomic and proteomic biomarkers are discussed.

1.1.2.1. High-Throughput Sequencing

Substantial progress in precision medicine has been from the introduction of high-throughput genomic technologies combined with computational frameworks and electronic health records. With sequencing time and cost following a trend similar to Moore's Law, today it is possible to sequence an entire human genome for under $1000 in a day [20, 21]. This accessibility has led to many clinical studies on genomics and, as expected, genomic information has revealed many of the genetic bases of cancer. Today molecular testing is routinely used for breast, lung, and colorectal cancers [22]. Further national efforts plan to combine electronic health records with newly acquired genomic information on large populations to create a database that can be data mined to discover new disease correlations [23]. The ambitious Precision Medicine Initiative (also known as All of Us) seeks to sequence one million American genomes with a near-term focus on cancers and a longer-term focus on other disease and health factors [4].

High-throughput sequencing allows analysis of an entire human genome in a single reaction. Typically, a genome (~3.2 billion bases) is fragmented into many shorter sequences, on the order of hundreds of bases, which are then read by a sequencer. Most modern sequencers use an optical readout (fluorophore) or changes in ionic concentration (detection of H^+ ions) to gather sequence information either during a DNA ligation reaction, where a fluorescently modified probe hybridizes to the DNA fragment, or during DNA synthesis, where polymerase and a probe are used to generate a signal during DNA elongation. In either case, the sequence of the fragments are obtained which are then compiled back into a complete genome [20]. At the most basic level, researchers and clinicians can then investigate a genome for known mutations or new biomarkers may be identified by correlating patient groups, disease and mutations.

Genomics offers insight into hereditary predisposition for many conditions but is unable to detect the extent of disease manifestation or the response of the disease to therapy. Moving one layer up, the transcriptome has also been extensively explored using the same techniques as genomic technologies.

High-throughput determination of the transcript levels of thousands of genes is possible, but this information is not easily translated to functional proteins and their post-translational modifications, which have long been recognized as important in many diseases [24-28].

Other –omics fields, such as proteomics, transcriptomics, and glycomics, among others, also contain a wealth of information relevant to health, disease and precision medicine. While 40,000 genes exist in the human genome, the human proteome is estimated to contain more than 500,000 proteins [29]. Adding to this complexity, half of the human proteins are further modified through glycosylation [30]. Protein biomarkers can be prognostic or predictive; however, there remain limited tools for the identification of non-nucleic acid biomarkers in disease [31].

1.1.3. Immunoassays for Biomarker Identification

Immunoassays, diagnostic tests which use an antibody with affinity and specificity for a molecule of interest, remain the gold standard and the most commonly used diagnostic assays for the measurement of phenotypic biomarkers [32]. In an immunoassay the presence or concentration of a biomarker is achieved through a specific binding interaction between the antibody and the biomarker [33]. The first immunoassays were developed in the 1960s using radioisotopes for labeling and a gamma counter for measuring [34]. While these tests can be performed at high sensitivity and low cost, the potential health and safety concerns led to the development of enzyme based methods, including the enzyme linked immunosorbent assay (ELISA) [35]. ELISA is usually performed in multiple steps where antigens from a sample are first conjugated to a surface. Then a specific antibody, with an enzyme linked to it, for the antigen of interest is applied to the surface. Finally a substrate for the enzyme is added which results in some detectable signal, usually a color change of the substrate.

ELISA is used in many clinical tests but it is limited by the quality and breadth of available antibodies. Successful assays rely on antibodies that are able to be immobilized while maintaining the activity of the antigen, that are accessible to antigens in solution and that have low non-specific absorption [32]. Furthermore, for a particular antigen to be measured with high sensitivity an antibody with high affinity must be available. While antibodies remain the fastest growing group of pharmaceutical molecules, the average time to develop an antibody is 8 years and the average cost is $2.8 billion [36]. Currently there are 30

monoclonal antibodies approved for clinical use by the FDA and, there are 205 assays approved by the FDA for measurement of proteins, translating to approximately 1% of the human protein gene products [37, 38]. In the last 15 years there have been only 1.5 new protein analytes introduced per year [39].

1.1.4. Mass Spectrometry

Mass spectrometry offers a high throughput method to analyze proteins in a sample. It is capable of determining the molecular weight, amino acid sequence, and post-translational modifications of its constituent sample [40]. The technique involves the ionization of chemical species and then the sorting of ions based on mass-to-charge ratio. As such, the technique involves two steps: ionization and detection. During ionization a neutral molecule becomes ionized through the addition or loss of charge by protonation, deprotonation, cationization, electron ejection, or electron capture. Each ionization method has advantages and limitations for particular classes of molecules. For example, deprotonation is very useful for acidic species, and peptides are often ionized by protonation. Once ionized the molecules travel through a vacuum, sometimes through a quadrupole, which filters or fragment ions, and finally to a detector. The result is a large set of data on the various mass and charges in the original sample, usually in the form of a spectrum of peaks at various mass points. This spectrum can be compared to known reference spectrum to identify the original contents of the sample [41-43]

While Mass spectrometry is a powerful tool that has been used in numerous precision proteomics applications the clinical adoption of mass spectrometry is still met with challenges [44-57]. Generally, the mass spectrometry field lacks standardization despite a multitude of normalization efforts [58]. This places a significant burden on preparative steps which has resulted in large variations in reproducibility [59]. Considering the wide range of concentrations peptides exist in serum, separation methods are usually necessary prior to MS to obtain sufficient resolution but this also limits its potential throughput [48]. Thus, disease biomarkers identified by mass spectrometry have still been from highly abundant proteins and less abundant proteins remain difficult to discern [60, 61]. Large proteins are not able to be analyzed in native form by MS and instead require fragmentation by trypsin prior to analysis, but this digestion introduces a major source of error and can produce variable results if reaction conditions are not carefully optimized [62, 63]. These shortcomings are perhaps best illustrated by the OVA1 test for ovarian cancer which was initially

developed on an MS based system but could not reach clinically acceptable levels of precision [64]. In the end, the test was re-engineered onto an immunoassay [65]. Ultimately mass spectrometry remains a seldom used tool in clinical practice, and no mass spectrometry devices have been approved for the measure of proteins and peptides by the FDA for marketing or for clinical trials [66].

1.2. Aptamers

Aptamers represent an emerging class of molecules with potential for sensitively detecting non-nucleic acid biomarkers in standardized assays, and therefore could be attractive reagents for identifying precision medicine biomarkers. Aptamers are single stranded oligonucleotides that can bind to a biomarker with high specificity and affinity. They were originally discovered in 1990 by the independent research of Larry Gold (who coined the term for the aptamer discovery process – systematic evolution of ligands by exponential enrichment) and Jack Szostak (who named these affinity reagents “aptamers”) [67, 68]. It was immediately clear from these early efforts that RNA was a “shape not a tape,” and a new affinity molecule had been discovered with potential for measuring a wide range of targets [69]. Indeed aptamers have been presented with affinities to basically all types of molecules including small molecules [70], peptides [71], amino acids [72, 73], proteins [74, 75], cells [76, 77], viruses [78, 79], inorganic compounds [80, 81] and bacteria [82].

Aptamers have several advantages over other affinity reagents (such as antibodies). First, new aptamers are discovered through a totally in-vitro process obviating the need for host animals and immunogenics [78, 83-86]. Once discovered, aptamers can be synthesized by a DNA synthesizer which can produce oligonucleotides at low cost and with limited batch-to-batch variability, and lyophilized allowing storage for long periods of time at room temperature without degradation. Binding interactions can be reversed with generally mild conditions which do not degrade the analyte or ligand and allow reusability of either or both molecules [87]. Aptamers also can be easily modified to incorporate fluorophores (fluorescein, TAMRA, Cy5, ROX, and Alexa among many others), attachment linkers (biotin, thiol, amine), or modified bases. Furthermore aptamers have little or no immunogenicity and have much lower molecular weight than antibodies allowing much higher diffusion rates [88]. The selection conditions can be modified to accommodate the conditions for which the aptamer is being developed to be used in (including physiological conditions), unlike antibodies which can only be selected for in physiological conditions [89].

Although early aptamers were composed of unmodified RNA, aptamers can also be composed of deoxyribosenucleicacids (DNA) [90]. While, double-stranded DNA forms a double helical structure, single-stranded DNA and RNA will form a three-dimensional secondary structure resultant from the intramolecular base pairing between complementary base pairs [87, 90]. In both cases helices, loops, bulges, and junctions are possible. No difference has been found between RNA and DNA aptamers in terms of the broadness of potential target molecules nor in the affinity of the aptamer towards the target; however, DNA aptamers benefit from the inherently more stable nature of DNA [87].

1.2.1. Isolation of Aptamers

Aptamers are generated through an *in-vitro* process termed systematic evolution of ligands by exponential enrichment (SELEX) which is a form of combinatorial chemistry where large libraries are synthesized and screened for their affinities towards a target [86, 87, 91]. This process relies on a synthesized starting library which features a randomized region (10-80 nucleotides long) flanked by a defined 5' end and a defined 3' end [92]. Consequently, a library will be composed of a large diversity of single-stranded oligonucleotides (10^{15} different sequence) that can all be amplified by a single set of polymerase chain reaction (PCR) primers due to the defined 5' and 3' regions. The diversity of the library is sufficiently large that it is assumed oligonucleotide strands exist with high affinity towards a target of interest in the library.

SELEX is a discovery process, where sequences of high affinity are found from a large, highly diverse library. In general, these high affinity strands are isolated from the library through repeated cycles of affinity selection, partitioning and amplification [87]. Affinity selection consists of incubating the library with a target molecule of interest, either by immobilizing the target on a column and flowing oligonucleotides across the column or by weakly immobilizing the library and using the target to elute binding strands. Once the library has been incubated with the target, non-binding and weakly binding candidates are removed from the target by buffer washes, leaving only library members which strongly bind to the target. Then the target is subjected to changes in temperature or ionic conditions to release the binding library members from the target. A second selection phase is also possible where the eluted library members which previously bound to the target are incubated with a molecule similar to the target (named the counter target)

for which the desired aptamer is sought not to bind. In this case, the sequences which do not bind to the counter target are collected and the sequences which bind to the counter target are discarded. This selection phase is termed counter selection and is designed to remove oligonucleotide members which non-specifically bind to the target. These released members are collected and amplified by PCR using forward and reverse primers complementing the defined region on the library. PCR generates double-stranded sequences that are reduced to single stranded sequences by affinity methods or other methods [93]. The now single-stranded DNA is reintroduced to the target to start another round. Therefore, the oligonucleotides which bound strongly in the first round must now compete with each other for binding in the second round. The process continues until the starting library has sufficiently converged to a few sequences of high affinity. It is possible to monitor the affinity of the entire oligonucleotide pool (which will contain many different sequences) or to sequence the members of the pool and test individual sequence's affinity and specificity (**Figure 1.3**).

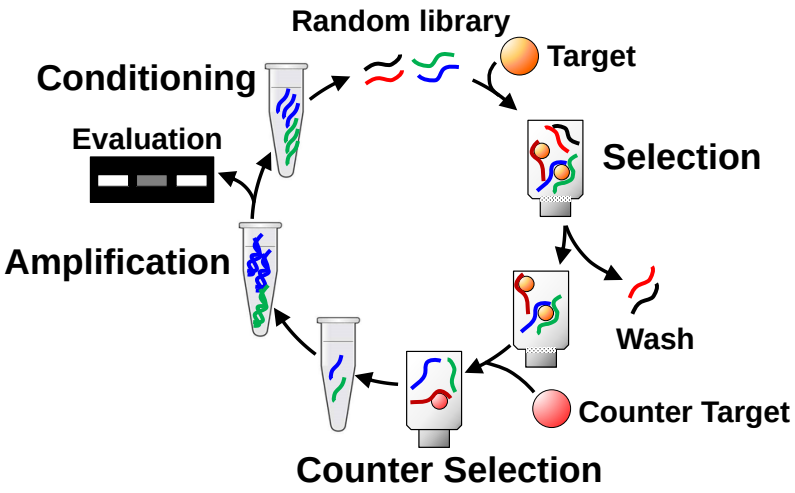

Figure 1.3: The SELEX process, consisting of multiple rounds of selection, counter selection, amplification, and conditioning. An aptamer library is incubated with a molecular target. Weakly binding oligonucleotides are removed by buffer washes. A counter target is then introduced, and oligonucleotides with affinity towards the counter target are removed. The remaining strands are PCR amplified, conditioned back to single-stranded oligonucleotides, and the process continues.

While aptamers have been employed in many relevant applications and for a wide range of targets, the application of aptamers to precision medicine fields remains unexplored because the time and resource consuming nature of the SELEX process. Significant effort has been placed on automating this process with coupled robotic selection and amplification; however, the sample consumption remains too wasteful to realistically approach precision applications.

1.3. Generation of Aptamers with Microfluidic Technology

Naturally microfluidic and lab-on-chip technologies which seek to provide integrated fluidic reaction modules in microscale geometries, have been under development for the rapid selection of aptamers at low cost [94, 95]. Generally, the selection stage of the SELEX process relies on the efficient and specific capture of candidate oligonucleotide strands on target functionalized surfaces. Because surface area scales at l^2 where l is the length of an object, and volume scales at l^3, the surface area to volume scales at l^{-1} meaning as objects become smaller the surface-area-to-volume ratio increases. The larger surface-area-to-volume ratios allow more intimate interactions between the aptamer candidates and targets with reduced surface area available for structural materials which can make the selection process unsuccessful from non-specific binding. As such, more binding sites are available for a given volume in microfluidic systems. Further, microfluidic systems can be highly integrated, efficiently transitioning from various stages of selection while handling small amounts of material, reducing the amount of waste generated and decreasing the amount of time spent on labor intensive procedures. Particularly attractive, these approaches have a high potential for automation and multiplexing to allow high-throughput SELEX.

In general, microfluidic SELEX approaches rely on the advances from the computing industry which made high resolution, high throughput, and small scale chips possible [96]. Most of the reported devices are made of polydimethylsiloxane (PDMS), a clear, biologically inert, polymer with the ability to have small features imprinted into its surface [97]. Furthermore, PDMS is able to be strongly sealed to many substrates by simply exposing both surfaces to oxygen plasma and then placing them in contact with one another [98]. Typically, a mold featuring chambers and channels is fabricated by photolithography in clean room settings onto a silicon substrate using additive processes [97]. Liquid PDMS is then poured onto the mold and allowed to harden by heating. The hardened PDMS is peeled off, inlets and outlets are punched, and it is

bonded to another substrate to complete the fabrication. More complicated architectures with multiple layers of PDMS bonded to each other are possible and are usually necessary when valves, pumps, or mixers are integrated into the system. [99].

1.3.1. CE-SELEX

Capillary-electrophoresis SELEX systems (CE-SELEX) were the first microfluidic systems applied to aptamer generation [100]. This method involves incubating an aptamer library with a target molecule and subjecting them to capillary electrophoresis based separation. Capillary electrophoresis can finely separate molecules based on size and charge, thus, a complex formed by an aptamer candidate binding to a target molecule can be distinguished and collected from free aptamer and from free target. The isolated complex is then amplified by PCR, conditioned back to single-stranded oligonucleotides are reintroduced to the target for further rounds of capillary electrophoresis. This approach has been used for proteins (IgE) [100], human immunodeficiency virus-reverse transcriptase (HIV-RT) [101], human vascular endothelial growth factor 165 (hVEGF165) [102], α-fetoprotein [103], and human epididymis protein 4 (HE4) [104]. The approach has been further improved to allow selections without intermediate amplification steps between selections and has been termed Non-Equilibrium Capillary Electrophoresis of Equilibrium Mixtures (NECEEM) [105]. The NECEEM method was used to isolate aptamers with affinity towards the h-RAS protein.

One advantage of the CE-SELEX method is the separation principle can also be used to evaluate binding parameters including dissociation equilibrium constants and rate constants [100-105]. This can be important because aptamers can be sensitive to the conditions they were selected in, resulting in aptamers with high affinity to the target during the selection stage but limited affinity towards the target in other binding assessment assays. Furthermore, CE-SELEX allows binding interactions to occur in solution without the need for potentially target altering functionalization onto a surface [100].

Conventional CE-SELEX is limited to molecules that generate large mobility shifts, including large, charged molecules, although examples have been presented with small molecules including the 580 Da small-molecule N-methyl mesoporphyrin IX when additional rounds of selection were used [102]. Another limitation of CE-SELEX is the small sample volumes the system is able to accommodate. Injection volumes

are less than 10 nL which limits the diversity of the library used in the selection process [95]. Even at high concentrations of DNA, a 10 nL volume practically features only 10^{12}-10^{13} oligonucleotides which is orders of magnitude less than traditional SELEX. Furthermore, the approach only seeks to speed up the selection stage and still relies on labor intensive conventional PCR and strand separation to start a new round of SELEX.

1.3.2. Magnetic SELEX

Microfluidic approaches which use carefully designed mixers to increase selection stringency have been developed to speed up the SELEX process. Soh and coworkers developed a system consisting of a microchannel with imbedded micropatterned ferromagnetic patterns to enable sensitive control of magnetic beads in the channel [106]. Target-functionalized magnetic beads were mixed with aptamer library and introduced under constant flow into two channel inlets on the outside of the channel while a magnet is held beneath the device. Ferromagentic structures focus the magnetic beads from the outside of the channel to the center of the channel under continuous laminar flow conditions. As a result, target functionalized magnetic beads and aptamer candidates which have bound to them traverse down the center channel to a center outlet while non-binding aptamer candidates remain in solution phase at the perimeter of the channel and exit the device through the two waste outlets. The collected sequences are then PCR amplified and conditioned back to single-stranded oligonucleotides. A bulk pool affinity (K_D) after only a single round of SELEX was found to be 33 nM [106]. An improved device was developed to reduce the dependence on carefully setting up the device under a microscope and to improve the device robustness. In the improved device, target functionalized beads are mixed with library and injected in the device [106]. Rather than focusing the magnetic beads to the center of the channel, the device immobilizes the magnetic target-functionalized beads on micro patterned Ni features while a magnetic field is applied by a permanent magnet. Buffer is then introduced to wash away weakly, and non-binding aptamer candidates. Finally, after sufficient washing, the magnetic field is removed and the target-functionalized beads and their bound aptamers were collected. These devices have been used to isolate aptamers in under 4 rounds towards streptavidin [107], Botulinum neurotoxin type A [108], apolipoprotein A [109], platelet derived growth factor B [107], and thrombin [109] with nanomolar dissociation constants. These devices improve the selection

stage of SELEX but do not offer improvements to the other phases of the SELEX including counter selection, amplification and strand separation processes.

1.3.3. Non-Magnetic Bead-Based SELEX

Magnetic beads provide a convenient method to immobilize a target functionalized surface within a chamber while increasing the binding sites but the high degree control afforded by microfabrication techniques make non-magnetic immobilization possible. A simplified selection chip consisting of a single channel with two pinched regions was developed [110]. Counter target-functionalized were injected through an inlet connected to one pinched region filling the channel with counter target beads up to the pinched region. Downstream to that pinched region was a second pinched region with another inlet. Target beads were introduced through this inlet to create a second region filled with target beads. The pinch regions prevented microbeads from passing allowing devoted regions of the channel to be filled with target and counter target beads. Thus, a fluidic channel with a counter target-functionalized bead region and a target-functionalized bead region was created. An aptamer library was then injected through this channel such that aptamer candidates would first interact with the counter-target beads, removing library members with affinity towards the counter target, before reaching the target-functionalized bead region and being allowed to bind to the target-functionalized beads. The target-functionalized region was then washed to remove weakly binding oligonucleotides, and finally eluted and collected. From the aptamer candidates were amplified off-chip and conditioned back to single stranded DNA, and reinjected into a freshly setup device. The chip was used for six rounds of SELEX to isolate an anti-myoglobulin aptamer (K_D = 4.93 nM).

Another microfluidic chip was presented foregoing beads altogether. Instead a protein microarray was created and then bonded to a microfluidic network of channels [111]. As such, aptamers flow across a series of counter-target regions before reaching the region of the target molecule. After interaction with the target molecule and washing, the fluidic network was torn off the microarray. Since a microarray was being used, it could be readily scanned to monitor the success of the selection process. The method was used to isolate a Lactoferrin aptamer in seven rounds with dissociation constants down to 0.92 nM. While, using a microarray to deposit target and counter target molecules allowed a straightforward immobilization

procedure it also limited the target region to a small area located on the bottom of the fluidic channel. Compared with bead filled channels, this method has reduced surface area devoted to target presentation.

SELEX on whole cells have been performed using an inertial device (termed I-SELEX) [112]. The I-SELEX device is a spiraling channel with inlets for sheath flow and samples, and outlets for waste and sample collection. Library was mixed with red blood cells and then injected in the sample inlet. Dean drag forces cause solution phase aptamers to migrate towards the outer wall while aptamers bound to the red blood cells remain on the inner channel. Similar to the magnetic bead based devices, this method allows efficient portioning of binding sequences from non-binders under constant flow conditions which have the additional benefit of simultaneously washing the target. After five rounds of SELEX, aptamers with nanomolar affinity were found towards cell surface markers.

1.3.4. Sol-Gel SELEX

Microfluidic approaches have also focused on increasing the target presentation to increase the selection efficiency. These techniques seek to overcome the concern for biased selection procedures which only select aptamers for targets immobilized in a specific manner. Sol-gels have been used to encapsulate and immobilize targets in a more native state within microfluidic channels [113-115]. Sol-gels with target proteins are mixed and deposited as a droplet onto a substrate. A PDMS mold with patterned microchannels is exposed to oxygen plasma, along with the sol-gel substrate, and is stamped onto the substrate to complete the fabrication. The porosity of the gel allows oligonucleotides to access the trapped target molecules and the device uses integrated heaters for thermal based elution to disrupt binding interactions between the target and aptamer candidates. Sol-gel SELEX device have identified aptamers towards the TATA binding protein [116], a yeast transcription factor [115], enhanced green fluorescent protein, and a heat shock factor. The sol-gels allow a high density of protein making it an attractive option for multiplexed selections which have been performed with 5 parallel selections each for aptamers with a different target. However, sol-gel preparation is a lengthy process that takes more than 12 hours, and the library must be incubated with the target for long periods of time (~1 hr) to allow diffusion of library members into the sol-gel, and presented devices use small reaction chambers (0.22 μL) during this incubation process limiting the diversity of the library for the selection process.

1.3.5. Integrated Microfluidic Systems

Rather than speed up a single stage of the SELEX process, researches have tried to use the ability of microfluidic devices to integrate the many different reactions of SELEX into a single fluidic architecture. The SELEX process relies on repeated rounds of affinity binding, partitioning and elution of binding library members, PCR based amplification of these members, and conditioning of the PCR product back to single-stranded DNA for further rounds of SELEX. Taken individually, all these steps have been demonstrated on dedicated microfluidic devices. By combining the substeps of SELEX onto a single-platform, the process can be performed with minimal sample loss between stages, low-volumes and thus low sample consumption for the entire process, and with a higher degree of automation.

1.3.5.1. Automatic Integrated Systems

An early effort in an integrated SELEX process was presented by Hybarger, et al. where a series of reagent-loaded microlines and a microline reaction chamber to fully automate the steps of transcription, selection, reverse-transcription, and amplification [117]. The automated system was used to find an anti-lysozyme aptamer. Despite the use of microfluidics the overall footprint of the system, and reagent consumption remained quite large. However, it remains the only integrated SELEX device demonstrated to be capable of performing reverse-transcription and transcription which are necessary for the handling RNA libraries.

1.3.5.2. Integrated Devices Capable of Accomplishing a Single Round of SELEX

The first chip-based microfluidic approaches were presented by Gwo-Bin Lee's group [114, 118]. The devices consisted of a glass substrate with a patterned heater and temperature sensor and two PDMS slabs – one bearing a fluidic network where SELEX would occur and the other bearing microfluidic flow control elements. The fluidic network featured reaction chambers for selection, PCR chambers, while the control elements consisted of micromixers and microvalves to direct oligonucleotides through the SELEX process. Targets are functionalized with magnetic beads off-chip, mixed with the aptamer library and this mixture is injected into the chip using the integrated micropumps while a magnet was held beneath the reaction chamber to immobilize the target functionalized beads. Buffer is then introduced into the chip to

remove solution-phase, weakly binding oligonucleotides from the target functionalized beads. Following washing, PCR reagents were introduced into the chamber and the integrated heater was used to amplify the remaining aptamer candidates. These systems have been further developed to include counter target chambers and dedicated PCR chambers [118]. Such embodiments rely on eluting target binding oligonucleotides by using off-chip heaters placed beneath the selection chamber. The eluted product was pumped through a chamber containing counter-targets before finally reaching the PCR chamber for amplification. Early devices were used to isolate anti-protein aptamers but later devices were used to isolate aptamers with affinity towards whole cells.

Ultimately, the presented integrated systems could complete a round of SELEX in ~1 hour which is a drastic improvement over conventional SELEX (~1 day). While these systems stored all reaction materials on the device itself, it severely limits the volumes for some of the SELEX stages. For example, washes to remove weakly binding oligonucleotides could only use volumes up to 300 µL. Moreover, the devices are only capable of performing a single round of the SELEX (one incubation, elution, partition of binding strands, and amplification of binding strands) and must be transferred to a new device for further rounds. Furthermore, the devices still rely on manual, off-chip processes to condition the amplified product back to a solution of single stranded oligonucleotides that does not include the complement generated during the PCR product.

1.3.5.3. Integrated Devices Capable of Accomplishing Multiple Rounds of SELEX

Integrated devices capable of multiple rounds of SELEX on a single device have also been pursued [119, 120]. These devices have, thus far, been PDMS fluidic networks bonded to a substrate featuring heaters and temperature sensors. Generally, the devices included two reaction chambers – one for affinity selection and one for PCR based amplification connected by microchannels. The SELEX process is achieved by oscillating between these two reaction chambers. Key to these devices was the incorporation of bead based reactions for all steps of the SELEX process. Target functionalized beads were used for the selection stages and reverse primer functionalized beads were used for the PCR stage. Target-functionalized beads were introduced into the selection chamber and held by microweir - a dam like constriction that allows buffer to pass but is too constrained to allow the passage of the much larger beads.

Library is injected through these selection beads causing library members with affinity towards the target of interest bound to target-beads in the selection chamber. The chamber is then washed to remove weakly binding strands. The remaining strands are eluted from their target molecules through modest increase in temperature and transferred to the PCR amplification chamber where they interact with reverse-primer functionalized beads. Due to the complimentary of the reverse primer and the 3' end of the library members, hybridization occurs between the transferred library members and the reverse primers resulting in library members hybridized to reverse primer beads which are in turn attached to bead surfaces. Reverse primer functionalized beads were created by mixing biotinylated reverse primer with streptavidin beads. The inclusion of the reverse primers only on bead surfaces results in the generation of double stranded DNA where the amplified input strand is hybridized to its compliment which is in-turn tethered to the bead surface through biotin-streptavidin interactions. Thus, under de-hybridizing conditions (e.g. thermal denaturation or mild NaOH treatment) the amplified aptamer DNA can be released into the solution phase while its compliment which was generated as a byproduct of the PCR process remains attached to the bead surface. Under flow conditions the released amplified product can be transferred back to the selection chamber (with replenished target) for further rounds of SELEX. Additionally, these devices were shown to be able to sensitively control the environmental conditions of the selection process to obtain aptamers with unique properties. For example, by using an integrated heater and temperature sensor located under the selection chamber the selection temperature could be set to physiological temperature. The resulting aptamer candidates exhibited increased binding at physiological conditions compared to room temperature conditions [120]. While the overall device operation and setup were simple, the device did not feature any barriers between selection and amplification processes which increased the potential for unintentional amplification of oligonucleotides with high non-specific interactions. Aptamers were isolated with affinity towards IgE and glucose-boronic acid using these methods.

Devices were also developed where the coupling between selection stages and amplification stages (and back) was achieved through electrokinetic methods which reduced the dependence on complicated fluidic handling components (e.g. syringe pumps and valves) [119]. The device featured a selection chamber and PCR amplification chamber which were separated by a channel filled with agarose gel. The agarose gel prevents diffusion from one channel to the other. When an electric field was applied

between the two chambers the agarose allowed migration of the aptamer candidates while preventing the migration of target molecules or other potential sources of cross contamination. In this way, selection and amplification could be performed in different buffers. In addition to demonstrating successful isolation of aptamers using surface immobilized targets, by weakly hybridizing DNA to beads and introducing the target in solution aptamers were isolated towards small molecule targets in solution. As such, the approach was capable of selecting aptamers towards a broad range of targets and was not limited to targets that are amenable to surface attachment chemistry. However, the agarose gel tended to break down after three rounds of selection limiting the amount of cycles performed on chip. Such an issue could be catastrophic for targets that require additional rounds of SELEX to obtain sufficient convergence of the starting library. Furthermore the device exposed the target to potentially deleterious electric fields prior to and during affinity selection which could compromise the integrity of the target or adversely affect target-aptamer binding.

1.3.6. Generation of Aptamers with Microfluidics Technology Summary

In summary, precision medicine lacks reagents for accessing non-nucleic acid molecules. Aptamers are affinity reagents with potential to allow the detection of many molecules, and when combined with microfluidic technology could rapidly isolate aptamers. Such approaches would allow the generation of many precision medicine probes at low cost. Microfluidic devices have been successful in isolating aptamer reagents for many targets but their full potential is yet to be achieved. Currently presented microfluidic SELEX devices either are only capable of improving the selection stage of SELEX or are poorly suited to handle the many rounds of SELEX that may be necessary for highly specific aptamer isolation. It is the goal of this thesis to develop an approach to rapidly isolate aptamers while reducing the amount of resources consumed and to apply this approach to several precision medicine relevant biomarkers.

1.4. Objective and Significance

This thesis seeks to develop methods for the rapid isolation of high affinity and high specificity affinity probes which can ultimately be applied to precision medicine. While the Human Genome Project, and next generation sequencing techniques have enabled much of the early applications for precision medicine, the human genome only represents a fraction of the information present and important to a person's health. Non-nucleic acid biomarkers (peptides, proteins, and their glycosylated versions) are strong indicators of health and disease but tools to detect and analyze these biomarkers remain scarce.

Furthermore, techniques to develop new detection assays are too time consuming and resource consumptive to be broadly applied within precision medicine applications. The specific objectives of this thesis are:

- Development of aptamer selection methods which can isolate aptamer candidates rapidly (within a day) for a wide range of targets while consuming small amounts of reagents and samples. Such methods will enable the isolation of probes at a scale capable of addressing the needs of precision medicine.
- Application of the methods to biomarkers relevant to precision medicine. Aptamers will be isolated against glycans, glycosylated peptides, monoclonal proteins, and a patient's tumor associated protein. These aptamers can potentially be applied to glycome profiling and personalized cancer diagnostics.

1.5. Contributions

1.5.1. Contributions to Engineering of Aptamer Isolation

The engineering contributions of the thesis primarily include the development of methods that reduce the amount of time and materials needed to isolate aptamers. These methods are realized with microfluidic devices which integrate the entire SELEX process.

- *Development of an electrophoretic, and pressure-driven hybrid SELEX method.* A microfluidic approach which combines electrophoretic and pressure-driven oligonucleotide transfers is used to integrate the SELEX process. The hybrid approach simplifies the device design and operation procedures by reduced pressure-driven flow control requirements, and avoids the potentially deleterious exposure of targets to electric fields prior to and during affinity selection.
- *Development of a free solution electrokinetic SELEX method.* A microfluidic approach which allows integration of the affinity selection and amplification stages of SELEX by combining bead-based biochemical reactions with free solution electrokinetic oligonucleotide transfer.
- *Development of a SELEX approach which integrates selection, counter selection and amplification.* Counter selection is incorporated into every selection round without any significant increase in selection time, materials, or reagents. The device is also designed to allow many rounds of SELEX without degradation of the device, thereby allowing selection of aptamers towards targets with high

similarity to their counter targets. Therefore, the device is suitable for isolating aptamers for precision medicine applications.

1.5.2. Contributions to Aptamer Isolation for Precision Medicine

This thesis contributes to precision medicine by isolating aptamers in two important applications to precision medicine. First, aptamers will be isolated as reagents for the study of the glycome, an emerging source of precision medicine biomarkers with potential to allow stratification of patients for individualized therapeutic strategies. Second, aptamers will also be isolated as personalized, patient-specific probes for cancer diagnostics.

Isolation of aptameric probes which recognize glycans. Glycans are involved in all human development activities, yet few tools to sensitively analyze glycan samples exist. Towards providing reagents for accessing the glycome, aptamers are selected for GM1, GM3, and GD3 gangliosides, and a glycosylated peptide.

Selection of personalized aptamers for multiple myeloma. Diagnosing multiple myeloma and monitoring the cancer progression relies on measuring cancer-affected monoclonal proteins in serum. Standard of care methods for detecting these monoclonal proteins are unspecific and are not sensitive Aptamers are selected from a multiple myeloma patient's monoclonal protein which was purified from a patient serum sample.

1.6. Organization of Thesis

The thesis is divided into two parts. The first part deals with the development of new microfluidic methods for aptamer development with the goal of developing a microfluidic technique capable of isolating aptamers relevant for precision medicine applications. Chapter 2 presents a hybrid microfluidic device using electrophoretic and pressure driven flow to isolate aptamers in an integrated manner. The approach is capable of performing the selection and amplification stages of the SELEX process on a single chip. However, the limitations of this device motivate the development of a purely electrokinetic device as presented in Chapter 3. This device uses free-solution electrokinetics to address the complicated handling procedures and limited reliability of the device presented in Chapter 2. The device is used to enrich an aptamer pool with affinity towards IgA. A third device is then developed in Chapter 4. The device employs

three chambers to perform selection, counter selection and amplification of aptamer candidates every round of SELEX. These stages of the SELEX process are connected in a fluidic loop with flow controlled through integrated valves. With this approach many rounds (up to six tested) of SELEX can be performed on a single device without degradation. Thus, the approach was attractive for precision medicine applications. Chapter 5 uses the approach developed in Chapter 4 to isolate aptamers towards glycans. Aptamers are generated with affinity towards gangliosides GM1, GM3, GD3 and a glycosylated peptide. The aptamers have potential to be used as glycome probes. Similar to Chapter 5, Chapter 6 uses the approach developed in Chapter 4 to isolate aptamers with affinity towards a multiple myeloma patient cancer associated monoclonal protein. Finally, Chapter 7 summarizes the thesis and discusses potential future directions for this research.

Chapter 2: An Integrated Microfluidic SELEX Approach using Combined Electrokinetic and Hydrodynamic Manipulation

2.1. Introduction

Aptamers are single-stranded oligonucleotides (typically 12-80 nucleotides long) that function as specific affinity receptors towards a broad spectrum of biological targets including small molecules [70], peptides [71], amino acids [72, 73], proteins [74, 75], cells [76, 77], viruses [78, 79], and bacteria [82]. With advantages such as synthetic availability through an *in vitro* process, ease of coupling to other functional molecular groups [121, 122], reversibility of binding, long-term stability, low immunogenicity [123], low batch-to-batch variability [124], and long shelf life aptamers offer an attractive alternative to other affinity receptors, (e.g, antibodies [86, 125]) and have broad applications to basic biological sciences[126], drug discovery [127], and clinical diagnostics and therapeutics [125, 128].

Aptamers are discovered from large randomized libraries of oligonucleotides through an *in-vitro* process termed systematic evolution of ligands by exponential enrichment (SELEX) [86, 87, 91]. SELEX involves iterative rounds of affinity selection against a target of interest, and amplification via the polymerase chain reaction (PCR), of target-binding oligonucleotides from large randomized libraries (up to 10^{14} members) [92]. Conventional SELEX platforms require extensive manual handling of reagents, and are time-consuming, typically requiring a month or more to complete a single experimental run. Robotic automation of the SELEX procedure can alleviate these issues but the cost is prohibitive [129].

Microfluidic technology has been emerging to enable rapid isolation of high-affinity aptamers with reduced reagent consumption and in much fewer rounds of iteration [118, 130]. Microfluidic affinity selection has been performed, in conjunction with off-chip amplification, against targets retained using silica capillary walls [117], microbeads [106-108, 131, 132] or sol-gels [113-115], or against cells in solution [133, 134], to increase selection stringency [106-108, 131-134], create more favorable biomolecular environments [113-115], or allow simultaneous positive and negative selections [110]. Moreover, microchips have been developed in an attempt to integrate the overall SELEX process using pneumatically based flow control for isolation of aptamers against viruses[135], cells [131, 136, 137] and proteins [138, 139]. While capable of performing individual affinity selection and PCR amplification processes on-chip, these devices apparently require an off-chip procedure to retrieve single-stranded DNA from amplified products between successive rounds of SELEX, and do not yet allow full integration of SELEX on a microchip. We have recently

demonstrated integration of the entire SELEX process using solid-phase capture and amplification of oligonucleotides on bead surfaces, which are manipulated using either pressure-driven flow or electrokinetics [119, 140]. In these works we found the use of electrokinetic manipulation simplified the device design but involved electric fields that can potentially comprise the integrity of the target or adversely affect the target-aptamer binding. Pressure-driven flow, on the other hand, in general requires extensive flow control operations that complicate the device design and operation.

This chapter presents a microfluidic approach to full integration of the SELEX process on a microchip. The approach combines the pressure-driven and electrokinetic transport of target-binding oligonucleotides to exploit the advantages of both methods while minimizing their individual limitations. In this hybrid oligonucleotide manipulation method, affinity selected oligonucleotides are electrokinetically transferred for PCR amplification, while the amplified oligonucleotides are subsequently transferred back using pressure-driven flow for further affinity selection. The hybrid approach simplifies the device design and operation procedures by reduced pressure-driven flow control requirements, and avoids the exposure of targets to electric fields prior to and during affinity selection. In addition, bead-based reactions are used to achieve the on-chip coupling of affinity selection and amplification of target-binding oligonucleotides, thereby realizing on-chip loop closure and integration of the entire SELEX process while leveraging the advantages of pressure-driven and electrokinetic transport without requiring offline procedures. The utility of this hybrid approach is demonstrated by isolation of high-affinity aptamer candidates (K_D = 12 nM) against the protein immunoglobulin E (IgE) via four rounds of selection and amplification within 10 hours.

2.2. Experimental

2.2.1. Microbead-Based SELEX Principle

A microbead-based SELEX procedure is integrated on a single chip using combined electrokinetic and pressure-driven transport of oligonucleotides for isolation of aptamers against a given target molecule (**Figure 2.1**). The procedure involves iterative rounds of affinity selection and amplification of target-binding oligonucleotides. Affinity selection occurs on microbeads that are functionalized with a biomolecular target. A randomized library of single-stranded DNA (ssDNA) oligonucleotides, each consisting of a randomized region flanked by two constant primer regions, is then introduced to the beads and bind to the immobilized

target. Weakly binding oligonucleotides are removed from the beads by multiple buffer washes. The remaining strongly binding oligonucleotides are released from the beads by thermally disrupting their binding with the target and transferred via electrokinetically migration to a second set of microbeads that are functionalized with reverse primers complementary to the 3' end of the ssDNA library. The target-binding oligonucleotides are captured by the beads via hybridization to the reverse primers. PCR reagents are then introduced and PCR is performed, resulting in double-stranded DNA (dsDNA) consisting duplicate copies of (i.e., amplified) target-binding oligonucleotides hybridized to bead-immobilized complementary strands. The amplified target-binding oligonucleotides are released from the beads via thermal denaturation, and then transferred via pressure-driven flow to a replenished set of target-functionalized microbeads, on which a new round of affinity selection is carried out without the presence of potentially damaging electric fields. This process is repeated in multiple rounds of affinity selection and amplification to yield aptamers with sufficient affinity to the target.

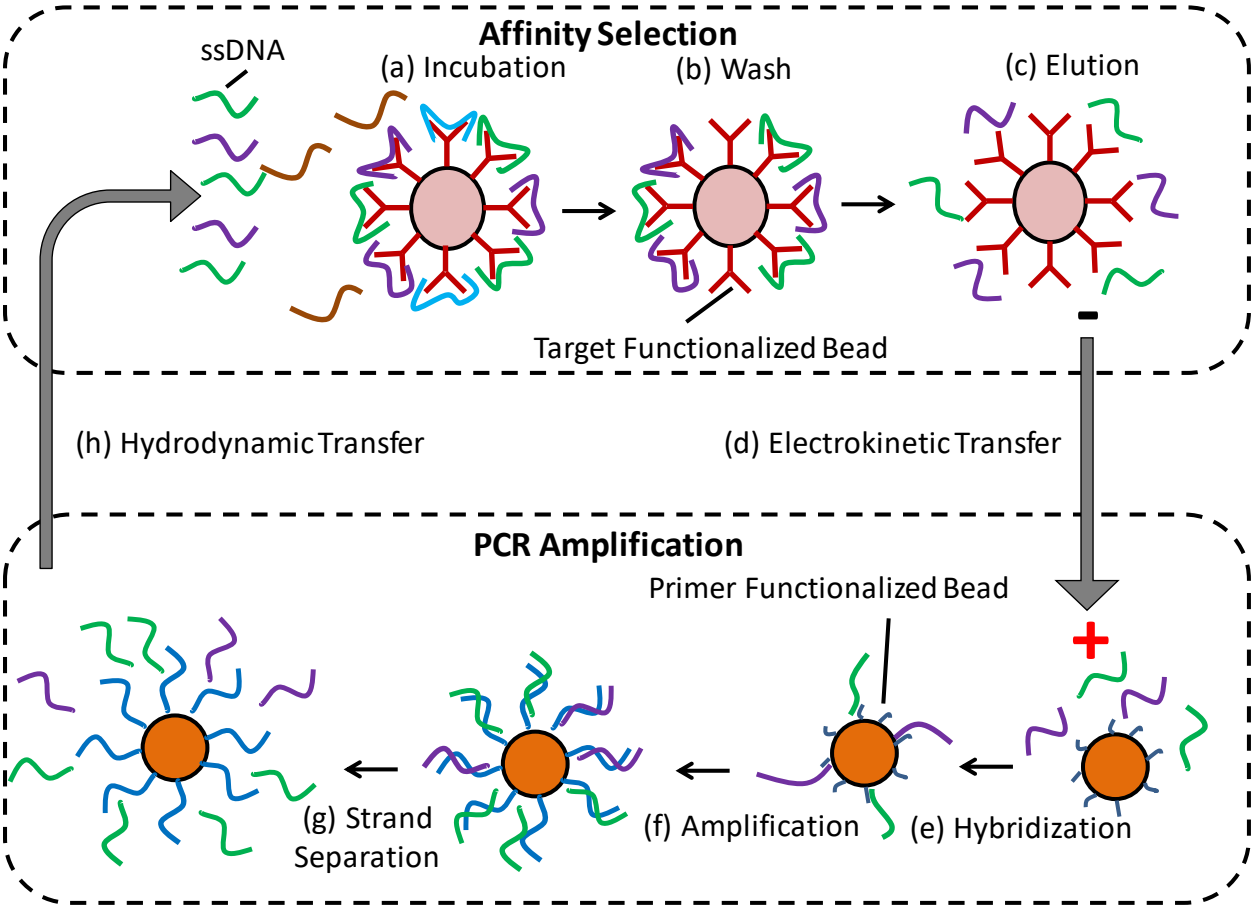

Figure 2.1: Microbead-based microfluidic SELEX principle. (a) Randomized ssDNA binds to target-functionalized microbeads. (b) Weak binders are removed by washing; (c) strong binders are thermally released and (d) transferred for PCR amplification via electrokinetic transport. (e) The strands are captured by magnetic microbeads with surface-immobilized reverse primers, and (f) amplified via PCR. (g) The amplified single strands are thermally released from bead surfaces, and (h) transported through pressure-driven flow for a new round of affinity selection.

2.2.2. Microfluidic Device Design and Operation

The microbead-based SELEX procedure is realized in an integrated microfluidic device (**Figure 2.2**). The device consists of two microchambers (respectively referred to as selection and amplification chambers), which are each integrated with thin-film resistive heaters and temperature sensors, and connected to an inlet and outlet used for the introduction of microbeads and buffers, as well as to an electrode port. The selection chamber also includes a microweir, a flow restriction structure (20 µm high) that retains microbeads while allowing fluid passage. The chambers (each 0.5 µL in volume) are

interconnected by reagent transport channels. One reagent transport channel (800 µm wide, 240 µm high, and 7 mm long) between the chambers is filled with agarose gel that allows electrokinetically driven oligonucleotide migration while preventing bulk flow (**Figure 2.2b**). The other transport channel (600 µm wide, 20 µm high, and 10 mm long), with a semi-circular cross section, lies below a second layer of control channels that are filled with pressurized oil (**Figure 2.2c**). Passage of reagent solution in the transport channel is prevented or enabled via changing the oil pressure in the control channels, which hence function as a microvalve. Two supplementary outlet channels sandwich the gel-filled transport channel and are used to allow buffer to fully fill the non-gel-occupied sections of the electrokinetic transport channel.

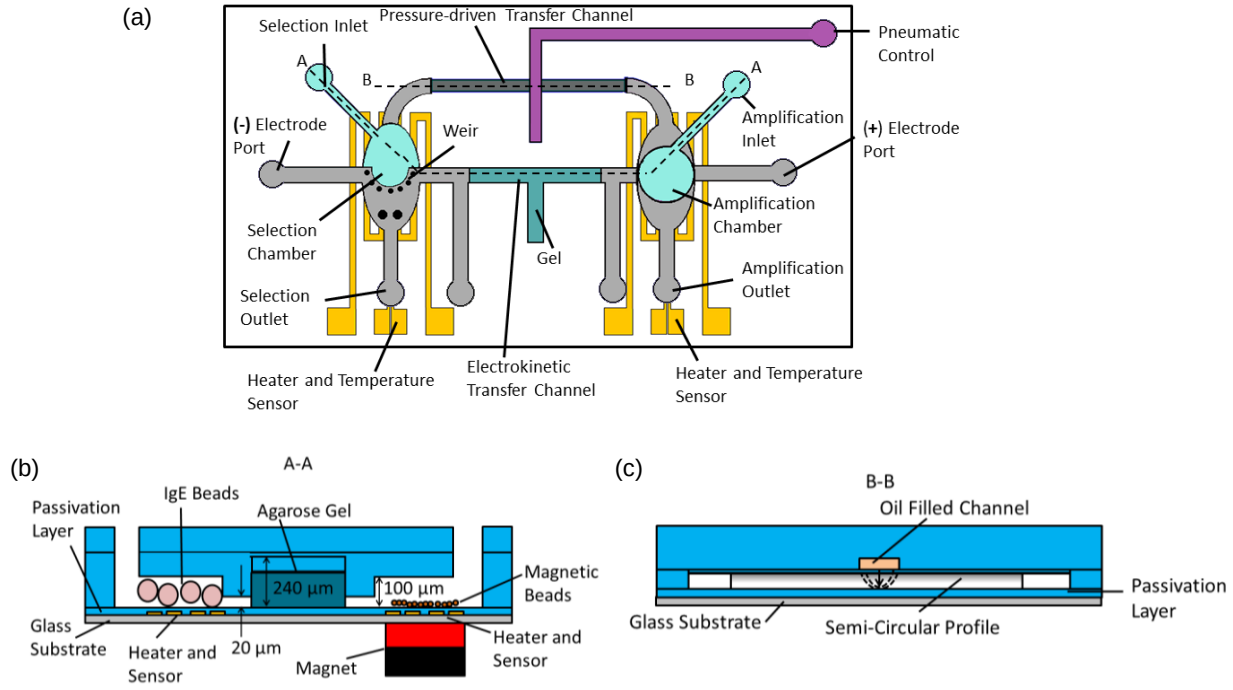

Figure 2.2: Schematic of the microfluidic SELEX device: (a) top view, (b) A-A cross-sectional view, and (c) B-B cross-sectional view. The selection chamber contains microbeads that are functionalized with a target protein and retained by a microweir. The amplification chamber contains magnetic beads that are functionalized with a DNA primer and retained by an external magnet. Oligonucleotides (ssDNA) strands are transferred by electorkinetics from the selection chamber to the amplification chamber, and reversely by pressure-driven flow.

The microfluidic device is capable of repeatedly performing iterative rounds of affinity selection and amplification. Affinity selection occurs in the selection chamber, where target-functionalized microbeads are introduced and immobilized by the microweir structure. A randomized ssDNA library is then introduced to the beads. Strongly binding oligonucleotides are captured by the target and weakly binding strands are removed by buffer washes. Next, reverse primer-functionalized magnetic beads are introduced into the amplification chamber and held via an external magnet. The oligonucleotides bound to the bead-immobilized target are thermally released from with the selection chamber's integrated heater, and electrokinetically transferred through the gel-filled channel to the amplification chamber, and captured therein by the bead-bound reverse primer[140]. PCR reagents are then introduced and PCR performed using the amplification chamber's integrated heater and temperature sensor. The amplified ssDNA is thermally released from the beads, and upon the opening of the microvalve, transferred via pressure-driven flow to the selection chamber for further affinity selection. As such, the bead-based protocol enables on-chip separation of amplified ssDNA from complementary strands and on-chip coupling of successive rounds of SELEX, thereby allowing integrated isolation of aptamers.

2.2.3. Materials

Agarose, PBS buffer, MgCl2, tris, boric acid, and molecular biology grade water were purchased from Sigma-Aldrich (St. Louis, MO). Deoxyribonucleotide triphosphates (dNTPs) and GoTaq Flexi DNA polymerase were obtained from Promega Corp. (Madison, WI). Randomized oligonucleotide library (5' – GCC TGT TGT GAG CCT CCT GTC GAA – 45N – TTG AGC GTT TAT TCT TGT CTC CC – 3') and primers (Forward Primer: 5' – FAM – GCC TGT TGT GAG CCT CCT GTC GAA -3', and Reverse Primer: 5' – dual biotin – GG GAG ACA AGA ATA AAC GCT CAA – 3') were synthesized and purified by Integrated DNA Technologies (Coralville, IA). Human Myeloma Immunoglubulin E (IgE) was purchased from Athens Research and Technology (Athens, GA), and NHS-activated microbeads were purchased from GE Healthcare (Little Chalfont, Buckinghamshire, United Kingdom). Dulbecco's phosphate-buffered saline (D-PBS), and streptavidin coupled magnetic beads (Dynabeads® M-270 Streptavidin) were purchased from Invitrogen (Carlsbad, CA). AZ-4620 positive photoresist was obtained from Clariant Corp. (Somerville, NJ) and SU-8 (2000, 2025, and 2075 series) negative photoresist was purchased from Microchem Corp.

(Westborough, MA). Polydimethylsiloxane (PDMS) was obtained from Robert McKeown Company (Somerville, NJ) and silicon wafers were purchased from Silicon Quest International, Inc. (San Jose, CA).

Agarose microbeads functionalized with a protein were used for selection and magnetic microbeads functionalized with reverse primers were used for amplification. The beads for selection were functionalized with a protein through covalent coupling between the NHS groups of the microbeads and the amine groups of the protein. Prior to an experiment, the protein was incubated with IgE under gentle rotation for 1 hour at room temperature, and washed with D-PBS buffer. Unreacted NHS groups were passivated by incubating the functionalized beads in Tris buffer. The functionalized beads were then suspended in D-PBS buffer. Similarly, streptavidin magnetic beads were functionalized by incubation with dual biotin conjugated reverse primers through covalent coupling for 30 minutes, washed with D-PBS buffer and suspended in D-PBS buffer.

2.2.4. Microfluidic Device Fabrication

The approach was demonstrated with a PDMS microfluidic device fabricated using standard multi-layer soft-lithography techniques. Two silicon wafers, one bearing four identical copies of the flow components of the device and the other bearing four identical copies of the control layer components were fabricated in a cleanroom setting. First, alignment marks were deposited onto the wafer so that multiple photolithography steps could be performed with high accuracy. This was achieved by thermally evaporating (Edwards 306 thermal evaporator) a silicon wafer with a 20 nm layer of chrome and a 100 nm layer of gold. Shipley photoresist S1813 was then spun onto the surface (6000 rpm for 50 seconds) and baked on a hot plate (115 ºC and 60 seconds). This coated wafer was then exposed to 80 mJ/cm^2 UV light through a mask defining aligner marks for subsequent layers. The exposed wafer was then submerged in AZ 300 MIF developer for 60 seconds. Following development the wafer was rinsed with water, dried with nitrogen, and submerged in gold etchant. The gold etched wafer was finally submerged in chrome etchant, rinsed with water, and dried with nitrogen. An acetone bath was used to remove remaining photoresist, and the wafer was rinsed with isopropanol and dried on a hot plate at 100 ºC for 10 minutes.

The valve controlled channel was then defined onto the wafer with alignment marks. First, a layer of AZ-4620 positive photoresist was spun on a silicon wafer in a two-step process. The photoresist was spun at 2000 rpm for 85 seconds, and baked for 85 seconds 110 ºC on a hot plate. Then the AZ-4620 was

reapplied to the wafer, spun again at 2000 rpm for 85 seconds and baked at 110 ºC on a hot plate for 165 seconds. The total thickness of the photoresist from this two-step process was approximately 30 µm. This photoresist covered silicon wafer was then exposed, through a photomask with desired channel features (designed using L-Edit and custom printed by Fineline Imaging), to 1400 mJ/cm^2 of energy from a mask aligner (SUSS MA6). The exposed wafer was submerged into AZ400K developer diluted 1:4 in water for 10 minutes. The developed wafer was placed on a programmable hotplate (Torrey Pines Scientific) where the temperature was ramped from room temperature to 200 ºC over an hour long period and let to stay at room temperature for 4 hours. This high-temperature bake served two purposes: first it hard baked the photoresist such that it would be more immune to the solvent effects in subsequent photolithography processes and second it caused the previously square shaped channel to reflow into a semi-circular shape. The reflow shape allows valves to tightly close channels without the compressive force causing unsealed corners [141].

Buffer channels were then built onto the silicon wafer. SU-8 2035 was spun at 4000 rpm for 50 seconds, baked at 65 ºC for 3 minutes on a hotplate, and baked at 95 ºC for 6 minutes on a hotplate. This wafer was exposed to 152 mJ/cm^2 of energy using a mask aligner and a custom drawn mask defining the desired channels. A post-bake was then performed consisting of 65 ºC for 1 minute on a hotplate and then 95 ºC for 5 minutes on a hotplate. Following, the wafer was submerged in SU-8 developer for 5 minutes and rinsed with isopropanol. A hard bake was then performed, placing the wafer on a hotplate at 125 ºC for 1 hour.

The final fluidic layer, consisting of the large chambers and gel channel, was then fabricated onto the wafer. SU-8 2075 was deposited on the wafer and left to spread on a flat surface for 15 minutes. The wafer was spun at 300 rpm for 15 seconds to spread the photoresist and then was ramped up to 1000 rpm for 45 seconds. The SU-8 coated wafer was then placed on a hotplate (65 ºC) for 7 minutes. Following the 7-minute bake the hotplate temperature was increased by 5 ºC every 10 minutes until reaching 95 ºC. After remaining on the hotplate for 1 hour the hotplate was cooled to room temperature with the wafer remaining on it. This on-plate cooling was to reduce thermal stress in the photoresist which can be caused by sudden changes in temperature and can potentially interfere with the adhesion of the SU-8 photosensitive epoxy to the silicon wafer. This pre-baked wafer was then exposed to 350 mJ/cm2 of energy through a film

photomask defining the chambers and gel channels. After exposure, the wafer was baked on a hotplate again, first at 65 ºC for 5 minutes and then at 95 ºC for 15 minutes. The hotplate was then cooled to room temperature with wafer remaining on the surface to reduce thermal stress. The baked wafer was then placed in SU-8 developer for 15 minutes and rinsed with isopropanol. This concluded the fabrication of the flow layer wafer of the microfluidic device.

Meanwhile, the control layer wafer was fabricated on a second silicon substrate. SU-8 2035 was spun onto a piranha (4 parts sulfuric acid, and one part 30% hydrogen peroxide) cleaned silicon wafer by spinning at 4000 rpm for 50 seconds. A pre-bake was performed by heating the wafer on a hotplate for 65 ºC for 3 minutes and increasing this to 95 ºC for 6 minutes. The pre-baked wafer was then exposed to 152 mJ/cm2 of energy from a mask aligner through a mask defining the control valves. The exposed wafer was then baked on a hotplate for 65 ºC for 1 minute and then 95 ºC for 5 minutes. Following the bake, the wafer was submerged in SU-8 developer for 5 minutes, rinsed with isopropanol and hard baked at 120 ºC for 1 hour on a hotplate.

Heaters and temperature sensors were created on piranha cleaned glass microscope slide substrates by depositing first 20 nm of chrome and then 100 nm of gold using a thermal evaporator. The heaters and temperature sensors were patterned into these thin films through photolithographic techniques. Shipley S1813 was spun on the gold surface of the glass slide with a spinner with a spinning program defined as 300 rpm for 15 seconds, and 3000 rpm for 45 seconds with a 400 rpm/second ramp rate. The glass slides were heated on a hotplate at 120 ºC for 2 minutes and then exposed to 95 mJ/cm^2 of energy with a mask aligner using a custom designed mask with defined heaters and temperature sensors. The exposed glass slides were immersed in AZ 300 MIF developer for 15 seconds and rinsed with water. Occasionally the development process was incomplete on the edges of the slides due to the beading effect caused during spinning. In these cases an isopropanol soaked cleanroom wipe (Texwipe TX49) was carefully used to remove excess photoresist. The developed slides were then immersed in first gold etchant for 10 seconds and then chrome etchant for 10 seconds. The etched substrate was then rinsed in water, dried with a nitrogen gun, and then placed on a hotplate for one hour at 120 ºC.

The two silicon wafers were used as molds to transfer the desired features into PDMS substrates. 30 mL of 10:1 (base: curing agent by weight) was poured onto the surface of the flow layer silicon wafer,

degassed in a vacuum desiccator for 30 minutes or until no bubbles were visible and heated on a hotplate set to 72 ºC for 30 minutes. Following complete curing the PDMS was peeled off the wafer and the four identical units were cut out of the slab to create individual devices. Inlets and outlets of the individual flow layers were then punched with a 1.2 mm autopsy punch (Harris). Meanwhile, the control layer wafer had 3 mL of PDMS deposited on it and was spun on a spinner for 15 seconds at 300 rpm and then 1000 rpm for 45 seconds with a 300 rpm/second ramp to create a thin film of PDMS on the surface of the wafer. This layer was placed on a hotplate for 20 minutes at 72 ºC. The four flow layer devices with flow channels facing up and the control layer silicon wafer with thin film PDMS were then placed in an oxygen plasma etcher together (Diener Plasma Etch) and exposed to 20 seconds of oxygen plasma at 50% power. Immediately after exposure to oxygen plasma, the four flow layer devices were aligned by hand onto the four control layer regions on the control layer silicon wafer and pressed with modest pressure to completely put the two oxygen plasma exposed surfaces in contact with each other. This wafer was then placed on a hotplate at 80 ºC for 1 hour.

While the control layer was on the hotplate, the glass slides bearing the heaters and temperature sensors had PDMS spun on them (300 rpm for 15 seconds, 1000 rpm for 45 seconds, 300 rpm/second ramp rate), and were baked at 72 ºC for 20 minutes. After the completion of the control layer with bonded flow layer devices baking, the flow layer devices were carefully peeled off the wafer such that the PDMS spun onto the control layer remained bonded to the flow layer devices and peeled off with the flow layer devices. The peeled off devices had inlets punched with a 1 mm autopsy punch. These four devices which consisted of two layers of PDMS (a thick flow layer PDMS block and a thin film control layer) were exposed to oxygen plasma along with the heater and temperature sensor glass slides with thin film PDMS for 20 seconds at 50 % power. Immediately after oxygen plasma exposure, each of the four PDMS devices were aligned to the heaters and temperature sensors of the glass slides and pressed with modest pressure to put the surfaces in contact. These devices were placed on a hotplate at 100 ºC overnight. Finally, molten agarose gel (3% agarose heated to 90 ºC and then cooled to 65 ºC) was injected in the gel inlet of the device and allowed to cure at room temperature to form the electrokinetic transfer channel and mineral oil was injected into pneumatic control channel. A fabricated device is shown in **Figure 2.3**.

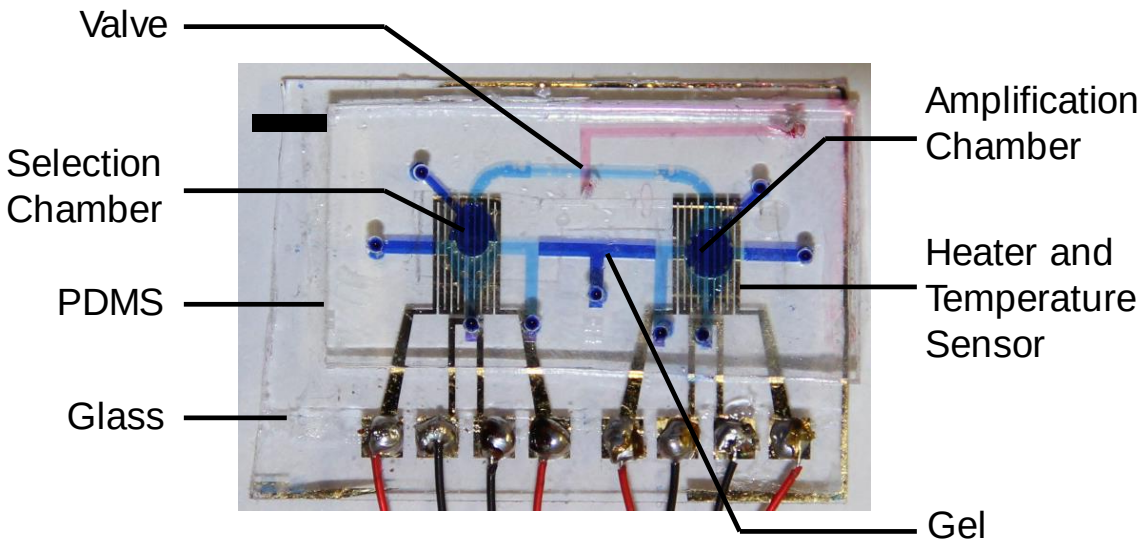

Figure 2.3: Photograph of a fabricated microfulidic device filled with dye solutions for visualizations. Scale bar: 5 mm.

2.2.5. Measurement of Electrokinetic Effects on Chamber Properties

Chamber pH was observed to evaluate the potential deleterious effects of prolonged electric fields on the selection chamber. A fabricated device was filled with TB buffer and an electric field (25 V/cm) was applied for varying lengths of time (0 min – 30 min) with cathode located in the selection chamber and anode located in the amplification chamber. After the prescribed amount of time elapsed the chamber volume was collected and the pH was measured. The process was repeated three times for each time course.

2.2.6. Integrated Aptamer Selection Procedure

The fabricated device was connected to a syringe pump (New Era Pump Systems, Inc., Farmingdale, NY), a multimeter (34420A, Agilent Technologies Inc., CA), a power supply (E3631, Agilent Technologies Inc., CA) and a nitrogen tank with pressure regulator (Concoa, Virginia Beach, Virginia). The syringe pump was used to introduce buffers, reagents, and beads. The multimeter and power supply measured the resistance of the temperature sensor and supplied power to the heater, respectively, and were connected to a computer which implements a Labview code for closed-loop temperature control of

the device. The pressure regulator was connected to the pneumatic control layer and allowed the oil filled channel to be pressurized thereby closing the valve.

Integrated SELEX occurred on-chip without the use of any offline processes. Protein functionalized microbeads were injected into the selection chamber of the device (20 μL/min) until approximately 40% of the selection chamber volume was occupied by beads. Selection of oligonucleotides was then performed by infusing randomized library (1 μM in D-PBS buffer) into the device (10 μL/min) for 10 minutes, followed by multiple washes with D-PBS buffer (20 μL/min) to remove weakly binding oligonucleotides which were collected in a tube and stored. Collected oligonucleotides were amplified off-chip (16 rounds of PCR) and imaged with gel electrophoresis to verify successful removal of weakly binding oligonucleotides and retention of strongly binding oligonucleotides that bind to targets functionalized on bead surfaces.

Next, primer functionalized magnetic beads were introduced into the amplification chamber of the device and held by an external magnet located beneath the chamber. Tris-boric acid electrolyte buffer (89 mM Tris, 89 mM boric acid, and 100 mM NaCl) was then injected into the device and platinum wires were inserted into the electrode inlets of each chamber to generate an electric field. Meanwhile, strongly bound oligonucleotides remaining in the selection chamber were thermally released (50 °C) using the integrated heater and temperature sensor. The released oligonucleotides were transferred from the selection chamber to the amplification by applying a 25 V/cm electric field for 40 minutes.

Following transfer of the oligonucleotides to the amplification chamber, the electric field was removed. PCR reagents were then introduced into the amplification chamber and bead-based PCR progressed utilizing the heater and temperature sensor located beneath the amplification chamber. A PCR process of 95 °C for 10 seconds, 59 °C for 30 seconds, and 72 °C for 10 seconds was used. After 20 cycles of PCR thermocycling, the protein functionalized microbeads were removed from the selection chamber and replaced with new protein functionalized microbeads. Bead based PCR was confirmed by introducing a fluorescently modified oligonucleotide library (100 pM) into the amplification chamber containing reverse primer functionalized beads and performing 20 cycles of PCR thermal cycling. Bead surfaces were imaged using an epifluorescence microscope (IX 71, Olympus, Center Valley, PA) equipped with a CCD (c8484, Hamamatsu, Boston, MA) before and after PCR, and after thermally induced ssDNA release. Additional information on the detailed procedure is included in the Supplementary Materials.

Following amplification, the valve was then opened and oligonucleotides were released from the bead surfaces by heating to 95 °C. The released oligonucleotides were transported back to the selection chamber through the opened valve via pressure-driven flow (20 uL/min) for further affinity selection with the replenished microbeads. This closed-loop process was repeated for a total of four affinity selections and three 20-cycle PCR amplifications.

2.2.7. Aptamer Characterization Procedure

The enriched aptamer pool collected following completion of SELEX was investigated for its affinity and specificity using a fluorescence binding assay [1]. Six different concentrations (100 nM, 50 nM, 25 nM, 12.5 nM, 6.25 nM and 3.125 nM) of fluorescently tagged oligonucleotides were incubated with IgE-functionalized beads in triplicate 100 µL volumes. After incubating the oligonucleotides with the beads for 30 minutes, the beads were washed and the bound oligonucleotides were thermally eluted (95 °C). The eluted oligonucleotdies were collected and their relative amounts were determined with a Wallac EnVision Multilabel Reader fluorescent spectrometer. The relative amounts were analyzed with a hyperbola saturation binding curve fitting (1:1 binding) using GraphPad Prism (GraphPad Software Inc., CA) to determine the binding affinity of the oligonucleotide pool towards the target molecule. The specificity of the aptamer candidate pool towards IgE was investigated by repeating the binding study with bare beads and beads that were functionalized with IgA.

2.3. Results and Discussion

We first present results from the characterization of the individual components of the microfluidic device, including pH effects, affinity selection, PCR amplification, and loop closure. We then describe results from the fully integrated SELEX process as well as the characterization of the resulting aptamer candidates. The protein immunoglobulin E (IgE) was used as a representative molecule throughout the experiments.

2.3.1. Electrokinetic Effects on Chamber pH

To demonstrate the benefits of the hybrid approach's ability to avoid the potentially deleterious effects of using each method alone we characterized the electrokinetic transfer process. The selection chamber pH was evaluated over various time courses (**Figure 2.4**) with electrodes oriented to allow migration from the amplification chamber to the selection chamber. A significant pH drop from 8.3 to 7.25 was observed in the selection chamber after the application of an electric field for 30 minutes, which can

be attributed to the generation hydroxide (OH-) and hydrogen (H+) ions at the cathode and anode, respectively[142, 143]. Thus, the electrolysis of buffer during electrokinetic transport of DNA can induce changes in the pH levels microchambers, which can potentially compromise the integrity of the target and disrupt the electrostatic interactions between the aptamer and oligonucleotides[142, 143]. While electrokinetic transport can significantly impact affinity selection, the hybridization interactions between complimentary oligonucleotides is more robust and for pH 5–9 the renaturation rate is practically independent of pH[144]. Thus, while electrophoresis of oligonucleotides from the amplification chamber to the selection chamber may not be desirable, electrokinetic oligonucleotide transport from the selection chamber to the amplification chamber is appropriate. These observations are consistent with the rationale for our hybrid oligonucleotide transport approach.

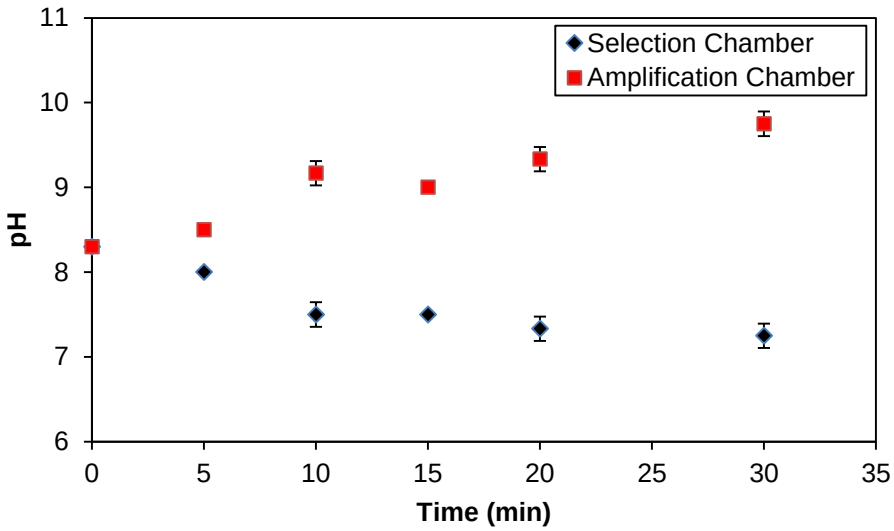

Figure 2.4: Electrokinetic effects on chamber pH. Electric field was applied for different time lengths (0 to 30 min.) and the chamber pH was measured. Error bars represent standard deviations from triplicate measurements.

2.3.2. Characterization of Affinity Selection

Eluates from affinity selection were collected and evaluated using gel electrophoresis (**Figure 2.5**). A band in the electropherogram indicates the presence of oligonucleotides; thus, the strong band in the first wash (W_1) demonstrates that not all oligonucleotides bound to the target molecule and some were flushed

out of the device during the washing stage. The decrease in band intensity from wash 1 to wash 20 shows that as washing progressed fewer oligonucleotides were eluted from the target, while the strong band intensity in the elution lane (E) demonstrates that oligonucleotides strongly bound to the bead surfaces were eluted when heating the chamber to 50° C. Therefore, the selection process partitioned non-binding oligonucleotides from binding oligonucleotides which could then be eluted by increasing the temperature. The thermally eluted oligonucleotides can be electrokinetically transferred and used for further rounds of selection to generate an aptamer pool with high affinity towards its target molecule.

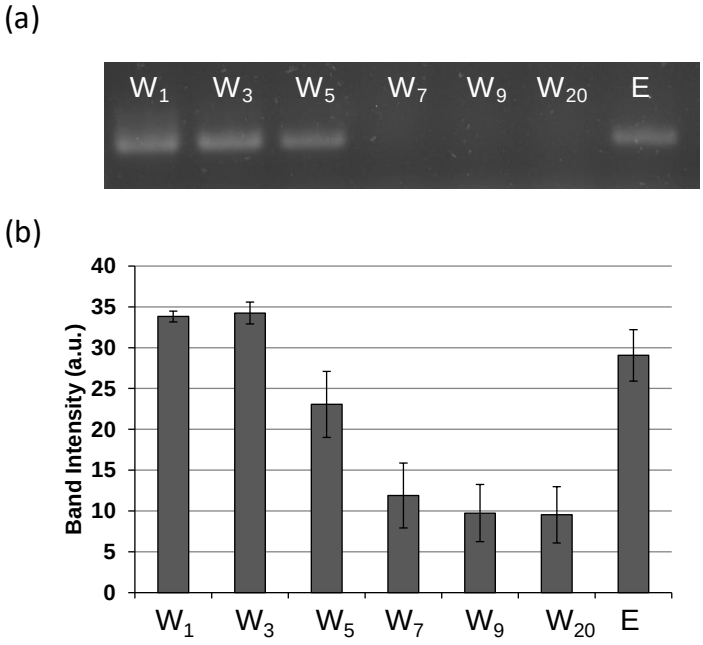

Figure 2.5: (a) Gel electropherogram of amplified eluents obtained during selection process; (b) bar graph depicting intensities of lanes W_1-E: washes 1, 3, 5, 7, 9, 20, and elution. Error bars represent standard deviations from triplicate measurements.

2.3.3. Characterization of Bead-Based PCR Amplification and Loop Closure

To characterize the bead-based PCR protocol, randomized library strands were amplified on-chip using a fluorescently tagged forward primer and monitored with fluorescent microscopy (**Figure 2.6**). During the amplification process, dsDNA is generated consisting of fluorescently labeled amplified library strands hybridized to their bead-bound complements. Thus, the increase in fluorescent intensity of beads following

20 cycles of PCR indicates that template oligonucleotides were successfully amplified on the bead surfaces within the device. The subsequent decrease in fluorescent intensity of the bead surfaces upon heating to 95 °C demonstrates that the fluorescently modified strands dehybridized from the complementary biotynalated strand bound to the bead surface. Affinity selected oligonucleotides can be transferred via electrokinetics to bead-based PCR to allow closed-loop aptamer enrichment. Eluates collected during the closed loop process showed successful coupling of affinity selection to bead-based amplification.

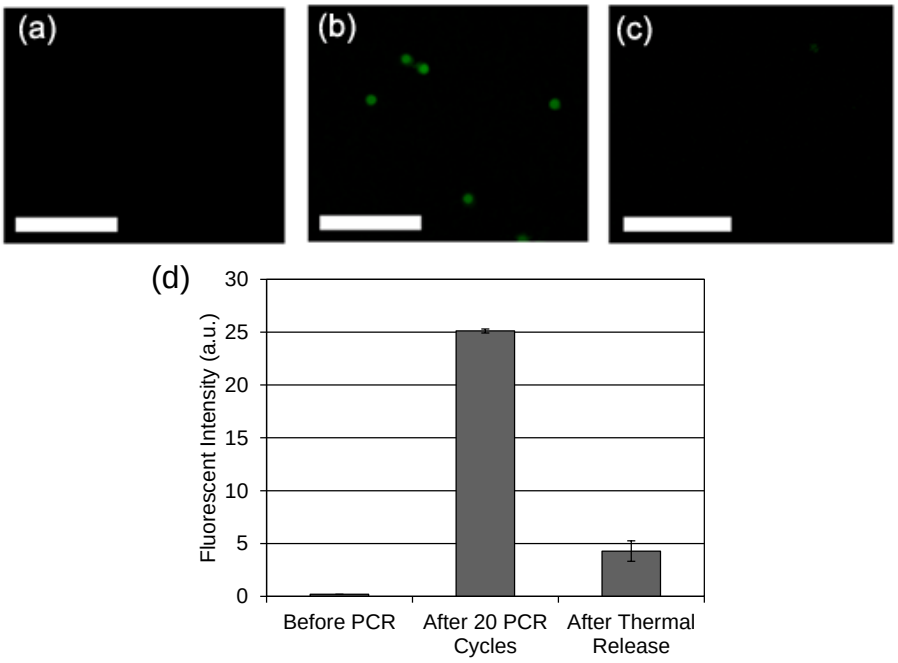

Figure 2.6: Fluorescent images of beads (a) before, (b) after 20 cycles of PCR, and (c) after 95 C thermally induced oligonucleotide elution. (d) Bar graph depicting the fluorescent intensities. Error bars represent standard deviations from triplicate measurements. Scale bar: 200 µm.

2.3.4. Integrated Multi-Round SELEX for Isolation of Aptamers

Having confirmed the approach's potential for closed-loop affinity selection and amplification, a microchip was used to demonstrate multiround hybrid SELEX where four rounds of affinity selection and three rounds of PCR amplification were performed on-chip (**Figure 2.7**). Eluates were collected during each round of affinity selection, amplified by PCR and analyzed using conventional gel electrophoresis. Since the brightness of bands in a gel image represents the amount of oligonucleotides in the eluent loaded in

the lane, comparison of the band intensities allowed investigation of the SELEX process. In the first round, some oligonucleotides were in the washing waste after the completion of the washing process as indicated by the presence of a band in lane S_1W_9. However, the increase in band intensity from S_1W_9 (selection 1, wash 9) to S_2W_1 (selection 2, wash 1) suggests that oligonucleotides were released from the bead surfaces, electrokinetically transferred and amplified by PCR. The lack of a band in S_2W_9 (selection 2, wash 9) shows that weakly bound oligonucleotides were removed from the washing process. The increase in band intensity in from S_2W_9 to S_3W_1 (selection 3, wash 1) and S_3W_9 (section 3, wash 9) to S_4W_1 (selection 4, wash 1) suggests that, again, oligonucleotides were thermally released, electrokinetically transferred to the amplification chamber, amplified by PCR, and transferred back to the selection chamber via pressure driven flow. The presence of oligonucleotides in the elution lane (E) and the lack of detectable oligonucleotides in S_4W_9 (selection 4, wash 9) suggests oligonucleotides were strongly bound to the target after four rounds of selection and amplification and were successfully released from the bead surfaces.

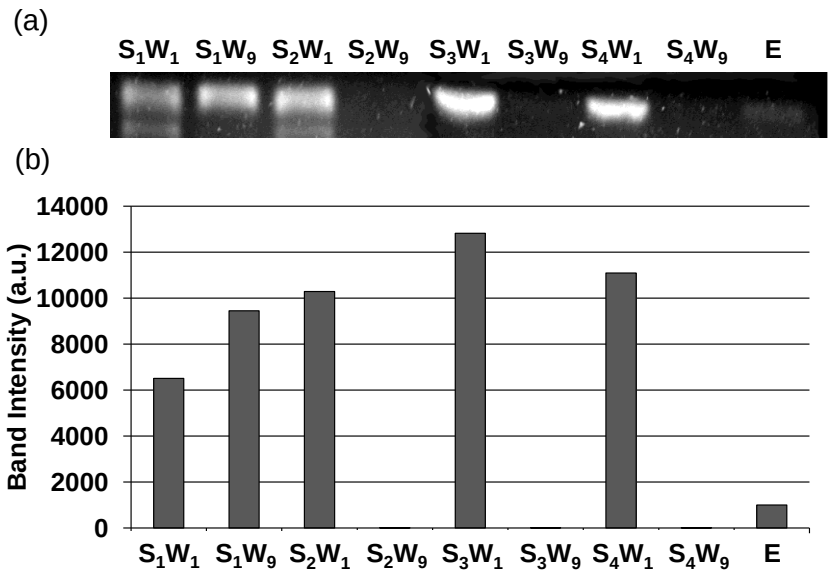

Figure 2.7: (A) Gel electropherogram of amplified eluents obtained during closed loop selection and amplification. (B) Bar graph depicting intensities, representing the amount ssDNA in the eluent, of lanes S_1W_1- S_4W_9: Lane S_1W_1: selection 1, wash 1; Lane S_1W_9: selection 1, wash 9; Lane S_2W_1: selection 2, wash 1; Lane S_2W_9: selection 2, wash 9; Lane S_3W_1: selection 3, wash 1; Lane S_3W_9: selection 3, wash 9; Lane S_4W_1: selection 4, wash 1; Lane S_4W_9: selection 4, wash 9; Lane E: thermally eluted ssDNA.

2.3.5. Binding Affinity and Specificity of Aptamers

The resulting aptamer candidate pool was analyzed for its affinity and specificity towards its intended target molecule. When the enriched pool was incubated with IgE-immobilized beads, washed, and bound oligonucleotides were thermally eluted and measured, the fluorescent intensity rapidly increased until reaching an asymptote (**Figure 2.8**). This indicated that the affinity of the enriched oligonucleotide pool considerably improved after the microfluidic SELEX process. Because this measurement relied on many manual transfers the error increases with higher concentrations of binding aptamer candidates. The data were well represented by a Langmuir monovalent binding model, with an equilibrium dissociation constant (K_D) of approximately 12 nM (obtained via nonlinear regression) as is consistent with that of existing IgE aptamers[75, 140]. In contrast, when the enriched pool was incubated with IgA functionalized beads or bare beads, washed, and bound oligonucleotides were eluted and measured, the fluorescently increased very slowly with the oligonucleotide concentration. This demonstrates the aptamer candidate pool binds much more strongly to the IgE functionalized beads than the bare beads, indicating the aptamer is indeed specifically binding to the protein target.

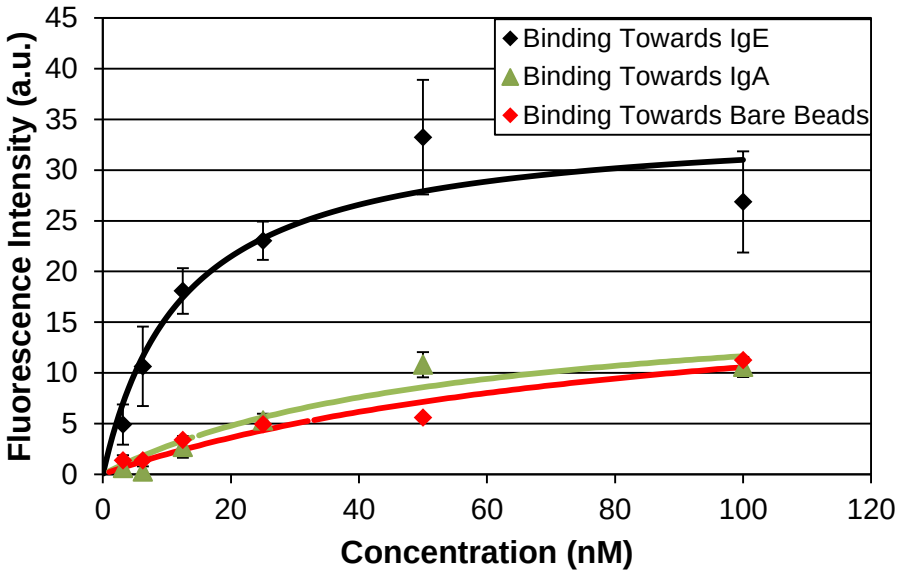

Figure 2.8: Fluorescence based binding affinity measurements of enriched pool towards IgE functionalized, IgA functionalized and bare microbeads. Error bars represent standard deviations from triplicate measurements.

2.4. Conclusion

A microfluidic approach to integrated isolation of aptamers against biological targets has been described. The approach employs a bead-based protocol for affinity selection and amplification of oligonucleotides, which are transported within the protocol via combined electrokinetic transport and pressure-driven flow. Specifically, oligonucleotides are affinity selected against target-functionalized beads and binding strands are transferred under an electric field for bead-based PCR amplification. The amplified product is then transferred back for further affinity selection through pressure-driven flow without relying on off-chip processes. This hybrid approach simplifies the microfluidic device design and operation by reduced pressure-driven flow control requirements, and avoids potentially deleterious effects of the exposure of targets to electric fields prior to and during affinity selection. The approach thus allows the entire iterative SELEX process to be integrated on a single chip without the requirement for any offline procedures, thereby enabling rapid isolation of aptamers.

The integrated hybrid microfluidic SELEX approach was demonstrated by isolating aptamers with high affinity towards the protein immungolubulin E (IgE). Binding oligonucleotides are affinity selected against IgE-functionalized beads, electrokinetically transferred to an amplification chamber, hybridized to microbeads, amplified by PCR, and transferred back to the selection chamber by pressure-driven flow for a new round of affinity selection. The SELEX process was completed in four rounds within a total runtime of approximately 10 hours. The resulting aptamer candidates displayed strong target-binding affinity, with an equilibrium dissociation constant of 12 nM. These results demonstrate the utility of the approach to rapidly isolate aptamers with high affinity to biological targets.

Chapter 3: Integrated Microfluidic SELEX using Free Solution Electrokinetics

3.1. Introduction

Aptamers are single-stranded oligonucleotides, including single-stranded deoxyribonucleic acid (DNA), ribonucleic acid (RNA) and peptide molecules, which can be used for specific molecular recognition towards a broad spectrum of targets including small molecules [70], peptides [71], amino acids [72, 73], proteins [74, 75], cells [76, 77], viruses [78, 79], and bacteria [82]. In many applications aptamers can be used as substitutes to antibodies but with the additional unique advantages of reversible binding, long shelf life, low batch-to-batch variability [124], low immunogenicity [123], long-term stability, ease of coupling to other functional molecular groups [121, 122], and ability to be discovered through an in vitro process [86, 125]. Thus, aptamers are being employed as biosensors, drug delivery devices, and bio-imaging probes in many applications within basic biological sciences [126], drug discovery [127], and clinical diagnostics and therapeutics [125, 128].

The *in vitro* process used to discover aptamers with high affinity for a particular target is known as systematic evolution of ligands by exponential enrichment (SELEX). During the SELEX process an aptamer is found from an initial library of randomized combinatorial oligonucleotides with approximately $10^{12} – 10^{15}$ unique members through iterative rounds of affinity selection and amplification [86, 87, 91]. Affinity selection involves incubating the library with a target of interest and then separating library members that bind to the target from those that do not bind to the target. The target-binding oligonucleotides are then amplified through the polymerase chain reaction (PCR) during the amplification stage and converted back to single-stranded oligonucleotides. These amplified single-stranded oligonucleotides are then incubated with the target as the affinity selection of a new round SELEX begins. Therefore, in every subsequent round of selection the oligonucleotides must compete for binding from the oligonucleotides that bound in the previous round. These rounds of affinity selection and amplification are repeated until a pool of oligonucleotides is isolated with high affinity and specificity towards the target. While effective, this process conventionally involves extensive manual handling of reagents, and is time consuming, typically requiring a month or more to complete a single SELEX run [129].

Microfluidic technology has been recently applied to the SELEX field to rapidly isolate aptamers at low cost in a highly integrated and automated fashion, and additionally with reduced reagent consumption

and in fewer rounds of iteration. Microfluidic affinity selection has been performed, in conjunction with off-chip amplification, against targets retained using silica capillary walls [117], microbeads [106-108, 119, 131, 132, 140, 145] or sol-gels [113-115], or against cells in solution [133, 134], to increase selection stringency [106-108, 131-134], create more favorable biomolecular environments [113-115], or allow simultaneous positive and negative selections [110]. Moreover, microchips have been developed in an attempt to integrate the overall SELEX process using pneumatically based flow control for isolation of aptamers against viruses [135], cells [131, 136, 137] and proteins [119, 138-140, 145]. While capable of isolating aptamers these microfluidic devices have relied on highly complex fabrication techniques not available to most researchers, extensive flow control components (integrated pumps, valves and mixers which all require additional off-chip equipment), sophisticated operating equipment, complicated designs, and integration of unstable gels.

This chapter presents a simplified microfluidic approach using free solution electrokinetic flow control to fully integrate the SELEX process on a single microchip. In this approach, electrophoretic transport of oligonucleotides occurs in free solution between selection and amplification chambers through a microchannel that is highly resistant to bulk flow and diffusion due to a relatively large length and small cross-sectional area. This high resistance prevents cross contamination between the chambers without significantly impeding electrophoretic oligonucleotide transport. The design hence obviates the use of complex flow handling or gel preparation, thereby allowing simple and efficient transfer of target-binding oligonucleotides as well as a high level of device integration. Also, the device is fabricated without the need for the multi-layer soft lithography techniques previously reported devices have required. These advantages are combined with a bead-based protocol to achieve on-chip coupling of affinity selection and amplification of target-binding oligonucleotides without requiring offline processes. The device is further simplified, while the reliability is improved, through optimized design of the microfluidic geometry and use of a magnetic microbead retention scheme that make the device considerably less prone to potentially catastrophic trapped bubbles [146]. The practical utility of the device is demonstrated with experimental results on isolation of DNA aptamers against human immunoglobulin A (IgA) as a representative target.

3.2. Experimental

3.2.1. Aptamer Selection Principle

The approach involves iterative rounds of microbead-based affinity selection and PCR amplification coupled by electrokinetic fluidic handling (**Figure 3.1**) carried out on a microchip. Aptamers are enriched from an initial single-stranded DNA (ssDNA) library comprised of oligonucleotides with a randomized region flanked by a forward primer region on the 5' end, and a region defined to be complementary to the reverse primer on the 3' end. This initial library is incubated with microbeads functionalized with biomolecular target (selection beads) during affinity selection. Through multiple buffer washes non-binding and weakly binding oligonucleotides are removed and discarded while strongly bound oligonucleotides remain attached to the target-functionalized microbeads. These strong binding oligonucleotides are thermally eluted from the target-functionalized microbeads and electrokinetically transferred to a second set of microbeads (amplification beads) which have been modified with reverse primers thus causing the library to hybridize to the reverse primers tethered to the amplification bead surfaces. PCR reagents are then introduced and PCR thermal cycling commences resulting in amplified copies of the target-binding oligonucleotides hybridized to the bead surfaces. The amplified product is thermally denatured from the bead bound complement and transferred back to replenished selection beads for further rounds of SELEX.

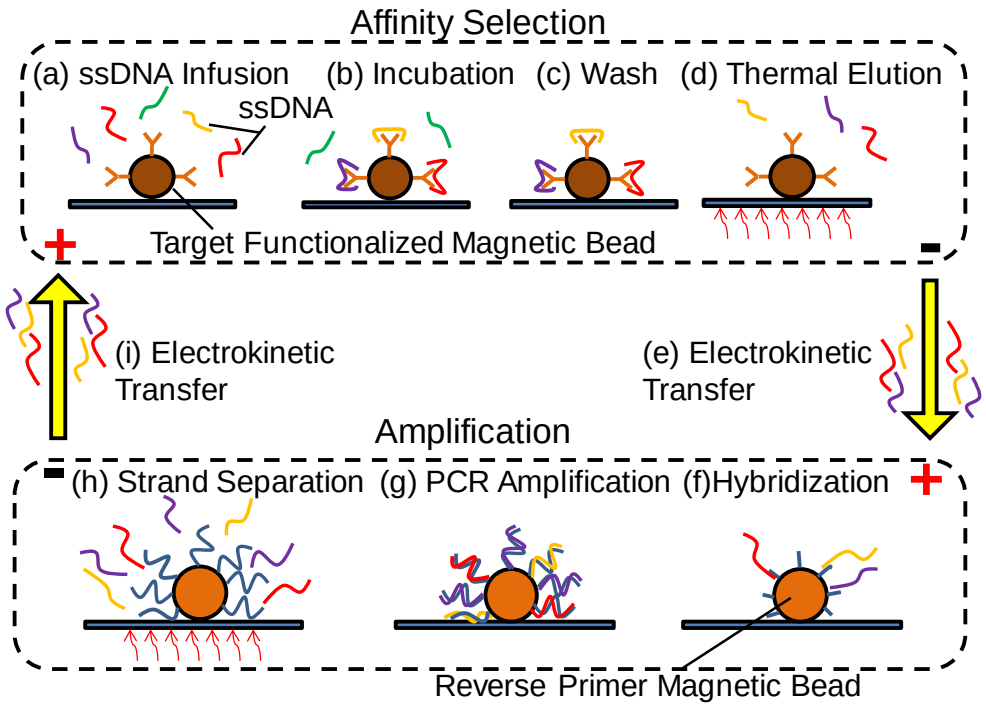

Figure 3.1: Principle of microfluidic aptamer development: (a) ssDNA with random sequence is introduced to the target. (b) ssDNA is allowed to bind to the target. (c) Weak binding and non-binding oligonucleotides are removed by multiple buffer washes. (d) Strong binders are thermally eluted and (e) transferred to the amplification chamber with electrokinetics. (f) Transferred oligonucleotides hybridize to surface-immobilized reverse primers and (g) amplified through PCR. (h) The amplified single strands are thermally released and (i) electrokinetically transported back to the selection chamber for further affinity selection.

3.2.2. Microfluidic Device Design and Operation

The electrokinetic microfluidic approach for aptamer enrichment is realized in an integrated microchip (**Figure 3.2**). The device consists of two (selection and amplification) microchambers of identical geometry (~2.8-μL) connected by a microchannel. The microchambers are hexagonal in shape with dimensions of 2 mm wide, 7 mm long and 250 um high. The hexagonal chamber shape has been demonstrated to be considerably less prone to trapping bubbles which can cause sample purging at increased temperatures, act as thermal insulators, create uneven temperature distributions, and reduce the effective volume of the chamber [146]. Each microchamber features a resistive heater and temperature sensor located beneath the chamber, an inlet, an outlet, and an electrode port. Connecting the two

chambers is a single serpentine shaped microchannel (14.75 mm long, 50 μm wide, 20 μm tall) which prevents diffusion between the microchambers but allows oligonucleotide migration under an electric field. Similarly the electrode port (2 mm diameter) is connected to its microchamber through a long, narrow microchannel (4.5 mm long, 50 μm wide, 20 μm tall). The electrode ports allow the insertion of platinum wire electrodes.

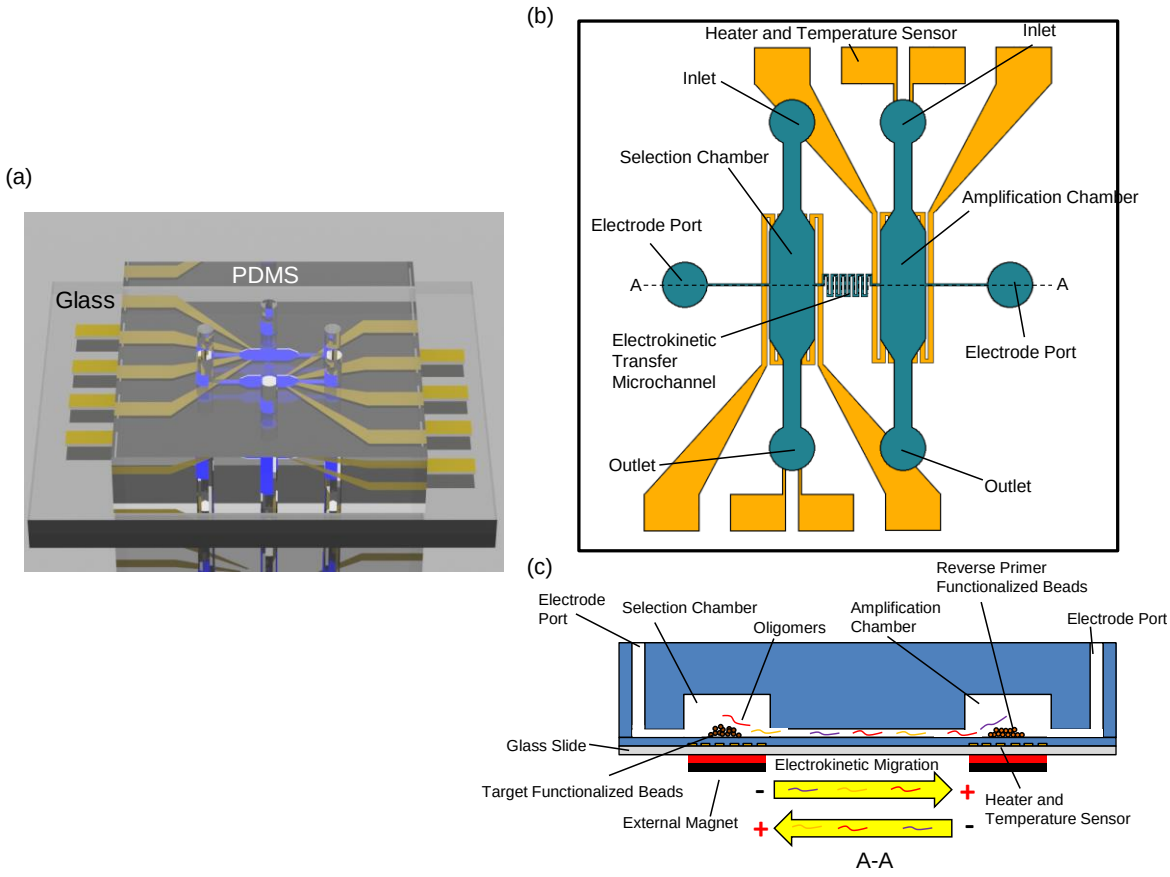

Figure 3.2: (a) Three-dimensional rendering of the microfluidic device. (b) Top view schematic of the microfluidic device. (c) Cross-sectional view of microfluidic device design along line A-A.

Repetitive, closed-loop cycles of affinity selection and PCR amplification can be achieved in the microdevice without the need for offline instruments. First target-functionalized beads are introduced into the selection chamber and retained via an external magnet. Affinity selection then occurs by flowing the initial randomized library across the beads from the inlet to the outlet, allowing oligonucleotides with affinity

towards the target to bind to the target-functionalized beads. The target-functionalized beads are washed with flowing buffer to remove weakly binding oligonucleotides. The remaining strongly bound oligonucleotides are then eluted by increasing the chamber temperature with the integrated heater located beneath the chamber. Meanwhile, an electric field is applied from the selection chamber electrode port to the amplification chamber port, inducing migration of the eluted oligonucleotides to the amplification chamber wherein amplification beads are located to capture and immobilize the oligonucleotides in the amplification chamber. PCR reagents are then introduced to the amplification chamber using the amplification chamber inlet and subsequently PCR thermal cycling commences using the integrated heater and temperature sensor located beneath the amplification chamber. The amplified product is thermally released using the integrated heater, an electric field of reversed polarity is applied, and the oligonucleotides are electrokinetically transferred back to the selection chamber where they interact with replenished target-functionalized beads as a new round of affinity selection begins. Note, the resulting amplified product of the PCR is double stranded oligonucleotides consisting of the amplified enriched library and the amplified complement of the enriched library. Partitioning of the desired amplified enriched strands from their complementary strands is achieved directly with the amplification beads. The complementary strand is an extended reverse primer which is coupled to the beads through temperature invariant streptavidin-biotin chemistry while the desired strand is attached to the beads through complementary base pairing to the complementary strand. Thus the desired strand can be released from the bead surfaces (while its complement remains attached to the beads), and subsequently transferred to the selection chamber, with elevated temperatures (~95 °C).

3.2.3. Materials

Human Imunnoglobulin A (IgA1) was purchased from Cell Sciences (Newburyport, MA), and Pierce NHS-activated microbeads were purchased from Thermo Fisher Scientific (Waltham, MA). Ethanolamine, $MgCl_2$, tris, boric acid, and molecular biology grade water were purchased from Sigma-Aldrich (St. Louis, MO). Deoxyribonucleotide triphosphates (dNTPs) and GoTaq Flexi DNA polymerase were obtained from Promega Corp. (Madison, WI). Randomized oligonucleotide library (5’ – GAA CTT CGC ATC TCA CGG TGG – 36N – GGA TCC GAT TCC ATC CTG CTC CTC– 3’) and primers (Forward Primer: 5' – FAM – GAA CTT CGC ATC TCA CGG TGG -3', and Reverse Primer: 5' – dual biotin – GAG GAG CAG GAT GGA ATC

GG – 3') were synthesized and purified by Integrated DNA Technologies (Coralville, IA). Dulbecco's phosphate-buffered saline (D-PBS), and streptavidin coupled magnetic beads (Dynabeads® M-270 Streptavidin) were purchased from Invitrogen (Carlsbad, CA). SU-8 (2000, 2025, and 2075 series) negative photoresist was purchased from Microchem Corp. (Westborough, MA). Polydimethylsiloxane (PDMS) was obtained from Robert McKeown Company (Somerville, NJ) and silicon wafers were purchased from Silicon Quest International, Inc. (San Jose, CA).

Magnetic microbeads (Pirece NHS-activated beads) functionalized with a protein were used for selection and magnetic microbeads (Dynabeads® M-270 steptavidin) functionalized with reverse primers were used for amplification. The beads for selection were functionalized with a protein (IgA1) through covalent coupling between the NHS groups of the microbeads and the amine groups of the protein. Prior to an experiment, the protein was incubated with IgA1 under gentle rotation for 1 hour at room temperature, and washed with D-PBS buffer. Unreacted NHS groups were passivated by incubating the functionalized beads in ethanolamine. The functionalized beads were then suspended in D-PBS buffer. Similarly, streptavidin magnetic beads were functionalized by incubation with dual biotin conjugated reverse primers through covalent coupling for 30 minutes, washed with D-PBS buffer and suspended in D-PBS buffer.

3.2.4. Fabrication

The microfluidic device was realized in polydimethylsiloxane using soft-lithography techniques (**Figure 3.3**). First, a layer of SU-8 was spun, and developed on a silicon wafer to define the narrow channels for oligonucleotide transfer. Then a second, thicker layer of SU-8 was spun, and developed to create the selection and amplification chambers to complete the fabrication of the flow-layer. On a separate glass-slide substrate chrome (10 nm) and gold (100 nm) were thermally evaporated and then patterned and etched to create a glass substrate bearing gold resistive heaters and temperature sensors. A thin layer of PDMS was spun on this glass slide and cured to passivate and allow reuse of the heater and temperature sensors. PDMS was poured on the wafer containing the flow layer features, degassed in a vacuum chamber, and cured at 72 °C for 30 minutes. The hardened PDMS was peeled off, cut, and had inlet and outlet holes punched with an autopsy punch. This flow layer was exposed to oxygen plasma along with the glass slide bearing the heater and temperature sensor and the two pieces were bonded and baked at 80 °C overnight.

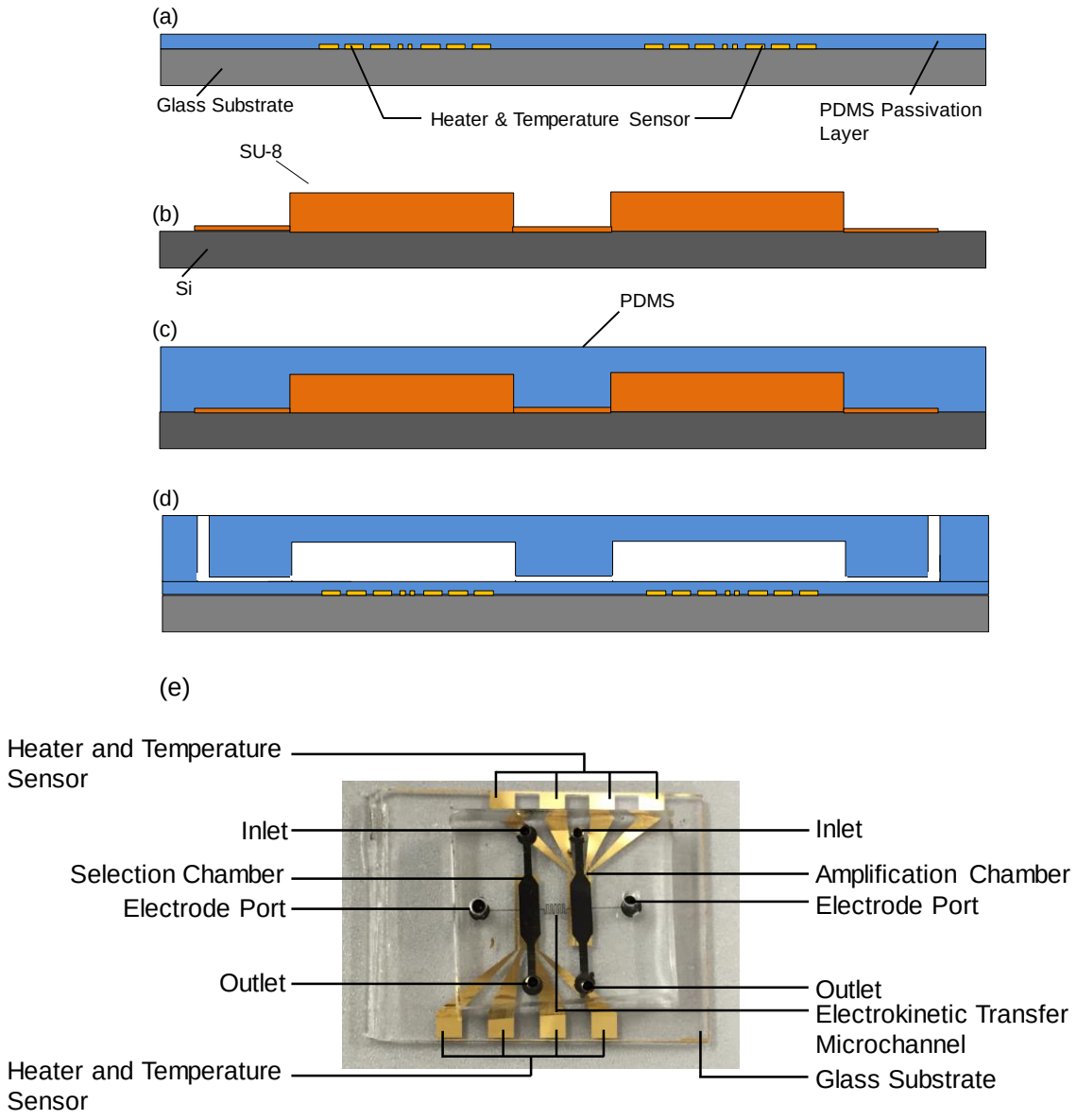

Figure 3.3: (a) Deposition, patterning and passivation of gold temperature sensors and heaters. (b) Fabrication of the SU-8 mold defining microfluidic chambers and channels. (c) Casting of the PDMS sheet of fluidic chambers and channels. (d) Punching of inlets and outlets and bonding of the PDMS sheet to temperature control substrate. (e) A fabricated microchip.

3.2.5. Detailed Aptamer Selection Procedure

A schematic of the device setup can be seen in **Figure 3.4**. The device was interfaced with a syringe pump (New Era Pump Systems, Inc., Farmingdale, NY), a power supply (E3631, Agilent

Technologies Inc., CA), and a multimeter (34420A, Agilent Technologies Inc., CA). During electrokinetic fluid handling platinum wires were inserted into the electrode ports and connected to the power supply. The multimeter was used to measure the resistance of the temperature sensor and ultimately interfaced with a computer which converted the resistance to a temperature using a calibration curve. The power supply was also interfaced to the computer which implemented a PID Labview (National Instruments, Austin, TX) algorithm for closed-loop temperature control in the chambers. The syringe pump was used for the buffer washes during affinity selection.

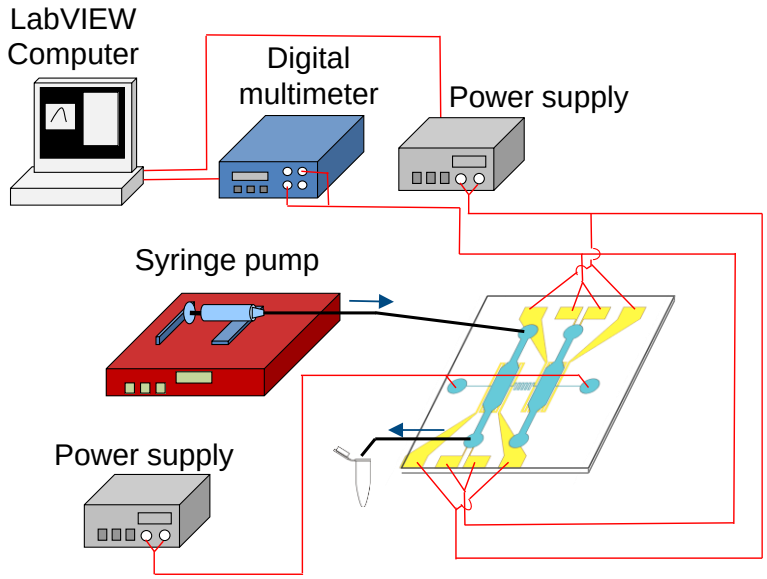

Figure 3.4: Experimental setup.

The device was first filled with tris-boric acid electrolyte buffer (TB buffer, 89 mM Tris, 89 mM boric acid, and 100 mM NaCl) and then target-functionalized magnetic beads (2 µL, 10 mg/mL) were introduced into the device using a pipette and an external magnet. A droplet merging technique was used where the liquid in the pipette tip was allowed to contact the fluid in the chip. Once this fluidic conduit was established an external magnet was used to pull the magnetic beads from the pipette tip into the chip. Library (1 µM, 100 µL in TB buffer) was then introduced into the selection chamber from the inlet (5 µL/min) and allowed to flow across the target-functionalized beads and ultimately to the outlet. An external magnet was held beneath the chamber to retain the beads in the selection chamber. The connecting microchannels provided sufficient fluidic resistance such that there was no observable flow to the amplification chamber or electrode

port. Following a 30-minute incubation with the library, the chamber was washed with eight 5 minute long buffer washes at a flow rate of 20 µL/min. The wash buffer exiting the device during this washing process, containing weak binding oligonucleotides, was collected, amplified off-chip, and imaged with a gel electropherogram to verify the removal of weakly binding oligonucleotides from the device.

Amplification beads (2 µL, 10 mg/mL) were then introduced into the amplification chamber using a pipette and external magnet. The Labview PID algorithm was implemented to increase the selection chamber temperature to 55 °C for 40 minutes thus inducing conformational changes in the oligonucleotides which disrupt the binding of the oligonucleotides to the target. Meanwhile a 40 V/cm electric field was applied for 40 minutes causing the thermally eluted oligonucleotides to migrate from the selection chamber to the amplification chamber wherein they bind to the amplification beads. The external magnet was kept beneath the chambers to retain the selection and amplification beads in their respective chambers. Following the migration process, PCR reagents were introduced into the amplification chamber using a pipette. A Labview algorithm was again implemented to thermally cycle the amplification chamber for 20 cycles of PCR (cycles of 5s at 95 °C, 15s at 55 °C, and 10s at 72 °C). For characterization purposes, bead surfaces were imaged using an epifluorescence microscope (IX 71, Olympus, Center Valley, PA) equipped with a CCD (c8484, Hamamatsu, Boston, MA) before and after PCR, and after thermally induced ssDNA release.

At the conclusion of PCR, the external magnet was removed to allow the selection beads in the amplification chamber to be removed and replaced with fresh selection beads with a pipette. With fresh selection beads in the selection chamber, the amplification chamber was heated to 95 °C inducing dehybridization of the single-stranded oligonucleotide from its complement and the electric field (40 V/cm) was again applied in reverse polarity to transfer the amplified oligonucleotides from the amplification chamber to the selection chamber. Once the oligonucleotides had travelled to the selection chamber, the selection chamber was again washed with eight 5 minute buffer washes at a flow rate of 20 µL/min. Following the wash the chamber was heated to 55 °C using the integrated heater and temperature sensor and the eluted oligonucleotides were collected and analyzed for their affinity towards the target.

3.2.6. Aptamer Characterization Procedure

The enriched aptamer pool collected following completion of SELEX was investigated for its affinity using a fluorescence binding assay [1]. The collected pool was amplified off-chip using a fluorescent forward primer and diluted to a final concentration of 100 nM. The 100 nM fluorescently tagged oligonucleotides were then incubated in triplicate 100 µL volumes with 20 µL (10 mg/mL) of washed target-functionalized beads. After incubation for 30 minutes, the beads were washed three times (100 µL each wash) and the bound oligonucleotides were eluted by heating to 95 °C. The relative amount of eluted oligonucleotides was measured with a Wallac EnVision Multilabel Reader (PerkinElmer, Waltham, MA) fluorescent spectrometer. This was repeated with the library used to initiate the aptamer development process.

3.3. Results and Discussion

The device was first characterized to ensure the device could sufficiently perform the individual sub-processes (affinity selection, elution, electrokinetic transport, and PCR amplification). Then closed-loop affinity selection and amplification were performed on-chip consisting of two rounds of affinity selection and one round of PCR amplification. The device can readily be used for additional cycles of affinity selection and amplification when necessitated by the application.

3.3.1. Heater and Temperature Sensor Characterization

The heater and temperature sensor were characterized by placing a fabricated device in an environmental chamber (Delta Designs 9023, Cohu, Poway, CA) and ramping the temperature from room temperature (~23 °C) to the maximum temperature used for PCR (95 °C) in 10 °C intervals. For every 10 °C interval the resistance and temperature was recorded (**Figure 3.5**). By fitting this highly linear data a temperature coefficient of resistance was obtained using the following expression.

$$\frac{R - R_0}{R_0} = \alpha(T - T_0)$$

In this expression R is the resistance for a given temperature, R_0 is the resistance at room temperature, T is the temperature, T_0 is the room temperature and alpha is the coefficient of resistance. A coefficient of resistance of 1.837 X 10^{-3} $°C^{-1}$ was obtained for the selection chamber temperature sensor and 1.902 X 10^{-3} $°C^{-1}$ for the amplification chamber temperature sensor.

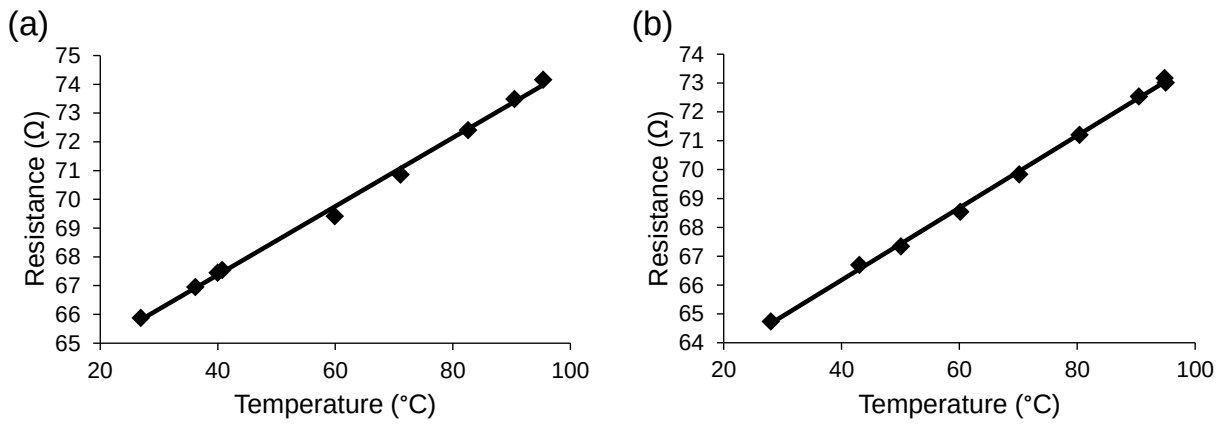

Figure 3.5: Characterization of the microchip temperature sensors. The linear relationship between temperature and resistor resistance for the (a) selection chamber and (b) amplification chamber resistors allows determination of a temperature coefficient of resistance

3.3.2. Affinity Selection

The affinity selection process must be able to provide an environment that allows potential aptamers in the initial starting library to bind to the target functionalized on the magnetic beads. The process must also be able to successfully partition binding oligonucleotides from weakly binding oligonucleotides. To verify successful affinity selection the initial starting library was introduced into the selection chamber which was preloaded with target-functionalized beads. Eight buffer washes were used to remove weakly binding oligonucleotides with effluents collected and analyzed. Finally the chamber temperature was increased to disrupt the binding between the binding oligonucleotides and the target molecules, and the chamber was washed using the same flow rate and volume of buffer that was used for the buffer washing. The effluent from this wash was collected and analyzed. All binding effluents were amplified off-chip by PCR (16 cycles) and imaged using gel electrophoresis (**Figure 3.6**). A decrease in band intensity in the gel electropherogram indicates fewer oligonucleotide molecules present. Thus, the decreasing band intensity from the first wash (W_1) to the final wash (W_8) indicates that in the initial washes many weakly binding oligonucleotides were removed from the selection chamber and as washing progressed few oligonucleotides remained that could be removed by washing alone. When the chamber was heated (55 °C),

represented by the elution (E) lane, a relatively high amount of oligonucleotides could be removed from the selection chamber. This suggests weakly binding oligonucleotides were removed by washing and upon heating the remaining strongly bound oligonucleotides could be eluted and collected or, if SELEX was to continue, transferred for PCR amplification. Therefore, the selection process was successful in portioning non-binding oligonucleotides, which were washed out of the chamber, from binding oligonucleotides, which could be eluted through a modest increase in temperature.

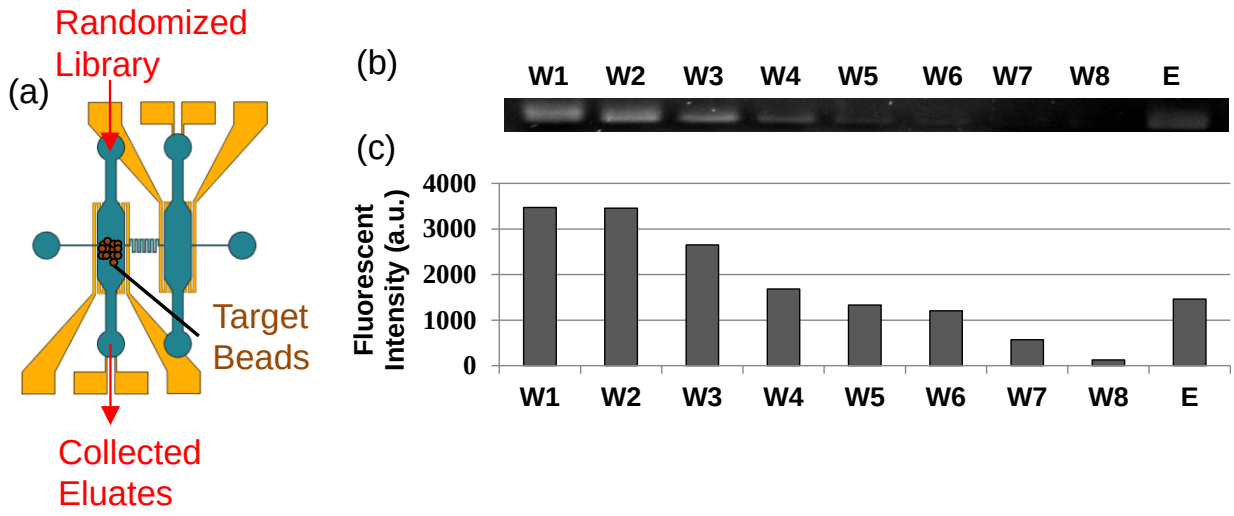

Figure 3.6: (a) Experiment schematic of the selection characterization. (b) Gel electropherogram and (c) measured band intensities of amplified eluents obtained during selection process with bar graph depicting intensities of lanes W_1-E: washes 1, 2, 3, 4, 5, 6, 7, 8, and elution.

3.3.3. Electrokinetic Transfer

Electrokinetic migration of oligomers was characterized by injecting fluorescently modified (fluorescein) oligomers into the selection chamber (100 nM) and applying an electric field (40 V/cm) with platinum wires from the selection chamber to the amplification chamber. While applying the electric field, an epifluorescent microscope (Eclipse 50i, Nikon, Tokyo, Japan) was focused on the amplification chamber and a micrograph of the chamber was acquired in one minute intervals with a charge-coupled device (Orca-

ER, Hamamatsu Photonics, Hamamatsu, Japan). This process was repeated three times with a 40 V/cm electric field and three times without applying an electric field.

The fluorescent signal of the fluorescein-modified library is shown **Figure 3.7**. The error bars indicate the standard deviation of three repeated measurements, representing experimental errors associated with sources such as the imprecision in the volume of nucleotide solution dispensed into the inlet well and time variation of the electroknetic properties of the PDMS surfaces [147]. When an electric field of 40 V/cm was applied, the intensity of fluorescence, representing the amount of oligonucleotides that had been transferred from the selection chamber to the amplification chamber, began increasing after 10 minutes and then saturated within approximately 37 minutes, In the absence of an electric field, the fluorescent intensity of the amplification chamber did not rise above background even for time durations longer than one hour (data not shown). Thus, to transfer oligonucleotides between functional chambers an electric field of 40 V/cm was applied for 40 minutes, which was considered sufficient for transferring oligonucleotides between the chambers.

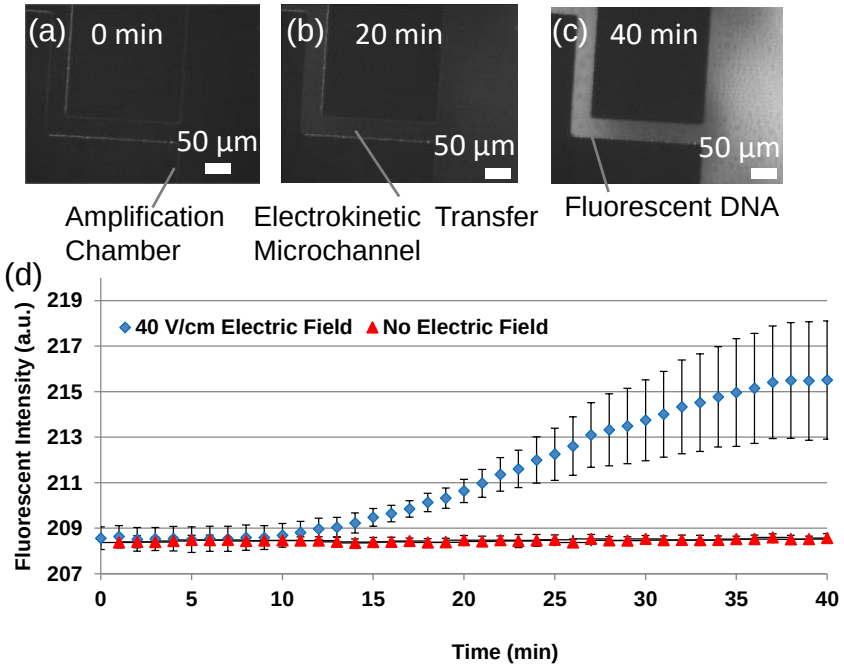

Figure 3.7: Fluorescent ssDNA was introduced to the selection chamber and fluorescent images were taken of the transfer microchannel at the amplification chamber after (a) 0 minutes, (b) 20 minutes, and (c) 40 minutes of applying a 40 V/cm electric field. (d) Time-course fluorescent intensity of selection chamber; error bars represent standard error; scale bars: 50 µm.

Considering a transfer channel 14.75 mm long, the oligonucleotide apparent velocity, v_{app}, was approximately 6.145 µm/s. Using this velocity along with the electric field strength, *E,* an apparent mobility electrokinetic, μ_{app}, of the solution can be defined.

$$\mu_{app} = \frac{v_{app}}{E}$$

From this expression an apparent mobility of 1.536 x 10^{-8} m^2/Vs is obtained which agrees with other PDMS/PDMS fabricated devices [148].

3.3.4. Amplification

On-chip bead-based PCR was verified by injecting fluorescently modified oligonucleotides into the amplification chamber containing reverse-primer beads. PCR reagents, including a fluorescently modified forward primer, were then introduced and 20 cycles of PCR thermal cycling. Following thermal cycling the beads in the chamber were washed to remove non-incorporated fluorescent primers. The fluorescent intensity of the beads was measured before thermal cycling, after thermal cycling, and after thermal elution. As a control the process was repeated without including taq polymerase (**Figure 3.8**). The increase in brightness of the bead surfaces after the PCR thermal cycling suggests that the PCR process successfully amplified the oligomers on the bead surfaces, while the decrease intensity after thermal elution indicates that single-stranded oligonucleotides were thermally released from the bead surfaces. The fluorescent intensity of the beads used in the no-taq experiment did no increase after thermal cycling.

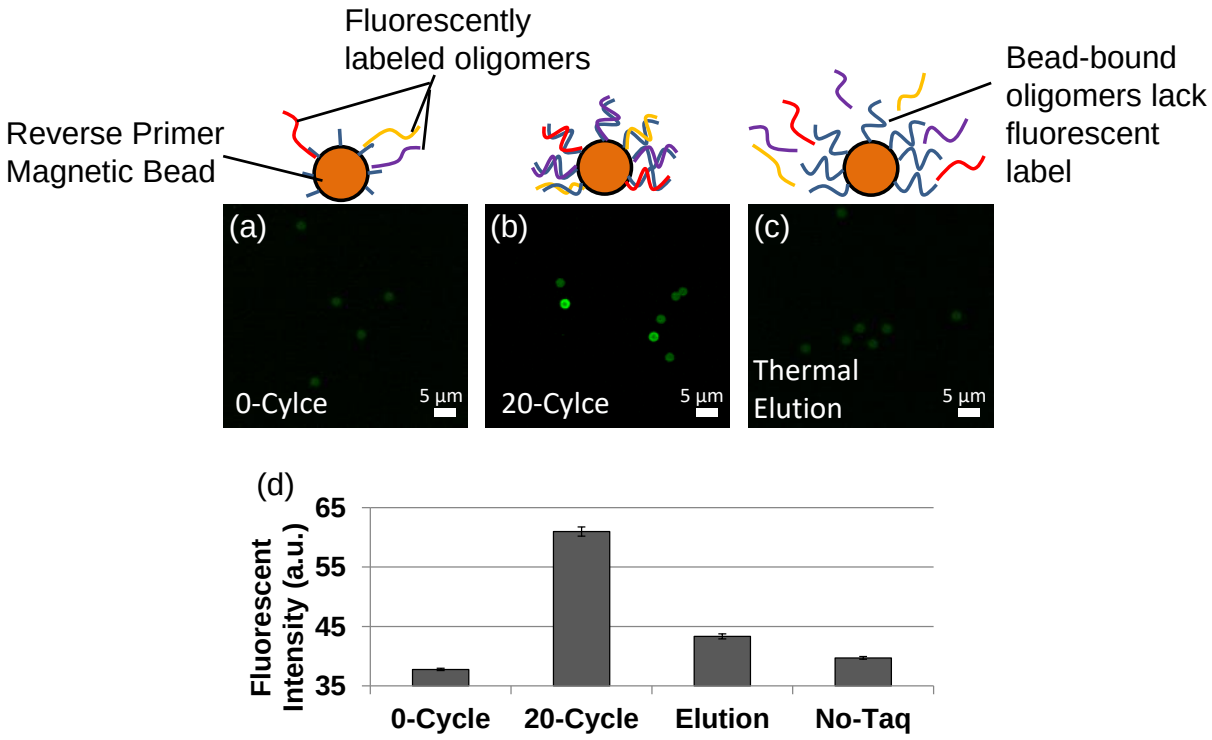

Figure 3.8: Fluorescent images of beads (A) before, (B) after 20 cycles of PCR, and (C) after 95°C thermally induced ssDNA elution. (D) Bar graph depicting fluorescent intensities. Error bars represent standard errors.

3.3.5. Closed-Loop SELEX

The microchip performed microfluidic SELEX, which primarily involved integrated affinity selection and amplification, for isolation of aptamer candidates that bind to protein IgA1. To investigate the progress of the multi-round SELEX experiment, weakly bound ssDNA in each wash in the affinity selection procedure of each round, as well as the thermally eluted, strongly protein-binding oligonucleotides in the final round, were collected from the selection chamber, amplified and analyzed with gel electrophoresis (**Figure 3.9**). In the first wash of the first round (S_1W_1) there were a significant amount of oligonucleotides present but this decreased as the washing process progressed. In the first wash of the second round (S_2W_1) there were many more oligonucleotides present than the last wash from the first round (S_1W_8). This indicates successful transfer of the oligonucleotides to the amplification, PCR amplification and transfer back to the selection chamber for a second round of affinity selection. At the final wash of the second round (S_2W_8) there was not a detectable amount of oligonucleotides present; however, upon thermal elution (S_2E) there were again detectable amounts of oligonucleotides. Thus, the affinity selection process in these rounds effectively removed weakly bound ssDNA as target-binding oligomers became more enriched. Moreover, high fluorescence intensity was observed in the thermal eluate (E) from the final round of SELEX, indicating that a significant amount of enriched protein-binding oligonucleotides (i.e., aptamer candidates) were generated from the SELEX process.

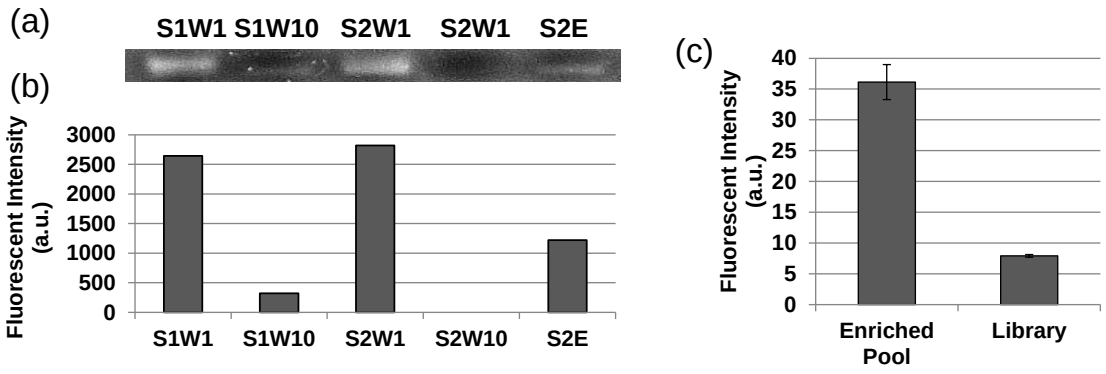

Figure 3.9: (a) Gel electropherogram of amplified eluents obtained during closed-loop selection and amplification. (b) Bar graph depicting intensities of lanes S_1W_1-S_2E: S_1W_1: selection 1, wash 1; S_1W_{10}: selection 1, wash 10; S_2W_1: selection 2, wash 1; S_2W_{10}: selection 2, wash 10; S_2E: oligomers released upon thermal elution. (c) Fluorescent intensity of fluorescently labeled enriched pool and library thermally eluted from target-functionalized beads after incubation and washing. Error bars represent standard error.

The oligonucleotides isolated from the microfluidic SELEX process were tested for their affinity towards IgA1 using a fluorescence binding assay. The background-subtracted average fluorescence intensity of the enriched aptamer candidate pool incubated with IgA was significantly higher than the fluorescence intensity of the library used to initiate the SELEX process. This indicates the enriched pool bound with considerably higher affinity and suggests that the mult-round SELEX process using the microchip was successful. Further enrichment of the candidate pool can be achieved with further rounds of affinity selection and amplification with the microchip.

3.4. Conclusion

We have presented an integrated, microfluidic approach to isolate aptamer against protein targets using a simplified electrokinetic transfer scheme. The approach involves bead-based reactions for electrokinetically coupled affinity selection and PCR amplification. The electrokinetic coupling allows highly

integrated migration of oligonucleotides with reduced flow control equipment and without the need for complicated fabrication methods or gels, while also preventing undesirable diffusion or cross-flow effects. Thus, the approach is capable of integrating the iterative cycles of affinity selection and amplification onto a single chip without requiring offline processes that are commonly used in existing microfluidic aptamer selection devices. The approach was demonstrated by selecting an enriched pool of aptamers with affinity towards IgA. Oligonucleotides were affinity selected from a randomized library, electrokinetically transferred, PCR amplified, and transferred back for further affinity selection. The approach is readily capable of repeating these cycles of selection and amplification to obtain a pool of aptamers with sufficient affinity to a target of interest. The resulting enriched pool showed increased affinity towards the target when compared with the starting library.

Chapter 4: Aptamer Selection with Microfluidic Three-Chamber Approach

4.1. Introduction

In Chapter 3 and Chapter 4, two different microfluidic approaches were presented. One which used a system combining electrophoresis transport and pneumatic valves, and the other removing valves altogether and employing a long channel with high diffusive resistance to separate two functional microchambers while still allowing electrokinetic transport between the two chambers. These approaches were successful in isolating aptamers with affinity and specificity towards model immunoglobulin subtypes (IgA, IgE). However, for the development of aptamers useful in precision medicine applications aptamers with a greater degree of discerning ability are needed, aptamers must be able to specifically recognize an epitope that shares many similarities with other biological molecules. Furthermore, both approaches had limitations which made accomplishing many rounds of SELEX in a single device challenging. The most direct way to increase the affinity and specificity of an aptamer pool is to do more SELEX cycles. As discussed in Chapter 2, the hybrid approach was dependent on an agarose gel which had a tendency to degrade after a few rounds of SELEX limiting the amount of cycles that could be performed on-chip. On the other hand, the electrokinetic approach needed careful control of the dynamic charge conditions in the microfluidic chip. Without careful control of the charge conditions, for a given electric field strength and direction, the flow between the two chambers could be dominated by either electroosmosis or electrophoretics [149]. Depending on which force dominates the flow could go from selection chamber to amplification or the other way around. Furthermore, the electrokinetic approach simplified the device operation with magnetic beads; however, it was found magnetic beads aggregated at the bottom of microchambers creating a flow situation where much of the aptamer library volume passed above the beads without interacting with the target molecules.

Moreover, both the hybrid and electrokinetic approaches were realized in devices with single selection and amplification chambers. While, this simplified the device design, it also limited the ability to incorporate rounds of counter selection. The importance of counter selection is lessoned when developing aptamers for a specific antibody class (e.g. IgE and IgA), but for precision medicine applications where aptamers must be specific for a single population of antibody within an antibody class, the counter selection remains an effective stage to increase an aptamer pool specificity. The previously presented approaches

could only effectively perform a single round of counter selection which was required to be at the end of the SELEX process.

Here we present a third microfluidic approach to accomplish the SELEX process on a microchip. The approach fully integrates selection, counter selection and amplification on a single microchip and is able to accomplish many rounds of SELEX without significant degradation. In this approach pressure-driven and pneumatically controlled valves are used to direct affinity-selected oligonucleotides through the SELEX process. The pneumatically controlled valves are not only capable of controlling flow direction but also able to fully close off functional chambers to reduce cross-contamination. Counter selection is achieved by the addition of a third microchamber which sits between selection and amplification chambers, such that counter selection occurs automatically as oligonucleotides are transferred for PCR amplification without increasing the overall time needed to complete a round of SELEX when compared to the hybrid and electrokinetic approaches. Moreover, the pneumatic microvalves employed in the approach can be used many times without risk of wear allowing many rounds of the SELEX process to be accomplished. These advantages are combined with high capacity agarose bead-based protocols to achieve on-chip coupling of affinity selection, counter selection and amplification of affinity selected oligonucleotides without relying on offline processes. In this chapter the functional ability of the device to accomplish affinity selection, and amplification and coupled multiround SELEX are demonstrated.

4.2. Experimental

4.2.1. Principle

The approach relies on isolating high affinity members from a highly diverse (10^18 member) oligonucleotide library through iterative rounds of affinity selection, affinity counter selection, and PCR amplification on a microfluidic device. The 87 nucleotide oligonucleotide library is composed of a 40 nucleotide randomized region surrounded by a fixed nucleotide region at the 5’ end and 3’ ends. Thus, the oligonucleotide library has a theoretical limit of 4^{40} members (10^{24}) that can be readily amplified through PCR with a reverse and forward primer. This library is passed through target-coupled beads and washed with buffer to remove library members that weakly bind to the target. Oligonucleotides that bind to the target glycan are eluted from the target beads by modest thermal denaturation and transferred through counter target beads before ultimately being captured by reverse-primer functionalized beads (amplification beads)

through complementary base pairing. In this way, library members with affinity towards the counter target are removed before hybridizing to the reverse-primer beads. The hybridized library is amplified by PCR and sense strands to produce double-stranded DNA products on the amplification beads. The amplified product is removed from its bead-bound complement through thermal denaturation and transferred back to target glycan beads as a new round of selection begins. This process is repeated until the library is sufficiently enriched to the point that oligonucleotides with high affinity and specificity can be identified (**Figure 4.1**).

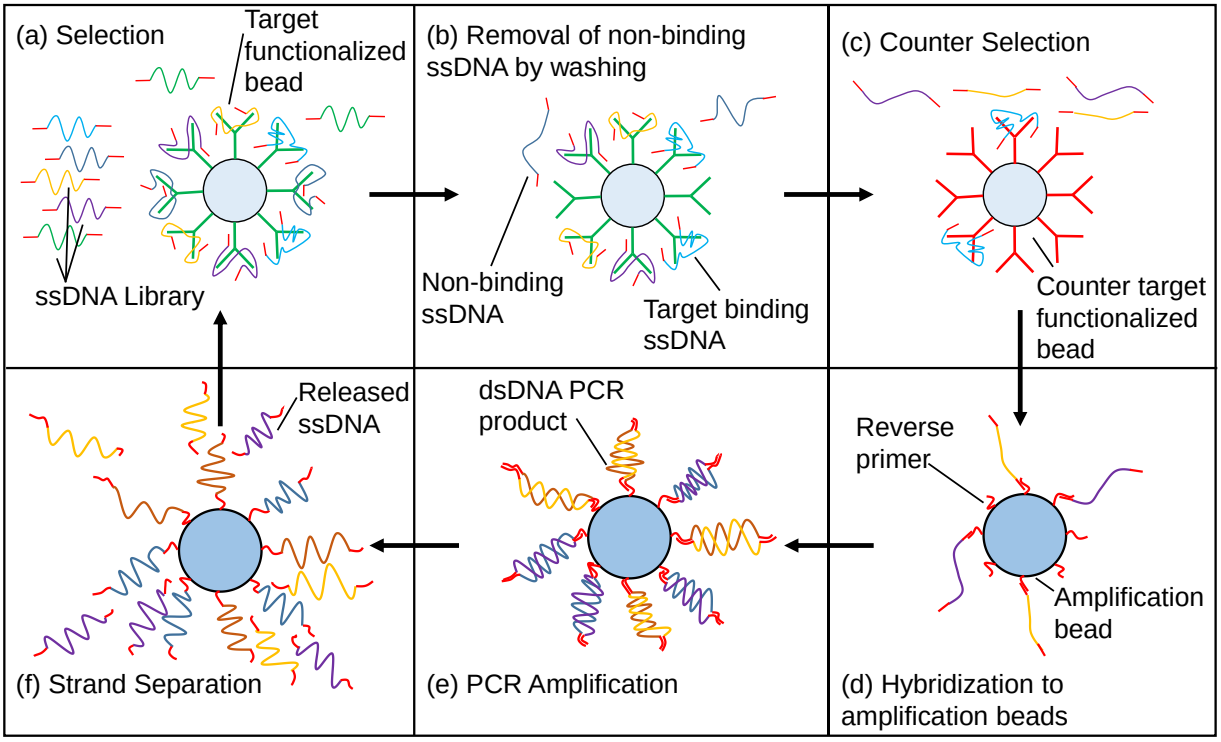

Figure 4.1: Aptamer selection procedure. (a) Library is introduced and allowed to bind to beads. (b) Non-binding and weakly binding ssDNA is removed with buffer washes and then (c) counter selected against a counter target. (d) ssDNA which binds to the target but does not bind to the counter target is transported to the amplification chamber where it hybridizes to reverse primers located on the surface of amplification beads. (e) Hybridized ssDNA is amplified by PCR which is then (f) thermally denatured to release the single stranded product. This product is transferred back to (a) for further rounds of SELEX.

4.2.2. Microfluidic Device Design

The approach is realized in a device consisting of 3 microchambers of similar geometry (~4.5 µL) connected by microchannels to form a SELEX capable loop (Figure 4.2). Each microchamber features a

fluidic weir which allows buffer to pass but is sufficiently small to prevent beads from passing between chambers (20 µm), a bead inlet, secondary inlet, and an outlet. The selection and amplification chamber are equipped with a temperature sensor and heater located beneath the chamber to allow temperature mediated release of oligonucleotides and PCR. Each chamber is connected to the other two through microchannels (~20 um height). Flow is directed between the three cambers by the integrated pneumatic microvalves [141]. Fluid moves in a clockwise direction from selection to counter selection to amplification and then back to selection.

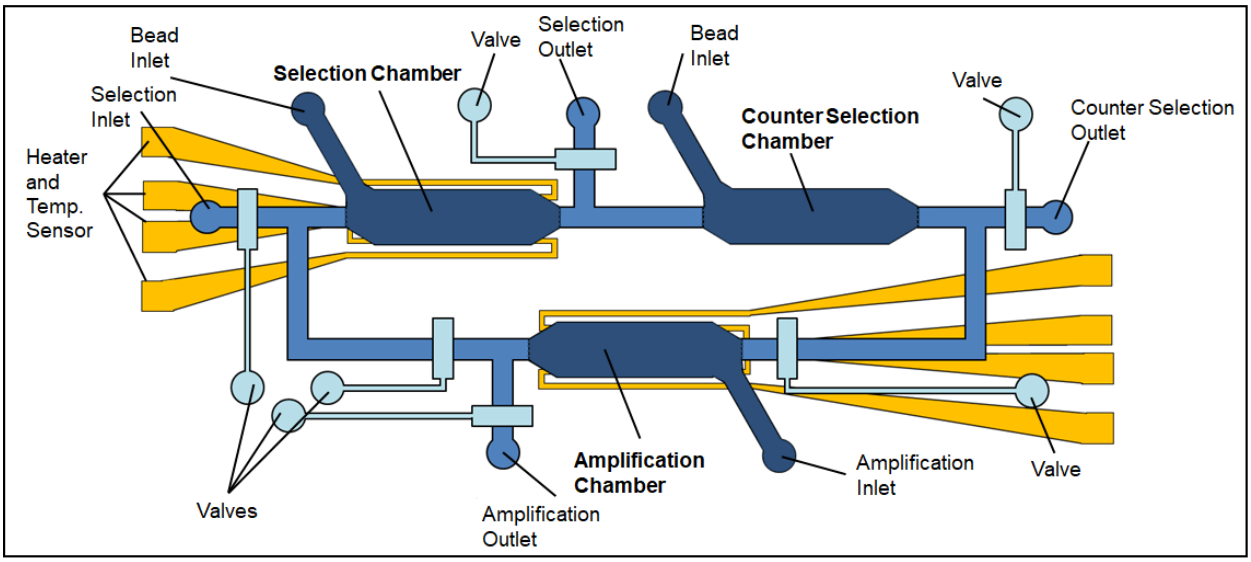

Figure 4.2: Device design. The approach is realized in a microfluidic device with dedicated chambers for selection, counter selection, and amplification. Valves are used to direct flow between these three chambers and allow controlled transport of ssDNA to complete rounds of SELEX.

Beads (selection, counter selection and amplification) are first introduced from the bead inlets and trapped by the weir structures in the three chambers. These inlets are then blocked and starting library is injected from the secondary inlet and allowed to incubate with the target. Valves are configured at this stage to allow buffer to flow from the inlet, across the selection chamber and then exit through the outlet. Following incubation, buffer is used to wash weakly binding aptamer candidates by exchanging the library with buffer at the inlet. Upon completion of washing only strongly binding oligonucleotides will remain in the device. The integrated heaters beneath the selection chamber are then activated to increase the selection chamber temperature and induce thermal based elution of binding oligonucleotides. Concurrently with this

temperature increase, the valve configuration is reoriented to create buffer flow from the selection chamber, through the counter selection chamber and amplification chamber, and out the amplification outlet. Thus oligonucleotides which strongly bound to the target molecule are released and are challenged by the counter target beads, with those members with affinity towards the counter target being trapped by the counter beads and the others ultimately hybridizing to the amplification beads. Once in the amplification chamber, PCR reagents are introduced and PCR based thermal cycling commences utilizing the temperature sensor and heater located beneath the amplification chamber. The amplified product is washed with buffer to remove free-solution oligonucleotides while oligonucleotides generated on bead surfaces remain. Selection and counter selection beads are replenished in their respective chambers. The heater and temperature sensor are employed again to heat the chamber to 95 ºC to induce thermal based dehybridization of the amplified product from its complementary strand used for PCR amplification. Meanwhile the valves are again reconfigured to allow flow carrying amplified oligonucleotides from the amplification chamber, across the selection chamber, and out the selection chamber outlet. Therefore, another cycle of SELEX begins. This process is repeated on a single chip until a pool of high-affinity aptamer candidates are generated.

4.2.3. Microfluidic Device Design

The integrated approach is achieved in a microfluidic device capable of performing iterative cycles of selection, counter selection and amplification. The device features three microfluidic chambers of hexagonal geometry, each 7.5 mm long, 2.5 mm wide and 240 um tall (~4.5 µL). Similar to the electrokinetic device in Chapter 3, the hexagonal shape is adopted because it is not as prone to trapping catastrophic bubbles [146]. Each selection chamber has a dedicated inlet for the introduction and removal of microbeads (700 µm wide, 4500 µm long and 240 um tall). Connecting each of the three chambers to the other two chambers is a microfluidic channel of 700 µm linewidth and 20 µm tall and variable length depending on the chambers the channel connects (either 16 mm or 28 mm). The reduced height of the connecting channels is smaller than the diameter of the microbeads used in the device; therefore, beads are retained in three taller chambers. The channel between the amplification chamber and counter selection chamber, and the channel between the amplification and selection chamber feature a region (3 mm long) of semicircular cross-section which overlaps with the valve channels in the control layer. This region of the

channel can be completely closed when the corresponding valve is actuated allowing controlled sealing of chambers and control of flow direction. The channel connecting the amplification chamber to the selection chamber and the amplification chamber to the counter selection chamber also feature an inlet and outlet to allow oligonucleotides and reagents to be introduced. A pair of heater and temperature sensors lie beneath the selection chamber and amplification chamber and are composed of 20 nm chrome and 100 nm thick gold. The temperature sensor is of rectangular shape with a linewidth of 30 μm and the heater is of serpentine shape, filling the area of the chambers and of line width 300 μm.

Multiple rounds are able to be achieved on the microdevice. First target beads, counter target beads, and amplification beads are respectively introduced in the selection, counter selection, and amplification chambers through the bead inlets. The reduction in chamber height from the inlet to the connecting chambers allows beads to be retained in the chamber. These inlets are blocked with plugs following bead introduction. Affinity selection is then performed by first flowing oligonucleotides, and then washing buffer from the selection inlet while the valves are configured to allow flow out the selection outlet. Following selection the valves are reconfigured to allow flow from the selection inlet, through the counter selection chamber, through the amplification chamber, and out the amplification outlet. Once reconfigured, the selection chamber heater and temperature sensor are engaged to increase the temperature and thermally elute binding oligonucleotides from their targets while buffer is flowing from the selection inlet to the amplification outlet. The oligonucleotides that do not bind to the counter target beads in the counter selection chamber hybridize to the amplification beads in the amplification chamber. Following this process, the valves are reconfigured again to allow flow from the amplification inlet and out the amplification outlet, and a pipette is used to inject PCR reagents from the amplification inlet. The amplification inlet is then plugged and the amplification chamber heater and temperature sensors are used to perform 12 cycles of PCR (55 ºC for 15 seconds, 72 ºC for 5 seconds, and 92 º C for 2 seconds). During PCR the amplification chamber is isolated from the other chambers with valves allowing the selection and counter selection chambers to be washed and their beads to be replenished. Following PCR the amplification chamber is rinsed with buffer to remove solution phase double stranded oligonucleotides. Then the heater and temperature sensor in the amplification chamber are again used to heat the chamber to 95 ºC to de-hybridize the amplified affinity selected oligonucleotides from their surface bound complements generated

during the PCR process. Meanwhile, the valves are once again reconfigured to allow flow from the amplification inlet through the selection chamber and out the selection outlet. Buffer flow carries the amplified oligonucleotides to the replenished selection chamber as a new cycle of SELEX commences. After the amplified product has be transferred, the amplification beads are replenished in the amplification chamber. This process continues until a pool of high affinity aptamers can be isolated.

4.2.4. Materials

Human Imunnoglobulin A (IgA1) was purchased from Cell Sciences (Newburyport, MA). CaptureSelect™ IgA affinity matrix, streptavidin coupled agarose beads (Pierce Streptavidin Agarose), and Dulbecco's phosphate-buffered saline (D-PBS) were purchased from Thermo Fisher Scientific (Waltham, MA). Ethanolamine, $MgCl_2$, tris, boric acid, and molecular biology grade water were purchased from Sigma-Aldrich (St. Louis, MO). Deoxyribonucleotide triphosphates (dNTPs) and GoTaq Flexi DNA polymerase were obtained from Promega Corp. (Madison, WI). Randomized oligonucleotide library (5' – TTG GAT TGA GAA ACA TCG CCG C – 40N – TTC CTC CTG ACC ACA TCC GAC– 3') and primers (Forward Primer: 5' – TTG GAT TGA GAA ACA TCG CCG C -3', and Reverse Primer: 5' - biotin – GTC GGA TGT GGT CAG GAG GAA – 3') were synthesized and purified by Integrated DNA Technologies (Coralville, IA). SU-8 (2000, 2025, and 2075 series) negative photoresist was purchased from Microchem Corp. (Westborough, MA). AZ 50XT was purchased from Integrated Micro Materials (Argyle, TX). Polydimethylsiloxane (PDMS) was obtained from Robert McKeown Company (Somerville, NJ) and silicon wafers were purchased from Silicon Quest International, Inc. (San Jose, CA). All other chemicals used for clean-room based fabrication were acquired from the City University of New York (CUNY) Advanced Science and Research NanoFabrication Facility.

Agarose microbeads (CaptureSelect™ IgA affinity matrix) functionalized with a protein were used for selection and agarose microbeads (Pierce Streptavidin Agarose) functionalized with reverse primers were used for amplification. The beads for selection were functionalized with a protein (IgA1) through affinity binding of the camelid CaptureSelect antibody which only binds IgA immunoglobulins. Prior to an experiment, a stock of selection beads were prepared by incubating the beads with IgA1 under gentle rotation for 1 hour at room temperature, and washing with D-PBS buffer. The functionalized beads were then suspended in D-PBS buffer. Similarly, streptavidin beads were functionalized by incubation with biotin

conjugated reverse primers for 30 minutes, and washing with D-PBS buffer. This coupling relies on the biotin-streptavidin affinity interaction. The functionalized beads were suspended in D-PBS buffer.

4.2.5. Fabrication

The devices used to realize the three chamber approach are fabricated in PDMS using standard photolithography techniques. First, a silicon wafer is cleaned with piranha (3 parts sulfuric acid and 1 part 30% hydrogen peroxide), rinsed with water, dried with nitrogen and placed on a hotplate set to 130 ºC for 1 hour. Following this cleaning process the wafer has chrome (20 nm) and gold (100 nm) deposited on its surface using a thermal evaporator (Edwards 306 Thermal Evaporator). Photoresist (AZ 1512, MicroChemicals GmbH) is then spun on the wafer (500 rpm for 10 seconds, 3000 rpm for 30 seconds, 500 rpm/s ramp) and baked on a hotplate at 120 ºC for 2 minutes. After the baking process, the wafer is exposed to 95 mJ/cm^2 of energy through a custom made mask defining alignment marks using a mask aligner. The exposed photoresist is then developed in AZ 300 MIF photoresist for 20 seconds and rinsed with water. The wafer is then submerged in first gold etchant (15 seconds), then chromium etchant (15 seconds), DI water, acetone, and finally IPA resulting in a silicon wafer with gold alignment marks which can be used for the multistep photolithography processes which are to follow.

The wafer with alignment marks could then be used for several additive fabrication steps. First AZ 50XT photoresist was spun onto the wafer (500 rpm for 20 seconds, 1500 rpm for 1 minute, 500 rpm/s ramp rate) and it was baked for 2 minutes on a hotplate at 85 ºC and then 5 minutes at 115 ºC. AZ 50XT was then deposited onto the wafer again and the wafer was spun using a spin coater (500 rpm for 20 seconds, 1500 rpm for 1 minute, 500 rpm/s ramp rate), and baked for 2 minutes at 85 ºC and then 5 minutes at 115 ºC. The wafer was allowed to rehydrate overnight. The wafer was then exposed to 2500 mJ/cm^2 of energy through a photomask bearing the valve controlled regions of flow layer with a mask aligner (EVG620 Mask Aligner). The exposed wafer was submerged in AZ 400K (1:4) developer for 15 minutes and rinsed with water. Excess photoresist on the edges of the wafer was removed using an acetone soaked cleanroom wipe (Texwipes). This wafer was then placed on a programmable hotplate (Torrey Pines Scientific) which ramped the hotplate temperature from room temperature to 200 ºC over 12 hours and then held the temperature at 200 ºC for 4 hours. Gradually heating allowed the photoresist to reflow into the semicircular shape necessary for valve control without causing bubbles to form in the photoresist. Furthermore, the

heating hard-bakes the photoresist so that the solvents in subsequent photolithography steps do not cause the dissolution of this layer.

A thin layer of SU-8 which includes the entire flow layer, sans the valve controlled regions, was then built on the wafer. SU-8 3005 was spun using a spin coater (2000 rpm, 1 minute, 500 rpm/s ramp rate) and baked at 95 ºC for 3 minutes. This layer was exposed to 250 mJ/cm2 of energy using a mask aligner and a custom designed mask, post baked (65 ºC for 1 minute and 95 C ºfor 2 minutes), and developed with SU-8 developer. The developed wafer was rinsed with isopropanol. This layer, while too thin to define channels in the final device, takes advantage of the increased adhesion of the 3000 series SU-8 to silicon substrates, thus creating an adhesion layer for the additional layers of SU-8 photolithography necessary to complete the fabrication of the device.

The flow layer bearing the connecting channels and chambers was then fabricated. SU-8 2025 was spun on the wafer using a spin coater (300 rpm for 15 seconds, 3000 rpm for 45 seconds, 300 rpm/second ramp rate), and baked (65 ºC for 3 minutes and 95 ºC for 6 minutes). The baked wafer was exposed to 400 mJ/cm^2 of energy through a custom made mask using a mask aligner, and returned to a hotplate at 65 ºC for 1 minute and 95 ºC for 6 minutes. The baked wafer was placed into SU-8 developer for 1 minute, rinsed with isopropanol and dried with a nitrogen gun. The chambers were then created in the wafer. SU-8 2075 was deposited on the wafer, allowed to settle on the wafer for 10 minutes, and then spun with a spinner (300 rpm for 15 seconds, 1000 rpm for 45 seconds, 300 rpm/second ramp rate). This was pre-baked on a hotplate at 65 ºC for 7 minutes which was ramped 10 ºC/minute to 95 ºC where it remained for 45 minutes. The pre-baked wafer was then exposed to 400 mJ/cm^2 energy with a custom mask defining the chambers using a mask aligner. Subsequently, the wafer was post-baked on a hotplate at 65 ºC for 5 minutes. The temperature was then slowly increased from 65 ºC to 95 ºC over 30 minutes and held at 95 ºC for 15 minutes. The hotplate was then turned off and allowed to return to room temperature with the wafer still remaining on its surface. The slow cooling to room temperature was to reduce the thermal stress on the thick SU-8 features which can cause adhesion problems during the development process. The wafer was then submerged in SU-8 developer for 10 minutes, rinsed with isopropanol and dried with compressed nitrogen thus completing the fabrication of the flow layer silicon mold.

The control layer was then similarly fabricated on a second wafer. SU-8 2025 was deposited onto a piranha cleaned wafer and spun using a spin coater (300 rpm for 15 seconds, 3000 rpm for 45 seconds, 300 rpm/second ramp rate). The spun photoresist was then baked on a hotplate at 65 ºC for 3 minutes and then at 95 ºC for 6 minutes. This pre-baked wafer was placed in a mask aligner along with a custom designed mask bearing the control layer features and exposed to 400 mJ/cm^2 of energy. A post-bake commenced consisting of 65 ºC for 1 minute and 95 ºC for 6 minutes on a hotplate. The post-baked wafer was then immersed in SU-8 developer for 1 minute, rinsed with isopropanol, and dried with compressed nitrogen.

Glass slides bearing heaters and temperature sensors were then fabricated. Chrome (20 nm) and gold (100 nm) were thermally evaporated onto piranha cleaned microscope slides. AZ 1512 was deposited onto them which were next spun (500 rpm for 10 seconds, 3000 rpm for 30 seconds, 500 rpm/s ramp) using a spinner. Following the spin, the slides were placed on a hotplate at 120 ºC for 2 minutes. The slides were then placed in a mask aligner along with a custom designed film mask bearing the heater and temperature sensor designs and exposed to 95 mJ/cm^2 of energy. These slides were developed in AZ 300 MIF, rinsed with water, and then immersed in first gold etchant (15 seconds) and then chrome etchant (15 seconds). Finally the slides were rinsed with acetone to remove remaining photoresist, rinsed in isopropanol, dried with compressed nitrogen and placed on a hotplate at 110 ºC for 1 hour to remove unevaporated solvent.

With flow and control layer wafers prepared, as well as substrates bearing heaters and temperature sensors, PDMS based fabrication began. 30 mL of PDMS (10:1 base: curing agent by weight) was poured onto the flow layer wafer, and placed in a vacuum desiccator for 30 minutes to remove bubbles. Following bubble removal, the flow layer wafer was placed on a hotplate set to 72 ºC for 30 minutes. The PDMS was then peeled off, cut into three identical flow layers, and had inlets and outlets punched using an autopsy punch. Meanwhile, 3 mL of PDMS was poured onto the control layer which was then spun using a spinner (300 rpm for 15 seconds, 1000 rpm for 45 seconds, 300 rpm/second ramp rate). The control layer was then placed on 72 ºC hotplate for 20 minutes. The three flow layer devices and the control layer were then placed in an oxygen plasma etcher (Diener Plasma Etch) and exposed to oxygen plasma for 20 seconds at 50% power. Immediately after exposure the flow layer devices were aligned to the three control layer features

on the flow layer wafer and gently pressed to put their surfaces in contact. The control layer wafer with flow layer devices on top of it were then placed on a hotplate at 75 ºC for 1 hour. Following this bake, the flow layer devices and the PDMS thin film coating the control layer were permanently bonded and could be peeled off together. The peeled off PDMS blocks which bore flow and control layers then had valve inlets punched into them. Meanwhile, 3 mL of PDMS were poured onto the glass slides bearing the heaters and temperature sensors, spun (300 rpm for 15 seconds, 1000 rpm for 45 seconds, 300 rpm/second ramp rate), and baked on a hotplate (72 ºC for 20 minutes). The heater and temperature sensors and the flow and control layer devices were then again exposed to oxygen plasma (20 seconds, 50 % power). The exposed devices were immediately aligned and gently pressed into the heater and temperature sensor glass slides. These were baked at 100 ºC overnight. Finally wires connected to the heaters and temperature sensors were soldered onto the contact pads. A fabricated device can be seen in **Figure 4.3**.

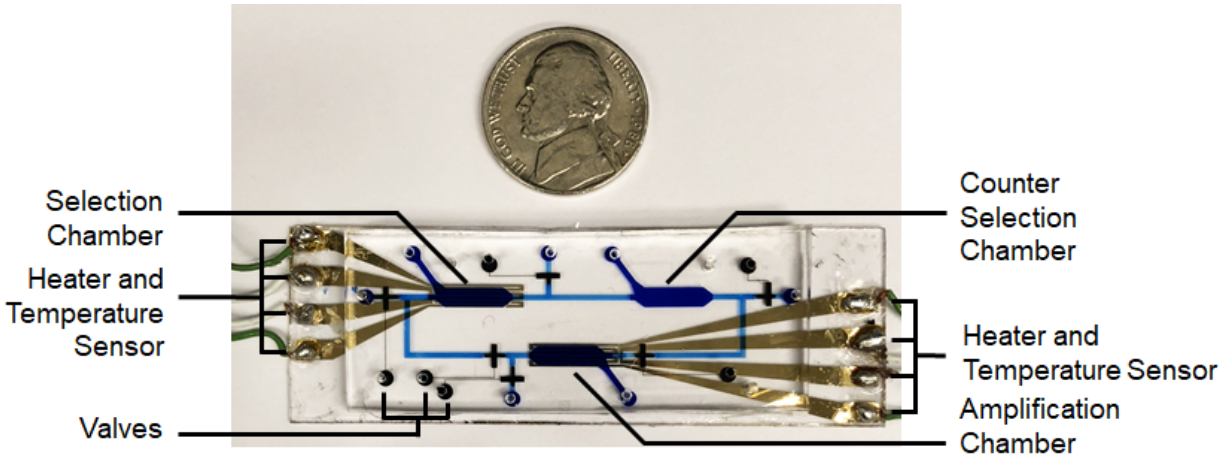

Figure 4.3: Photograph of a fabricated device.

4.2.6. On-chip Procedure

The microfluidic chip was interfaced with a syringe pump (New Era NE-1002X), a nitrogen tank, a multimeter (HP 3478A) and a power supply (Agilent E3631A). The syringe pump was responsible for supplying a fluid source, while the nitrogen tank was used to actuate the valves that controlled the direction of this fluid source. The multimeter and power supply were in turn connected a computer which implemented a LabView code to control the temperature of functional chambers in the device. This code

could implement simple temperature control for the elution of binding oligonucleotides or could perform the thermal cycling necessary for PCR amplification.

Multiround integrated SELEX occurred on-chip without the use of offline processes or equipment. First, the appropriate beads (selection, counter selection, and amplification) were pipetted into the three chambers (selection, counter selection, and amplification) until the beads filled approximately half of the chamber. Next, 100 µL of 100 nM (10 pmoles) of library, which has previously be heated to 95 ºC for 5 minutes and cooled back to room temperature, was pumped into the device (10 µL/min) using a syringe pump. Once the total library volume has passed through the selection chamber, the washing stage commenced where buffer (PBS with 2 mM $MgCl_2$) was infused (20 µL/min) through the selection chamber to remove weakly binding oligonucleotides for 35 minutes. Buffer flow-through was collected in 5 minute intervals, amplified by PCR, and imaged with a gel electropherogram to verify successful removal of non-binding oligonucleotides through the washes and the retention of strong-binding oligonucleotides.

Following this wash the valves were reconfigured to allow flow from the selection chamber through the counter selection chamber and into the amplification chamber. Once in this configuration, the heater and temperature sensor located beneath the selection chamber were used to increase the selection chamber temperature to 55 ºC. 20 µL/min flow over a 10 minute period was used to transfer heat released oligonucleotides from the selection chamber through the counter selection chamber and finally to the amplification chamber where oligonucleotides that do not bind to the counter target hybridize to the reverse primer functionalized beads in the amplification chamber. PCR reagents were then pipetted into the amplification chamber and all the valves were closed to seal the amplification chamber for PCR. The heater and temperature sensor located beneath the amplification chamber were used for 12 rounds of PCR thermal cycling (55 ºC for 15 seconds, 72 ºC for 5 seconds, and 92 º C for 3 seconds). PCR amplification was confirmed through the amplification of a 100 fM library. An agarose gel was used to determine the presence of amplified DNA before amplification, and after amplification and thermally induced single-stranded DNA release.

During the PCR process the selection and counter selection chambers were prepared for the second round of SELEX. The beads in the selection chamber and counter selection chamber were removed

and the chambers were refilled with fresh selection and counter selection beads. The amplification chamber was then washed with buffer (PBS with 2 mM $MgCl_2$) for 10 mins using a volumetric flow rate of 20 µL/min. After the completion of the washing, the heater and temperature sensor were again used to increase the amplification chamber temperature to 95 ºC which caused single stranded DNA to be released from their bead bound complements while the valves were again reconfigured to allow flow from the amplification chamber to the selection chamber. A flow rate of 20 µL/min was used for this process. After 5 minutes, the amplification chamber heater was turned off and the chamber returned to room temperature. The washing of the selection chamber then began (20 µL/min) and lasted for 35 minutes as the second round of the SELEX process continued. This sequence of events repeated until high affinity aptamer sequences could be identified.

4.3. Results and Discussion

Results are presented characterizing the performance of the individual components of the 3-chamber device. A complete two round process (selection, counter selection, amplification, selection, and finally counter selection) is then performed to demonstrate the ability of the device to realize a multi-round SELEX process.

4.3.1. Heater and Temperature Sensor

Tight control over the heater and temperature sensor are necessary to ensure consisitent thermal based elution of strongly binding oligonucleotides and to ensure PCR amplification can successfully occur. The device uses thin film gold resistive temperature sensors and heaters. The heater and temperature sensor were first characterized using an environmental chamber (Delta Designs 9023, Cohu, Poway, CA) with a temperature probe. The device was placed inside the chamber with its temperature sensor connected to a multimeter and the temperature was ramped from room temperature to 95 ºC. The corresponding resistance of the device temperature sensors were recorded every 10 ºC **(Figure 4.4**).

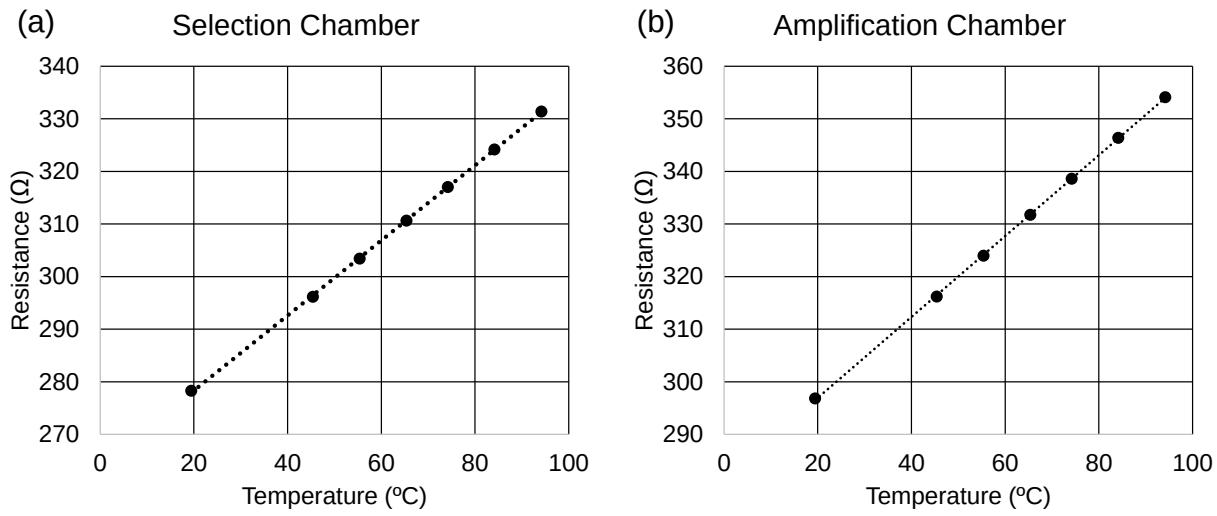

Figure 4.4: Resistance of the (a) selection and (b) amplification chamber temperature sensors at various temperatures.

The temperature and resistance information for the device was then plotted and fitted with the following expression.

$$\frac{R - R_0}{R_0} = \alpha(T - T_0)$$

In this expression R is the resistance for a given temperature, R_0 is the resistance at room temperature, T is the temperature, T_0 is the room temperature and alpha is the coefficient of resistance. A coefficient of resistance of 2.527 X 10^{-3} °C^{-1} was obtained for the selection chamber temperature sensor and 2.556 X 10^{-3} °C^{-1} for the amplification chamber temperature sensor.

4.3.2. Affinity Selection

The affinity selection was evaluated by performing a single selection and assessing collected oligonucleotides. Selection beads were injected into the selection chamber until it was approximately half full of beads. The valves were configured to allow flow through the selection chamber inlet and out the selection chamber outlet. 100 µL and 100 nM of library (preheated off-chip) was injected into the chip at 10 µL/min for 10 minutes. Wash buffer (PBS with 2 mM $MgCl_2$) was then injected (20 µL/min) for 35 minutes. During the wash the flow through was collected in tubes, exchanging the outflow to a new tube every 5

minutes (~100 µL per tube). Finally, the temperature of the chamber was increased to 55 ºC and the outflow volume was collected in 5 minute intervals for 10 minutes. These collected volumes were amplified by PCR (20 cycles) and imaged with an agarose gel (**Figure 4.5**).

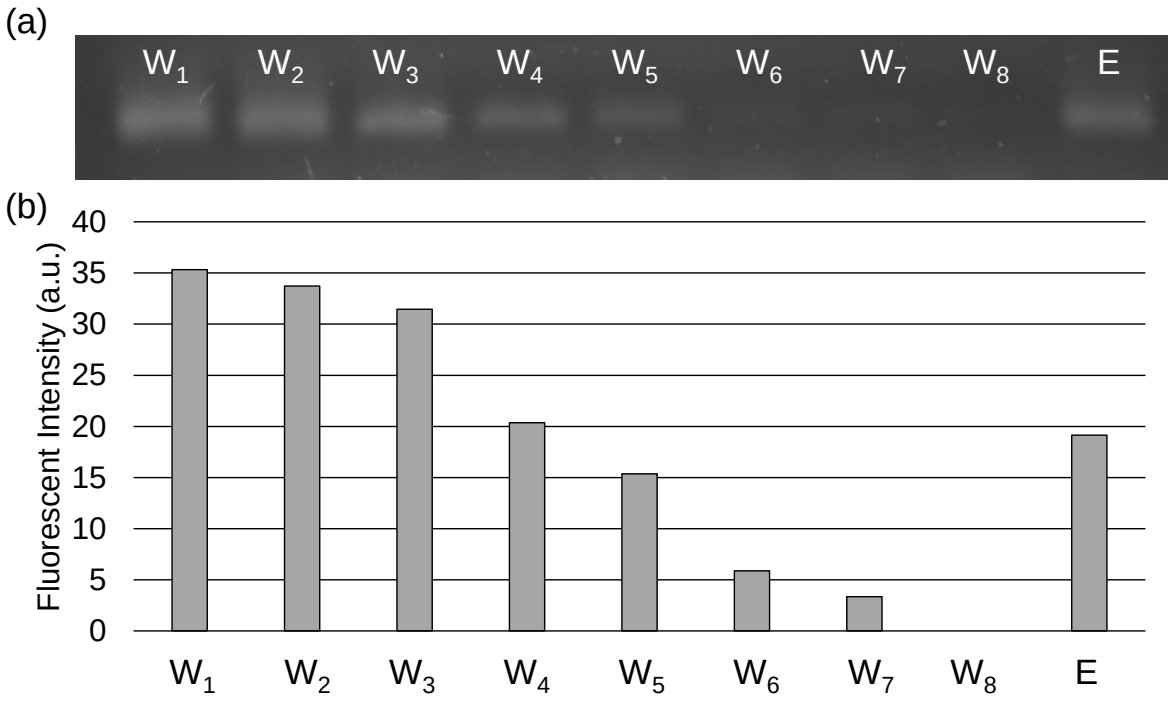

Figure 4.5: Elution profile for the selection process. Collected eluents were amplified by PCR and imaged by gel electrophoresis. (a) Gel electropherogram of the amplified eluates and (b) fluorescent intensity readings from the gel electropherogram in (A). W_1: wash 1, W_2: wash 2, W_3: wash 3, W_4: wash 4, W_5: wash 5, W_6: wash 6: W_7: wash 7, W_8: wash 8, E: eluted product.

It can be seen that during the washing process the brightness of the bands, which is a measure of the amount of DNA in each tube, decreased from W_1 to W_8 (**Figure 4.5**). This demonstrates that the washing process initially removed many weakly binding oligonucleotides but as the washing progressed fewer oligonucleotides were able to be removed from the chamber. The elution band (E) is comparatively bright compared to the final wash (W_8) indicating that after the increase in temperature oligonucleotides which were unable to be removed by washing alone could be eluted. These oligonucleotides strongly bound to the target and the binding was only disrupted by the modest increase in temperature.

4.3.3. Amplification

The PCR amplification was confirmed by amplifying a low concentration library and imaging with an agarose gel. First buffer was injected into an amplification chamber containing amplification beads and the chamber was heated to 95 ºC while exiting solution was collected. This was to provide a no template control for the PCR process. Then, 100 µL of 100 fM library was injected (20 µL/min) into the amplification containing amplification beads. PCR reagents were pipetted into the chamber, and 12-cycles of PCR amplification commenced. The chamber was washed to remove unincorporated primers and double stranded DNA in solution. The chamber was then heated to 95 ºC under 20 µL/min flow conditions for 5 minutes and the exiting solution was collected. This was repeated with a new device where library was injected and then heated to remove ssDNA without performing PCR thermal cycling. Collected eluates were amplified by PCR off-chip (10 cycles) and imaged by gel electrophoresis. It can be seen that there is only a band in the gel for the case where PCR amplification occurred with a template in the device (**Figure 4.6**).

(a)

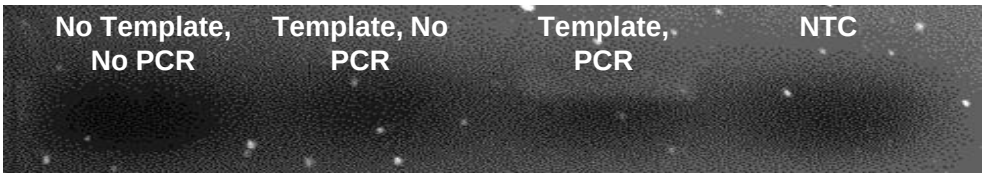

(b)

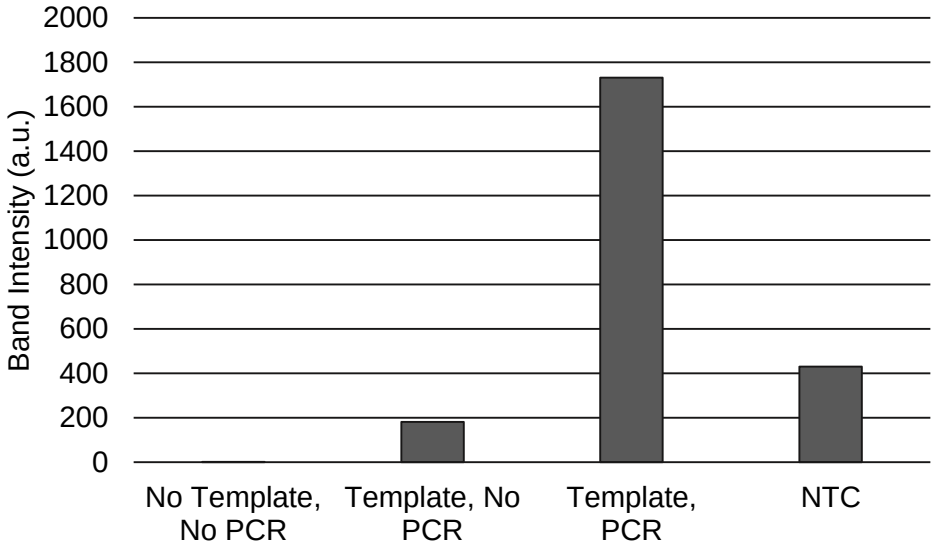

Figure 4.6: (a) Gel electropherogram of collected eluates from the amplification chamber in conditions where no template was included and no thermal cycling was used, where template was injected but thermal cycling was not used, where template was injected and thermal cycling was used, and a no template control. (b) Measured band brightness from the gel electropherogram.

4.3.4. Integrated Multi-round SELEX

A complete 4-round SELEX was performed to confirm the devices ability to transition from selection steps to the amplification stage and back. Four rounds of selection, and counter selection were performed with a three rounds of PCR amplification and strand separation (**Figure 4.7**). Eluates during the process were collected, amplified off-chip by 20 cycles of PCR and imaged with a gel to analyze the closed-loop process.

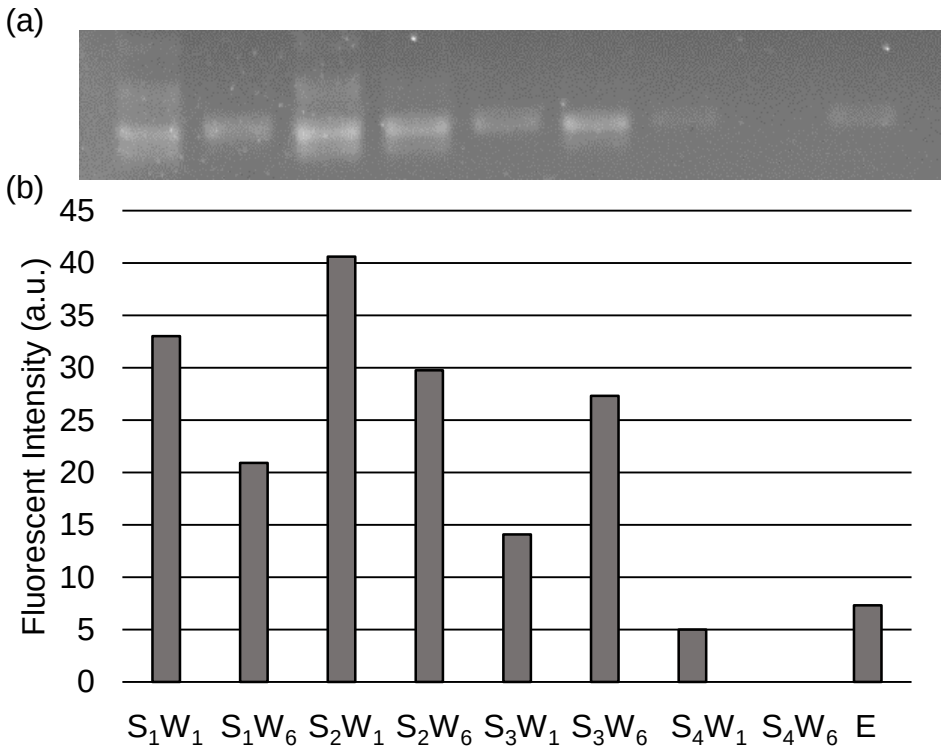

Figure 4.7: Gel electropherograms from the four round selection process. (A) Amplified eluents measured with a gel electropherogram. (B) Measured band intensity from (A). Labeling is as follows, S_1W_1: Selection round 1, wash 1; S_1W_6: selection round 1, wash 6; S_2W_1: selection round 2, wash 1; S_2W_6: selection round 2, wash 6; S_3W_1: selection round 3, wash 1; S_3W_6: selection round 3, wash 6; S_4W_1: selection round 4, wash 1; S_4W_6: selection round 4, wash 6; E: elution.

The brightness of the bands in a gel electrophorogram correlates to the initial amount of oligonucleotides in the collected eluate which can be compared to investigate the SELEX process. During the first round, the brightness of the bands monotonously decreases from the first wash (S_1W_1) to the last wash (S_1W_6) indicating that the washing process removed weakly binding oligonucleotides. The band intensity then increased from the last wash of the first round (S_1W_6) to the first wash of the second round (S_2W_1). This suggests the ssDNA were successfully transferred to the amplification, amplified by PCR and transferred back to the selection chamber. The decrease in band intensity from the first wash of the second round (S_2W_1) to the final wash of the second round (S_2W_6) again indicates the washing process removed weakly binding oligonucleotides. The presence of a band in the elution lane (E) combined with the absence

of a band in the final wash of the fourth round shows that oligonucleotides that could not be removed by washing were eluted by a change in thermal conditions and were able to be counter selected and collected. It is further important to note that during this closed-loop process there was no observed wear on the device suggesting the device could be used for many rounds of the SELEX process without deterioration.

4.4. Conclusion

The three chamber microfluidic approach with pressure driven reactions has been described. The approach leveraged bead-based reactions within three functional chambers (selection, counter selection, and amplification) connected in a loop by microchannels. As such, oligonucleotides are affinity selected against target functionalized beads, affinity counter selected against counter target functionalized beads, and amplified by reverse primer functionalized beads. The single-stranded amplified product is transferred back to the selection chamber for further rounds of SELEX. Therefore, the approach integrates the entire SELEX process on a single microchip without the need for offline procedures and drastically reduces the time required to obtain aptamer candidates. These components were characterized using IgA as a model target. Furthermore, the device showed no appreciable degradation indicating it could be used for SELEX beyond four rounds if needed.

Chapter 5: Selection of Aptamers to Glycans and Glycosylated Peptides

5.1. Introduction

Glycans, one of the four major classes of molecules making up cells (the others being nucleic acids, proteins and lipids) [150], are involved in all human developmental activities including structural roles, modulatory, intercellular signaling and adhesion [151, 152]. Furthermore, more than 50% of proteins are modified by glycosylation [30] which occurs in the Golgi apparatus (for *O*-linked glycosylation) or endoplasmic reticulum (for *N*-linked glycosylation). Expectantly, aberrant expression of glycans, including under- and overexpression, has been found to be associated with many diseases, attracting considerable interest in using glycans as disease markers [153-155]. Glycans represent a potential source of biomarkers that could stratify patients and allow tailored disease treatment strategies [7].

Despite their importance in many biological functions, methods to rapidly and sensitively analyze glycan samples remains an unmet challenge [156]. The entire human glycome (estimated to range from hundreds to thousands of structures) can be built by branched and linear combinations of only 9 glycome building blocks and are recognized by only 70 different glycan binding proteins [151]. The structure of glycans cannot be predicted by genomic information [155, 157]. Multi-dimensional liquid chromatogoraphy (LC) which separates glycans based on differences in chemical structures (size, hydrophobicity, etc.) has been used to discriminate over 500 glycans but has low throughput [158]. Mass spectrometry (MS) is able to achieve superior accuracy but glycan samples need extensive preparation steps before use and structural isomers (enantiomers, diastereomers, anomers) are challenging to discriminate [159]. Affinity receptor methods also remain underdeveloped. Lectins, glycan binding proteins from natural sources, have been used in many examples [159-163] but they suffer from low affinity, broad specificities, and, in some cases, high toxicity limiting their applications. Anti-carbohydrate antibodies have reduced affinities compared to protein or peptide antigens and lack the potential to bind to the full spectrum of the glycome [164]. Further, the amount of glycan material needed to generate a specific antibody is often prohibitively consumptive.

Oligonucleotide-based receptors or aptamers can be straightforwardly applied and are adapted/engineered to have new properties even in non-specialist laboratories [165, 166]. Thus, aptamers have the potential to be customizable synthetic reagents that can be reproducibly used across a wide range

of laboratories. There is a substantial number of individual demonstrations of the isolation of aptamers [167] binding to sugars [168-179], spanning from complex saccharides [173, 174] to disaccharides (with specificity for particular anomeric configurations) [179], and even monosaccharides [180]. However, lacking is a systematic approach to generate individual aptamers, while consuming modest amounts of glycans, against thousands of possible oligosaccharide structural motifs in order to implement aptamers as widely available off-the-shelf structural and discovery tools available to general users.

Here we apply the microfluidic approach developed in Chapter 4 to rapidly isolate aptamers with high affinity and specificity towards glycan targets with low sample consumption. As discussed in Chapter 4, the approach relies on the use of an integrated microfluidic chip that is capable of performing the iterative, and repeated steps of the aptamer generation process – termed systematic evolution of ligands by exponential enrichment (SELEX), while leveraging the high surface to volume ratios and small sample consumption afforded by microfluidics. In particular, the device includes dedicated chambers that allow the selection and counter selection stages of the SELEX process, as well as a dedicated chamber which can perform polymerase chain reaction (PCR) based amplification of enriched aptamer candidates and strand separation. Thus, multiple rounds of affinity selection and amplification are coupled in one fluidic device. As a result, the device is able to isolate aptamer candidates in a rapid manner (4 rounds of SELEX in 9 hours) while consuming <500 µg of purified glycan. The device is applied to the isolation of aptamers with affinity towards gangliosides GM1, GM3, and GD3 with limited cross-reactivity. Furthermore, the approach is applied to the selection of aptamers with affinity towards a glycosylation pattern in a peptide. This is demonstrated through the isolation of aptamers for an IgA hinge region peptide with *N*-acetylgalactosaminyl (GalNAc) glycosylation.

5.2. Materials and Methods

5.2.1. Materials

$MgCl_2$, imMedia Growth Media, TOPO TA Cloning Kit for Sequencing with One Shot, lyso-GM1 ganglioside and molecular biology grade water were purchased from Sigma-Aldrich (St. Louis, MO). Deoxyribonucleotide triphosphates (dNTPs) and GoTaq Flexi DNA polymerase were obtained from Promega Corp. (Madison, WI). Protein G ELISA plates, Dulbecco's phosphate buffered saline (D-PBS), Pierce NHS-Activated Agarose Slurry, and streptavidin coupled agarose beads (Pierce Streptavidin

Agarose) were purchased from ThermoFisher (Waltham, MA). Streptavidin surface plasmon resonance chips and 2D carboxydimethyldextran (2D CMD) chips were purchased from BioNavis (Tampere, Finland). E.Z.N.A. DNA Extraction kit was purchased from Omega Bio-tek (Norcross, GA). Randomized oligonucleotide library (5' – TTG GAT TGA GAA ACA TCG CCG C – 40N – TTC CTC CTG ACC ACA TCC GAC– 3') and primers (Forward Primer: 5' – TTG GAT TGA GAA ACA TCG CCG C -3', and Reverse Primer: 5' – biotin – GTC GGA TGT GGT CAG GAG GAA – 3') were synthesized and purified by Integrated DNA Technologies (Coralville, IA).Gangliosides GM1, GM3 and GD3 were purchased from Avanti (Alabaster, AL). Gangliosides GD3, and GM3 with stearic acid cleaved were acquired from Milan Stojanovic. IgA hinge region peptide VPSTPPTPSPSTPPTPSPSCCHPR and its GalNAcosylated version were acquired from Jan Novak. Tube-O-DIALYZER was purchased from VWR (Radnor, PA).

5.2.2. Aptamer Selection

Aptamers were selected using the methodology developed in Chapter 5 with some modifications. Selection beads were prepared by washing NHS agarose beads three times in PBS buffer. Then lyso-ganglioside was incubated for one hour. The beads were then washed five times in selection buffer (PBS with 2 mM $MgCl_2$) and then blocked with ethanolamine (1 M) for 30 minutes. The beads were washed 10 times and stored at 4 ºC. Similarly, counter selection beads were prepared by first washing NHS agarose beads with PBS three times and then incubating with ethanolamine (1 M) for 30 minutes. The beads were then washed 10 times with 200 µL of selection buffer and stored at 4 ºC.

To reduce non-specific binding of the library to agarose beads, a pre-selected library was created. Prior to selection, a library (300 nM and 1 mL) was passed through an ethanolamine blocked agarose column three times. The column effluent was then passed through a second ethanolamine blocked column three times. The oligonucleotides that did not bind to the column were collected, measured for concentration and diluted as necessary for microfluidic SELEX.

The preselected library (300 nM and 1 mL) was then injected into a microfluidic device that has previously been prepared with selection and counter selection beads at a flow rate of 10 µL/min for 10 minutes. Following this library introduction, the beads were washed with buffer (PBS with 2 mM $MgCl_2$) for 35 minutes at 20 µL/min. An additional wash with sialic acid, chosen because sialic acid is a shared component amongst all gangliosides, was then performed for 10 minutes at 20 µL/min. Strongly bound

oligonucleotides that were not removed by washing with buffer or with counter target were eluted by heating the selection chamber to 55 °C using the heater and temperature sensor located beneath the selection chamber. Eluted oligonucleotides were carried by 20 µL/min buffer flow through the counter selection bead filled counter selection chamber until finally they reach the amplification chamber. Thus, oligonucleotides were counter selected before reaching the amplification chamber where they hybridized to the reverse primers conjugated to the amplification beads and remain in the amplification chamber. PCR reagents were then injected using a pipette into the amplification chamber and the heater and temperature sensor beneath the amplification chamber are used to thermal cycle the amplification chamber for PCR. Following 12 cycles of PCR, the chamber was washed to remove in-solution double stranded DNA. Then the amplification chamber heater and temperature sensor were again used to the increase the chamber temperature to 95 °C inducing de-hybridization of the single-stranded DNA from its bead-bound complement. Meanwhile, buffer flow (20 µL/min) transported this single stranded DNA from the amplification chamber back to the selection chamber as another round of SELEX begins. As the SELEX process continues longer sialic acid washes were used in an effort to increase the specificity of the aptamer pool. In the first round, 10 minutes of sialic acid washing was used. This was increased to 15 minutes in the second round, 20 minutes in the third, and 25 minutes in the fourth round. After four rounds of selection and counter selection, aptamer candidates were removed the device, sequenced and characterized for their binding properties. The same process was employed for the GM1, GM3 and GD3 gangliosides.

Aliquots collected during this process were PCR amplified with 20 cycles of PCR in an off-chip thermal cycler and analyzed through gel electrophoresis. The relative fluorescent brightness of a band in gel electrophoresis can be correlated to the amount of DNA present in the lane and this indicated the amount of DNA in the various stages of the selection process. Relative amounts of DNA during the selection informed the success of the selection process.

5.2.3. Subcloning and Sequencing

Aptamer candidates were identified by first subcloning the pool and then sequencing selected colonies from the subcloning. Aliquots from the aptamer selection process were PCR amplified for 20 cycles and then precipitated in ethanol with 10% sodium acetate overnight at -20 ºC. The precipitate was centrifuged, washed with 70% ethanol, resuspended in water and measured with a spectrophotometer

(Implen). This DNA was then used with a TOPO vector kit following the manufacturer's instructions. Briefly, the DNA was combined with the TOPO vector and one shot *E. coli* at 4 ºC, heat shocked at 42 ºC, and then combined with SOC solution. This was then spread onto Amp Blue culture dishes and incubated overnight at 37 ºC. Colonies were selected from the dish by contacting a pipette tip to a colony. This tip was then dropped into a 1.5 mL tube containing sugar culture media and cultured at 37 ºC on a shaking incubator for 16 hours. DNA from these cultures were extracted with an EZNA cleanup kit following the manufacturer's instructions and measured with a spectrophotometer. The resulting DNA was sequenced by Genewiz through a Sanger Sequencing protocol.

5.2.4. Surface Plasmon Resonance (SPR)

Aptamer candidates are characterized for their specificity and affinity using multi-parametric SPR (MP-SPR). In MP-SPR, a ligand (the aptamer in our case), is functionalized onto a gold surface. Then an analyte in solution (glycan or aptamer) is injected through microfluidic channels located on top of the functionalized gold surface. A surface plasmon is generated by directing a beam of light at a specific wavelength through a prism at the resonance angle. This resonant angle will depend on the wavelength of light, material properties of gold, and the prism. As the mass changes on the gold surface, as would happen during an analyte-ligand binding interaction, the properties of the sensing surface deviates resulting in a change in the angle needed to generate a surface plasmon. This change in angle is detectable by the intensity of light reflecting from the laser, off the gold and into a detector. Thus, it is possible to measure binding interactions without the use of a label and to provide kinetic information on binding including equilibrium constant, association constant, and dissociation constant. Unlike conventional SPR that uses a fixed angle for the incoming light, MP-SPR sweeps the angle of the incoming light to obtain the full SPR curve. The angle at which the surface plasmon effect is produced, which is the angle that produces the minimum reflection to the detector, is used as the measurement metric informing the binding interactions of the analyte and the ligand.

MP-SPR was used in both configurations where the aptamer was bound to the surface as the ligand and the glycan served as the analyte, and also with the glycan conjugated to the surface as ligand and the aptamer being used as analyte. When the aptamer was used as a ligand, it was bound to a regenerable avidin chip (BioNavis, Tampere, Finland) which has a mutated avidin surface that can be completely

removed upon citric acid washing. The avidin chip was rinsed in double distilled water, dried with compressed air, and placed into the SPR instrument (Naavi 220A, BioNavis, Tampere, Finland). Once the chip was inserted into the instrument, a series of injections were setup to prepare the sensor surface and to functionalize the surface with the aptamer. First, the surface was washed with the manufacturer provided Regeneration Solution 2 (2.5% citric acid with 0.5% SDS) for two minutes at 20 µL/min. A wait time of two minutes was used after the first regeneration solution and then Regeneration Solution 1 (0.5% SDS) was injected for two minutes at 20 µL/min. An avidin solution (50 µg/mL) was injected for two minutes after this this injection over both fluidic channels at flow rate of 20 µL/min for ten minutes with a five minute post wait time. Biotinylated aptamer (25 µg/mL) was then injected for 7 minutes at 20 µL/min in one fluidic channel while a scrambled sequence (identical 5' primer and 3' end to the aptamer sequence but a random 40 nucleotide middle region). The baseline was allowed to stabilize before injecting analyte and recording the interaction (**Figure 5.1**). All analytes were injected at 20 µL/min for five minutes with a dissociation wait time of at least ten minutes. After every analyte injection the process of injecting regeneration solutions and aptamer were repeated to strip the surface of the aptamer and replace it with fresh aptamer. Binding curves for different concentrations of analyte were analyzed to determine the kinetic binding parameters.

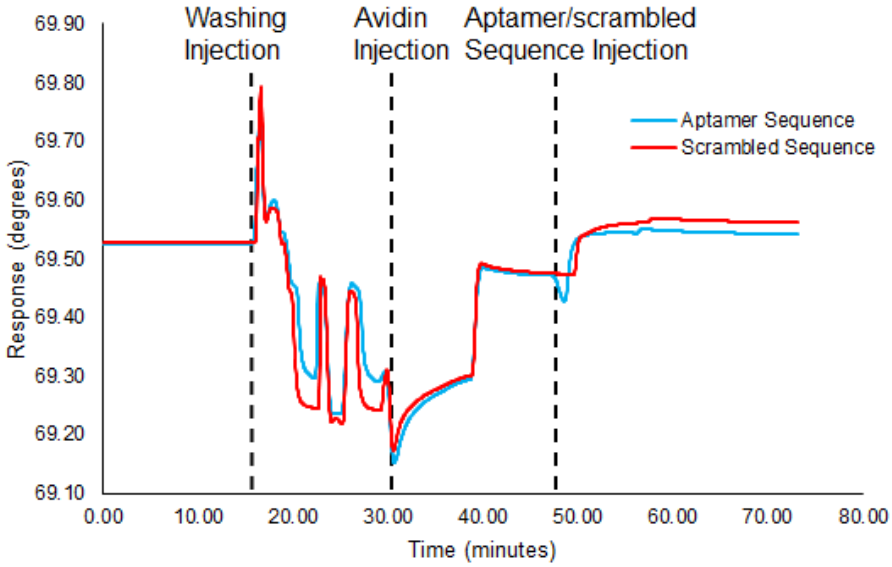

Figure 5.1: Avidin SPR chip setup. The surface is washed, then avidin is injected and finally aptamer is injected on one channel while a scrambled sequence is injected on the other

Aptamer candidates were also analyzed by SPR with glycan acting as ligand and the aptamer serving as the in-solution analyte. This SPR format was only possible for lyso-gangliosides that have an amine group exposed by the cleavage of the stearic acid. A 2-D carboxymethyldextran (CMD 2D) chip was rinsed with double-distilled water, dried with compressed air and placed into the SPR instrument. A series of injections were then performed to covalently attach the glycan to the sensor surface. First, a solution of 2 M NaCL and 0.01 M NaOH were injected to clean the sensing surface for seven minutes at 20 µL/min. The dextran surface was then activated by injecting freshly made 0.05 M NHS and 0.2 M EDC were mixed 1:1 and injected for seven minutes at 20 µL/min. Glycan (0.2 mg/mL) in PBS buffer (pH 8.5) was injected over one of the activated channels at 10 µL/min for 15 minutes to covalently attach the glycan through the amine group. Following this, ethanolamine (1 M) was injected (20 µL/min for 5 minutes) over both channels to block unreacted NHS groups. Once the chip surface was prepared, a series of analyte injections were performed. All analytes were injected with a flow rate of 20 µL/min for five minutes with 10 minutes allowed for dissociation. The surface was regenerated with injections of ammonium sulfate (1 M) at 20 µL/min for five minutes. After the injection of regeneration solutions the baseline was allowed to stabilize for at least 45 minutes before injecting a new solution of analyte. The functionalization of the sensor surface can be seen in **Figure 5.2**.

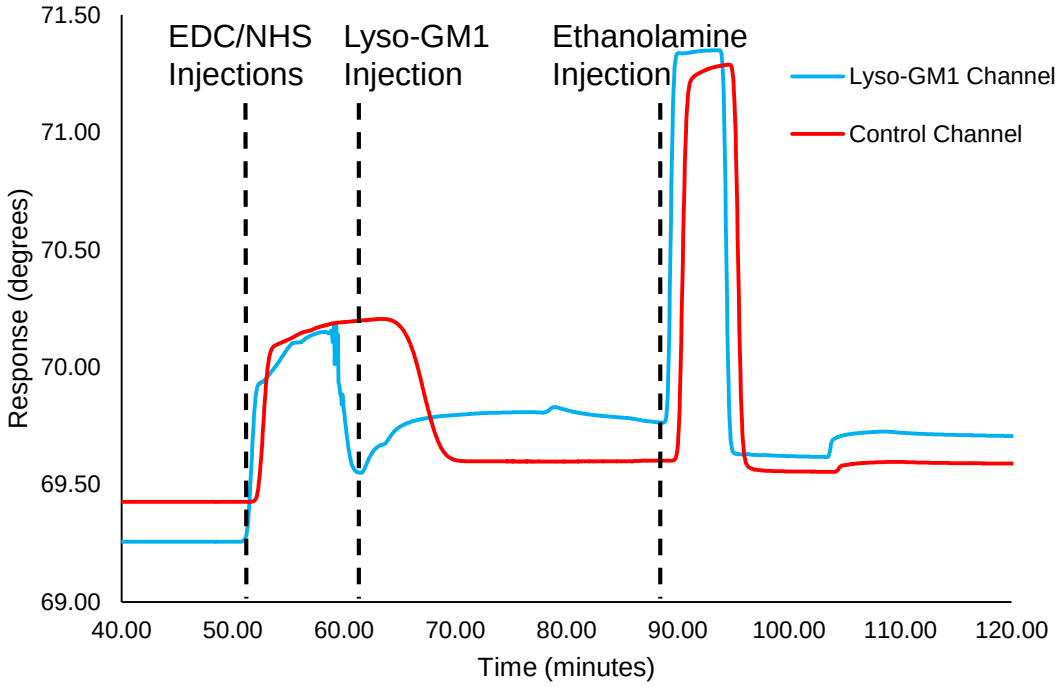

Figure 5.2: Functionalization of the sensor surface. First ECD/NHS was injected over a cleaned surface. Lyso-GM1 was then injected over one of the flow channels. Finally, both of the channels were blocked with ethanolamine.

All the data collected from the SPR instrument was formatted and exported with BioNavis Data Viewer. Centroid data was used as the measurement of binding to the surface as it was found to have the lowest measurement noise and the highest sensitivity. The reference channel was subtracted from the experimental channel in all data collection such that the binding data only captured the specific binding of the aptamer to the glycan. Saturation binding curves were developed from the binding interaction curves and analyzed by GraphPad Prism (GraphPad Software Inc., La Jolla, CA) with a specific 1:1 binding model. Aberrant curve spikes were removed from the data to facilitate the rate constant curve fitting process.

5.2.5. Isothermal Titration Calorimetry (ITC)

Aptamers were also characterized for their binding parameters through isothermal titration calorimetry (ITC). In ITC binding constants and the thermodynamics of bindings are obtained by diluting and injecting the ligand into a sample cell. During this interaction, the instrument maintains constant

temperature and records the amount of power needed to maintain a constant temperature. Thus, the data consists of a series of power spikes of varying heights depending on the dilution of the injection. These spikes can be integrated over time to get the heat of the interaction between the macromolecule in the sample cell and the ligand, which can also be correlated to the molarity of the injection and fitted to a sigmoidal curve to obtain the dissociation constant. With the dissociation constant and enthalpy of interaction, the Gibb's free energy and entropy can be found through the following equation:

$$\Delta G = -RTlnK_a = \Delta H - T\Delta S$$

Where G is the Gibb's free energy, R is the gas constant, T is temperature, K_a is the association constant, H is the enthalpy and S is the entropy.

Aptamers were dialyzed in 2 L of selection buffer (PBS with 2 mM $MgCl_2$) with a Tube-O-Dialyzer for 24 hours. Aptamer (300 µM) was used as the ligand and glycan (30 µM) was used as the macromolecule in a MicroCAL ITC 200 instrument. First aptamer was loaded into the syringe and injected in a series of dilutions into selection buffer to provide the heat of dilution. These injections were used as a reference for the aptamer-glycan interaction. Then aptamer was injected in a series of dilutions into the glycan macromolecule. The buffer reference was subtracted from the glycan-aptamer interaction curves. The resulting curves were analyzed in Origin (OriginLabs, Northampton, MA) for thermodynamic and binding constant information.

5.3. Results and Discussion

This section introduces the results of the SELEX process for the three ganglioside targets and the glycosylated peptide. First, it is confirmed that SELEX was completed on chip as designed by analyzing binding effluents from the selection process. Then, the sequences from the selection process are identified and presented. Finally, the binding ability of isolated sequences are assessed using SPR and ITC.

5.3.1. Aptamer Selection

Four rounds of closed-loop aptamer selection were performed on the chip. Aptamers were selected for GM1, GM3, GD3 and glycosylated peptide. For each of the ganglioside cases, solution phase sialic acid was used as a counter as well as ethanolamine blocked beads. For the glycosylated peptide, the counter

target consisted of agarose beads with the same peptide as the target but without glycosylation. A gel electropherogram was used to assess the success of the selection process prior to characterization of the aptamer pool (**Figure 5.3**). Aliquots from the selection washing effluents were amplified by 20 cycles of PCR and imaged on an agarose gel. From the gel electropherogram, the bright band in the first wash of every selection round indicates that weakly binding DNA is washed off of bead surfaces during the early wash. While, the decrease in band intensity in the final wash of every SELEX round indicates that less DNA is being washed from the surfaces. The increase in band intensity from the final wash of one SELEX round to the first wash in the next round of SELEX demonstrates that the PCR amplification, which occurred between these rounds, was successful and increased the amount of DNA such that the SELEX process could continue on-chip. Also, the increase intensity from the last wash of the final round to the elution suggests that strongly bound DNA strands that could not be removed from washing were eluted by the increase in temperature and could be collected for further analysis.

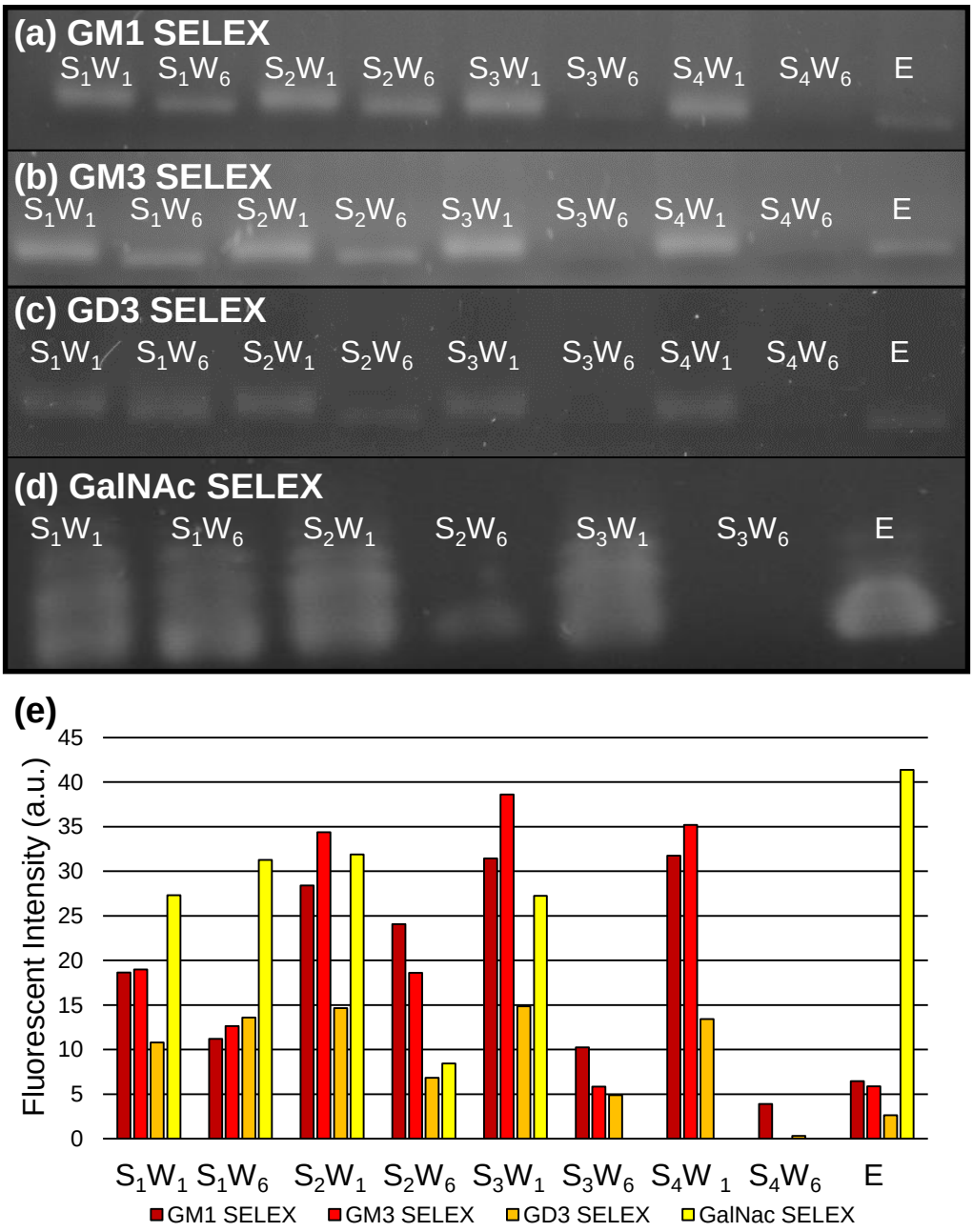

Figure 5.3: Gel electropherograms from the selection process for glycan targets. (a) GM1 SELEX eluents. (b) GM3 SELEX eluents. (c) GD3 SELEX eluents. (d) GalNAc SELEX eluents. (e) Measured band intensity from (a)-(d). (a)-(e) labeling is as follows, S_1W_1: Selection round 1, wash 1; S_1W_6: selection round1, wash 6; S_2W_1: selection round 2, wash 1; S_2W_6: selection round 2, wash 6; S_3W_1: selection round 3, wash 1; S_3W_6: selection round 3, wash 6; S_4W_1: selection round 4, wash 1; S_4W_6: selection round 4,

wash 6; E: elution. Note the GalNAc SELEX consisted of three rounds of selection so round 4 bar graphs in (E) omit GalNAc information.

5.3.2. Sequencing

The resulting pool from the SELEX process was collected and sequenced. Approximately 28 clones were chosen at random for sequencing (Table 5.1). From the sequencing results, it can be seen that while the library did not fully converge onto a few sequences, repeated sequences were present for each target indicating the pools were converging. Furthermore, the SELEXs for different targets did not yield overlapping sequences. Thus, the resulting sequences were unique to each target and appreciable library contamination was not observed. Four aptamers candidates from each pool were selected based on shared motifs and synthesized to be further characterized for their binding affinities and specificities.

Table 5.1: Sequences for Ganglioside SELEX

GM1 Sequences	
GM1S1	TGGAGTTTAAGGTCTCATTCTTGGATTACGGGACTTAAG
GM1S2	TTCCGGTTTGTTATTCGGGTATCGACATAAATAAGTGTAA
GM1S3	GGGGGTGCTATGTACGGTTGGTTGACTGTAGGGCTAAGGC
GM1S4	CAATAGCAATAGGAATCTAATTGTCAAGTGTGCTTCTCTG
GM1S5	AGTTTGGATCCACGTTCCCTAGAGCTGAAGATGGCATCGG
GM1S6	TTGAGTCGCGTCATTATATTCATTGTCAAGGCTTTAAACA
GM1S7	TTGGATTATTTGAAGTATATTTATTTTAGGCTAATAATTA
GM1S8	TCATCGATCTTGTTTTGTGGGTTATGTTGTAATATTCGTC
GM1S10	AAAGACCGGGTGCCTGGGTAGATGTTGCGGGGATAATTAG
GM1S11	AAGAACCGTACGCTTTAAAAATCATTAAGTGAGTTTCTAA
GM1S12	TCGTCCTTAGTTCGAAAGCACTTGGTTTATCGGCAACTGT
GM1S13	AGCCCGCGAGGTTGCACAAGACAGAGAGTCACAACGGCTC
GM1S14	TTTGGCGCGCACCTGTAGCTCTACATCTTGAAGCGGTGAG
GM1S15	CGAAGGTGCTTTTATACGAGCCTATCTTCGTATTCGTTTG
GM1S16	TATTTGGCTAAGAGATGACTGTCCGCCTGCCGAATAAGGT
GM1S17	TGATTAGGCAAATGGCCACTTCTAGTGCGCGGATCGTTGG
GM1S18	TGATTGGGCTTAGATTAATGATTCAGGACTACTGTCTTGG
GM1S19	TAGTTAACGTTTTTACCTCAAAAATGTGTATGAGTGCGGC
GM1S20	GCCATGTGTTGGTCTTCTAAATGGTTGAGGTATTGCCGCG
GM1S21	ACCTAATCTTAAGCTTTGGGACTATGCTCCATACCTGTAT
GM1S22	AGTTTGGATCCACGTTCCCTAGAGCTGAAGATGGCATCGG
GM1S23	TAGAGGTCAATACAACTTTTAACGAGTATGCCGAATCGTT
GM1S24	ATCCTTCTTAGTCACAGGATCAACCGAAGAGGCCGTTCAT

GM3 Sequences	
GM3S1	CTGCAGAACTATGG
GM3S2	TCCAATTTTAACAGATCTTCTTTCTCTGTATCTTTTCTAT
GM3S3	TTATTTACGTAGGGCTAATCGTAGTTTTGCTGACGTAGTT
GM3S4	TAGCAATAGAAATTTATAGTTAACAACCTTTGATTACGTA
GM3S5	CAATCCCCTGTGACACTACCAGTCACGGTACGAGTTACGT
GM3S6	TCCTTTGAAAAGCTAATCTACGGGCGGATCCATATTATGG
GM3S7	GCTGGTTACCTTTGTTTGTTGTACATAGTTTTTCACACGT
GM3S8	TCTATGCCTTGTTGTTTTAGGTATATAGATTTAGGCCCTG
GM3S9	GCACAGACTAGCATGACGTGAAAGGTAGGTAGGTGGGTTA
GM3S10	CCGTAGTTAATGTCATTATTGGGTAGCCAGACGTTAAGCA
GM3S11	CGCCTTTTTTGTTAAGTTGACTTGAGTTTCCTTATTATCT
GM3S12	ATAGGTTTTCAGGATTGTCCTGCTATTCATTTGTCCATTG
GM3S13	ACTGCCTTCTTGAGTTCTTGGGTTTTACCACTTCACAGGG
GM3S14	GATTTGATTAGTTTGCCATGATTTTACCGTAAGCTTAACC
GM3S15	GGCCAAGTACGGCAAGCAATATCGCTAATCGTACTCTCGA
GM3S16	TTTTATACTCTGGTAATTTACTCTATAGGATTCATGCAAT
GM3S17	CAGATACTTGACTAGCTGTTTATGGATCGTATTAGCGCTT
GM3S18	AGGGATCACAGGATAACTGAGTTATCATGGAATCNATAAG
GM3S19	AACGTTACGTCTCGTTATATGAATTAAGGACTCCGACAGA
GM3S20	CTATATGGAGGGGGAAACAAAACTTATCGTCATTGAAAGC
GM3S21	ATAAGATACTTTCTTTCTTTAGTACAAACTAATGATTTAA
GM3S22	CGTATCCTTTTGAATAGTTGTAATATACTTTTTCTGCAGG
GM3S23	ATAACATGAATATCTAAGATATATTTTTAATGAAGTATCT
GM3S24	TTTCGTGGGGCGATAGTACGACGATAATCGCGGAACGGCG
GM3S25	GGTGTAAAAGATAAGTGAAGCCTTGTTGTATTAGTTGGTG
GM3S26	GGGGATATGAGCTTCTCTTAAAAATTAATGCACCATTCTA
GM3S27	CCAATATAATTATTTGTCTCTTACCCTCACGGTAGAGTCT
GM3S28	AACCTCCAATTACTAAGATCCTACAATAATTGTCTCACTA
GD3 Sequences	
GD3S1	TAATATCGCTAGTGCAAACGGATCTTAGGTAGGGCAGCAA
GD3S2	CTCTGCGCATGCAGATTTTTTACAGGTCCTTGTAAGCCTT
GD3S4	GCAGGGTAAGTCCGACGGTATCGTTTGAGCGAGCTCGATA
GD3S5	TATATGTTTGTTTAGATAGAATTCACCTGACTCAGGGGGA
GD3S6	GTTTTTCGCTGTCAAATCTCGCAATTATACGCTAACCCGG
GD3S7	TGAGTAAGCCAGCAGGGGAGATGTGAGTGGGGAAGTCGGT
GD3S8	GTTCGTCGGGTAACTTAACGACGTACCAGTTCGGCTGGGA
GD3S9	GGTAGCTCTTATAATTACATTAATCTTGTTTTATAGGTTA
GD3S10	CTGGTGGATATCAGCTCGGTAGGCTGTGTGATCCTGACGT
GD3S11	AGTATCAACACTCTTTAGTAGCGCACGAAGATTACGTTTA
GD3S12	GCTATGTTACAACAAAGGCAAGTTCCCTAACGGGATCGCC

GD3S13	TTGCTCCCGCAAAGTAATTAAAGCATGTGTGTACTAGCAA
GD3S14	AGAATAAATTGCTTGTTCTTCATAGCCGGTACGGTGAACG
GD3S15	TGAGGTTTTCTGAGTATCATGCCGAACGGTGACCTGCATC
GD3S16	GCTTGGTATTGATCTAATTCCCGCCTGCCAGGAGTGTAAT
GD3S17	GTTATTGGGCATTCGATATTAGAGCATAAAGCCCACTCGG
GD3S18	GTGATCACTTCTTTGGAGCAGCCAGTAGACATTTCATACG
GD3S19	TTGTAGGCTGGTCACAACAGACGGCCAGGTTAGCACAT
GD3S20	CGCATGGCCCGCCGTCAGGGGCTTTAGGTGGCAGGTGGGG
GD3S22	TAGAAACCTACCTCGAGTTCGCGCTTCTCACGTGGACTTC
GD3S23	GTGACATGTGTGTTTTTATTCGGCAGATACGCGTTAAGTA
GD3S24	AATGAGGGTAGCGGTTTGAGCAGACGTTTCTAAGCCCATG
GD3S25	ATCAATGTCATGGCGTGTTAAGAACAGTGCCATTAACTTT
GD3S26	TCGCCTGGTGGCTAACTTAAATCCAACGTCTAACTGTTGC
GD3S27	TCATGGGCGTATTCCGCGCGCACGCGGGATATAAGGGAAC
GD3S28	TGTGAGGTTTTACAACTAGAACACATCTTCTGTCGGGACG
GalNAc Sequences	
GalNAcS1	TCATGGATTACACCGTATGAATCAGCATCGCAGTTTTACA
GalNAcS2	CGGACAAATGAAGTTGATTGGTTTGAAGTCTAGGTGAGAT
GalNAcS4	CACTTTATCAGTTCGATACCGTGATGGCTAGTGTAAGGGT
GalNAcS5	GGAGGCTTAGTGGGGCGTAGCGCATTTCCAGCAACAAGCA
GalNAcS6	GCTTTGATGTCTGTGTAGATCTATACTAATGGCCCCGTAG
GalNAcS7	ACTAGTCCAGGTGAACGCCGTTGGGGGTTGCCCGGGCTAA
GalNAcS8	CCATGGAAACTTGGTGGGTTCTGGGATACCCCATTCTATT
GalNAcS9	CTAGCGTAAATATGGGGAGGTCTGCGTCTGTCTTTGCTAC
GalNAcS10	TGGAGGAACACTTAAGCACGGCGACAAGATGCTGCGGTGT
GalNAcS11	ATTATGAACTCTCAACATGGCTCGAAATACCCGGTTTTTT
GalNAcS12	AACATATTCGAGGCCCTAAGCTCACTTCACTACCAAGCAT
GalNAcS13	CAAGTGTAGCAGACAGTCGGAAGAGGGACTGCGTCGCAGG
GalNAcS14	GGCTAGTGGGTAACATCAATTCGCCCTAGCGGTTGCCCCA
GalNAcS16	TTGAACTTTTAGCCGCCGATAGTAGCTTGTTATTGAAGTA
GalNAcS17	TCCTTAAAATCGGGGAAACATCGCGTCAACAAATAACTCCCG
GalNAcS18	CACATGGGACAAGTTTACTCGCACCGAGTACTGGGACACC
GalNAcS20	TCGCGTAGCAATCGGTGCGAACAGGGCGTGCAATAATGGG
GalNAcS21	GTGCTGTCCCGAGCACACACTTCTGAGTTATTTAATCACT
GalNAcS22	TTGTTATATTCGAATTTAGCCTTAATGATCGCGTTTGTGT
GalNAcS23	CTGGATATAATTGCCAGAAATGTCTATCTTCTTGTATTTC
GalNAcS24	TTACTTCTGACGGAACTGGGTCGACGGACTCGACCGGGA
GalNAcS25	TAGTCACTCACAACAAATTTTCTATTCCGTCTTAACGCAG
GalNAcS26	CAGCTGGTTTTTATTTTCCATAGTAATATAGGCAGATTCG
GalNAcS27	TTTGCTCCATGCCGCTTTATTATGATAGGTATGGGGAACG
GalNAcS28	GTCTAGAAGACTTTGGATTGCCCTGAGTATGGGCATGCAT

5.3.3. Lyso-Ganglioside SPR

Aptamer candidates were screened by SPR to determine equilibrium binding constants. Lyso-GM1 and lyso-GM3 were conjugated to the SPR sensor surface and aptamers were driven through the flow channel while binding interaction information was collected. Injections were increased from a low concentration to successively higher concentrations (31.25 nM, 62.5 nM, 125 nM, 250 nM and 500 nM of aptamer). This was repeated three times on the same sensor surface (**Figure 5.4**). Resulting interaction curves were analyzed to discern binding parameters. Sequence GM1S6 was found to have the greatest affinity towards GM1 with a binding dissociation constant (K_d) of 35.23 ± 9.575 nM while GM3S256 was found to have the greatest affinity towards GM3 with a binding dissociation constant of 33.49 ± 3.445 nM. These binding affinities are orders of magnitude lower than known probes for GM1 and GM3 suggesting these aptamers could be used for ganglioside analytical assays. Binding data for the sequences tested can be seen in **Table 5.2**.

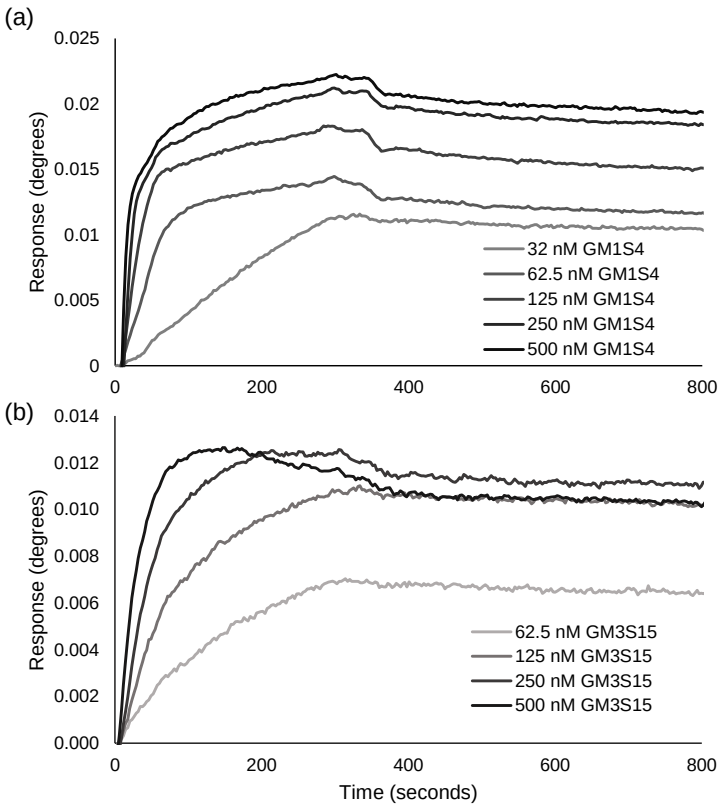

Figure 5.4: Representative surface plasmon resonance responses of various concentrations of aptamer. All curves are the resultant curves after subtracting an ethanolamine control channel response. (a) GM1S4 over a lyso-GM1 surface. This was repeated three times and yielded an average K_d value of 49.6 ± 9.978 nM through curve fitting with a 1:1 binding model. (b) GM3S15 over a lyso-GM3 surface. This was repeated three times and yielded an average K_d value of 43.59 ± 8.58 nM.

Table 5.2: Binding affinities of lyso-GM1 and lyso-GM3 aptamers towards their target molecule.

	Average K_D (nM)	Standard Deviation (nM)
GM1S4	49.6	9.978
GM1S5	88.79	23.05
GM1S6	35.23	9.575
GM1S16	52.58	7.937
GM3S3	47.45	13
GM3S15	43.59	8.58
GM3S21	64.84	23.44
GM3S25	33.49	3.445

The binding of these aptamer candidates were compared to a scrambled sequence. Triplicate injections of 500 nM aptamer or scrambled sequence were performed and the average response from the 100th second to the 300th second was recorded and compared. All of the aptamers all displayed much greater binding to the target than the scrambled sequence (**Figure 5.5**).

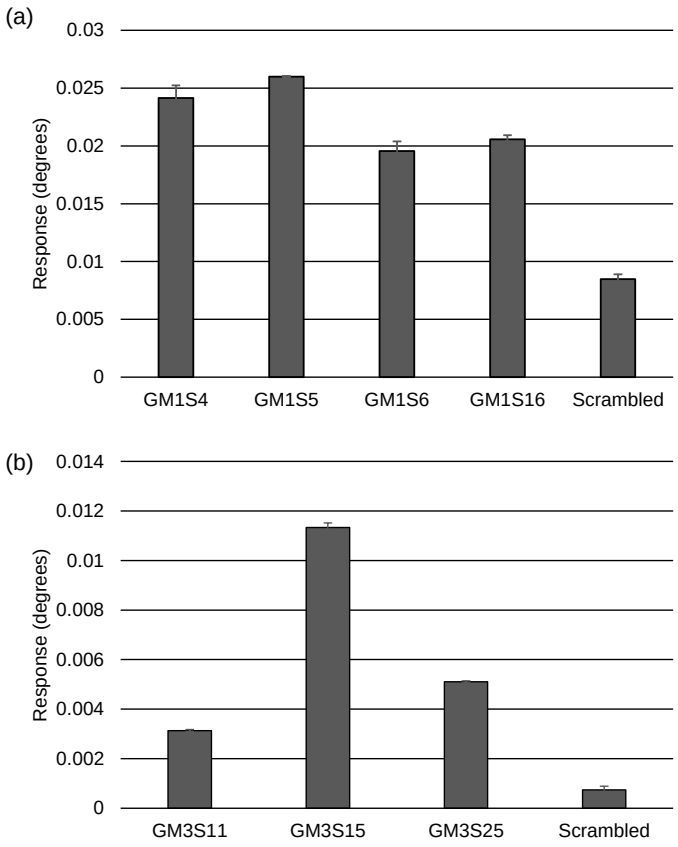

Figure 5.5: Sequence binding during a 500 nM injection compared to a scrambled control. All sequences were injected three times with error bars representing the standard deviations from these injections. (a) GM1 aptamer sequence injections over a lyso-GM1 surface. (b) GM3 aptamer sequence injections over a lyso-GM3 surface.

5.3.4. Full Ganglioside SPR

Full gangliosides were also investigated for the GM1, and GD3 aptamer candidates. For these cases, aptamer was functionalized to the SPR sensor surface by biotin/streptavidin interactions and the ganglioside was introduced in solution while binding interaction data was collected. From these studies it was found that GM1S4 had an affinity of 741 nM towards the intact ganglioside GM1 with minimal cross reactivity to the other gangliosides (**Figure 5.6**). Similarly, GD3S16 had an affinity of 2.48 µM with limited cross reactivity.

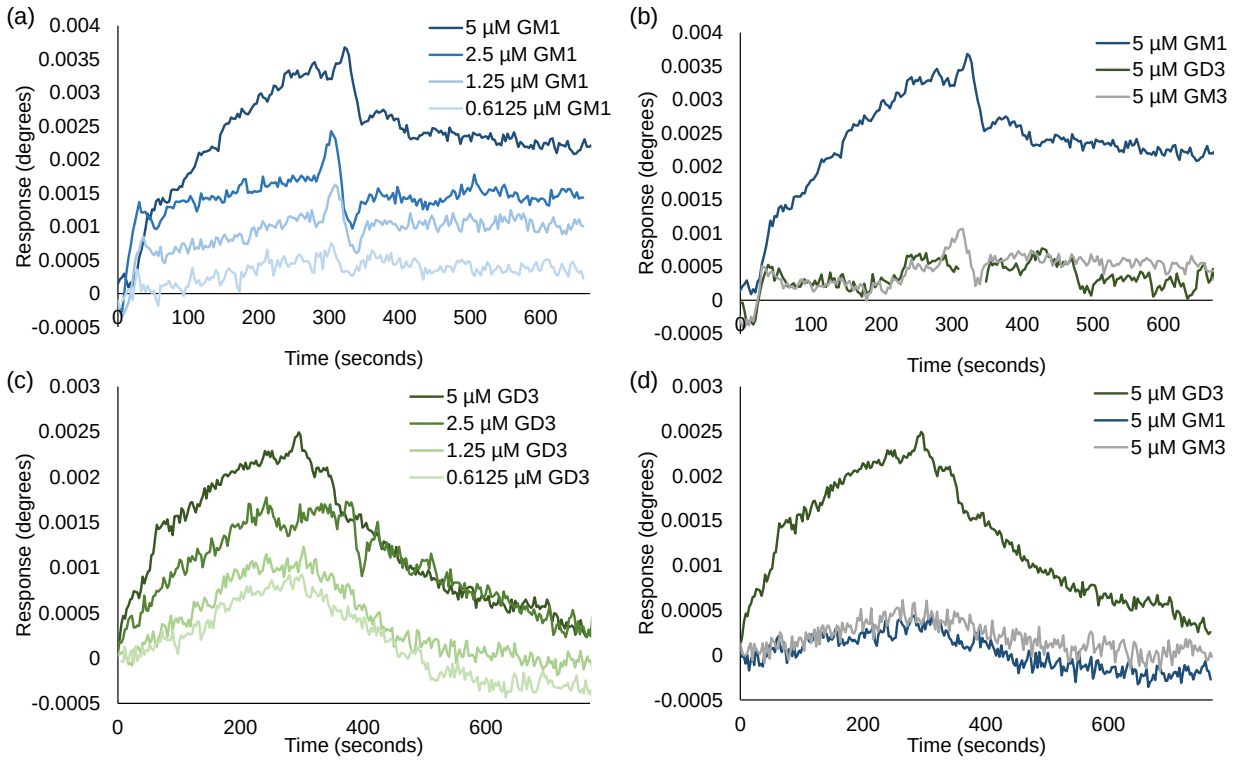

Figure 5.6: (a) SPR curves for GM1 aptamer sequence 4 with various concentrations of full GM1 ganglioside injected. (b) SPR curves for GM1 sequence 4 responding to 5 µM injections of GM1, GM3 and GD3. (c) Response curves for GD3S16 towards various concentrations of full GD3 ganglioside injections. (d) SPR curves with GD3 sequence 16 on the surface and 5 µM of GM1, GM3 and GD3 injected.

Full ganglioside binding was challenged by the inherent tendency of gangliosides to form micelles. Micelles are an aggregate of gangliosides in a sphere or bilayer sheet. Once in this form the molecule is no longer in a similar orientation to that used for the aptamer selection process which interferes with the aptamer's ability to recognize the target. Micelles form at micromolar concentrations that coincides with the measurement range needed for dissociation constant determination in the SPR instrument [181]. On the other hand, lyso-GM1 has a stearic acid removed so micelles are not possible and is bound to a solid support preventing micelle formation in any case. The discrepancy between lyso-GM1 binding affinity (2.5 nM) and full GM1 binding affinity (741 nM) may be explained by the formation of micelles interfering with the aptamer binding to the target. The test format could also contribute to the difference in binding as the

lyso-GM1 was immobilized while the aptamer was in solution. It is possible the immobilized GM1 is more recognizable by the aptamer, and indeed that would match selection conditions more closely. Furthermore, it is possible the aptamer loses some recognition ability when constrained to the surface of the sensor through the biotin-streptavidin link.

5.3.5. Isothermal Titration Calorimetry

Aptamer candidates that demonstrated binding affinity towards the target in SPR were examined by ITC. A high concentration of aptamer (300 uM) was used in the syringe and diluted into a lower concentration of the sugar group of each ganglioside remaining in the cell (30 uM). Each binding pair used a series of 25 dilutions. Results were compared to injections into a reference cell (**Figure 5.7**).

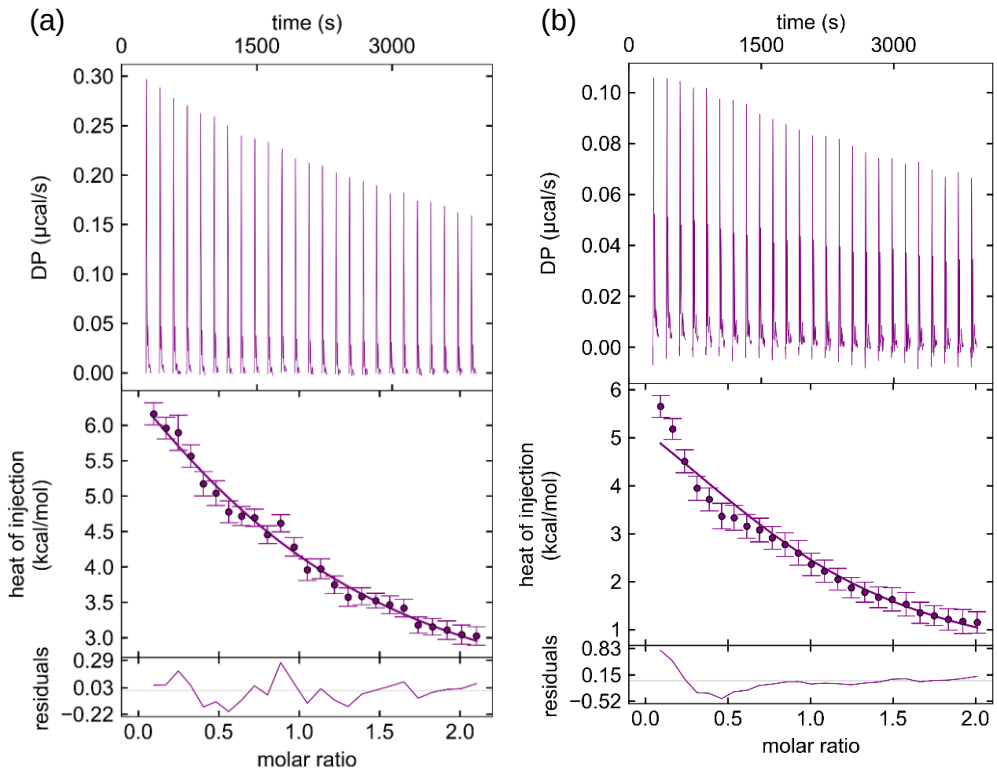

Figure 5.7: ITC curves for gangliosides. (A) ITC curves for GM1 ganglioside with GM1S4 in the syringe. (B) ITC curves for GM3 gangliosides with GM3S16 in the syringe.

For GM1 a binding affinity of 18.76 µM was found with a ΔH of 14.92 kcal/mol. The ΔH indicates this was an exothermic reaction. Exothermic reactions are not uncommon for aptamers and they typically

suggest an entropy driven binding process. Electrostatic based binding is possible for entropy driven processes and that can also drive aptamer-target recognition. The binding affinity characterized by ITC was similar to the full ganglioside binding affinity found through SPR but indicated much weaker binding than the lyso-GM1 binding in SPR. This could be because the aptamer does not bind as well to the sugar group as it does to the entire molecule.

For GM3 the binding affinity was found to be 17.51 μM with a ΔH of 8 kcal/mol. Again the reaction was exothermic which could indicate that the aptamer binds to the GM3 target through electrostatic forces. The GD3 aptamer did not bind in the isothermal titration calorimeter. This could be overcome with full ganglioside injections in the ITC; however, micelle formation may prevent the binding of the aptamer to the target at these concentrations. ITC fluid cells with lower concentrations of ganglioside may overcome the issues presented by micelle formation; however, lowering the concentration may move the measurement outside the useful range to determine the binding affinity of the aptamer candidates. The binding affinities of the sequences with the highest affinity towards the ganglioside target for the various formats tested are summarized in **Table 5.3**.

Table 5.3: Aptamer affinity towards gangliosides in various formats

	Lyso-Ganglioside Dissociation Constant (nM)	**Full Ganglioside Dissociation Constant SPR (μM)**	**Sugar Group Dissociation Constant ITC (μM)**
GM1	49.6	0.741	18.76
GM3	43.59	NA	17.51
GD3	NA	2.48	NA

5.3.6. Glycosylated Peptide

A glycosylated peptide was characterized using SPR. The binding assessment was considerably more straightforward than the gangliosides considering the size of the glycosylated peptide. Biotinylated aptamer was conjugated to the streptavidin sensor surface through the biotin-streptavidin affinity interaction. Various concentrations (62.5 nM, 125 nM, 250 nM, and 500 nM) of glycosylated peptide were then injected. This was repeated using the non-glycosylated version of the peptide such that binding dissociation

constants were found for the target molecule and for the counter target molecule (**Figure 5.8**). Binding data was found for three sequences that were selected from the cloning (**Table 5.4**).

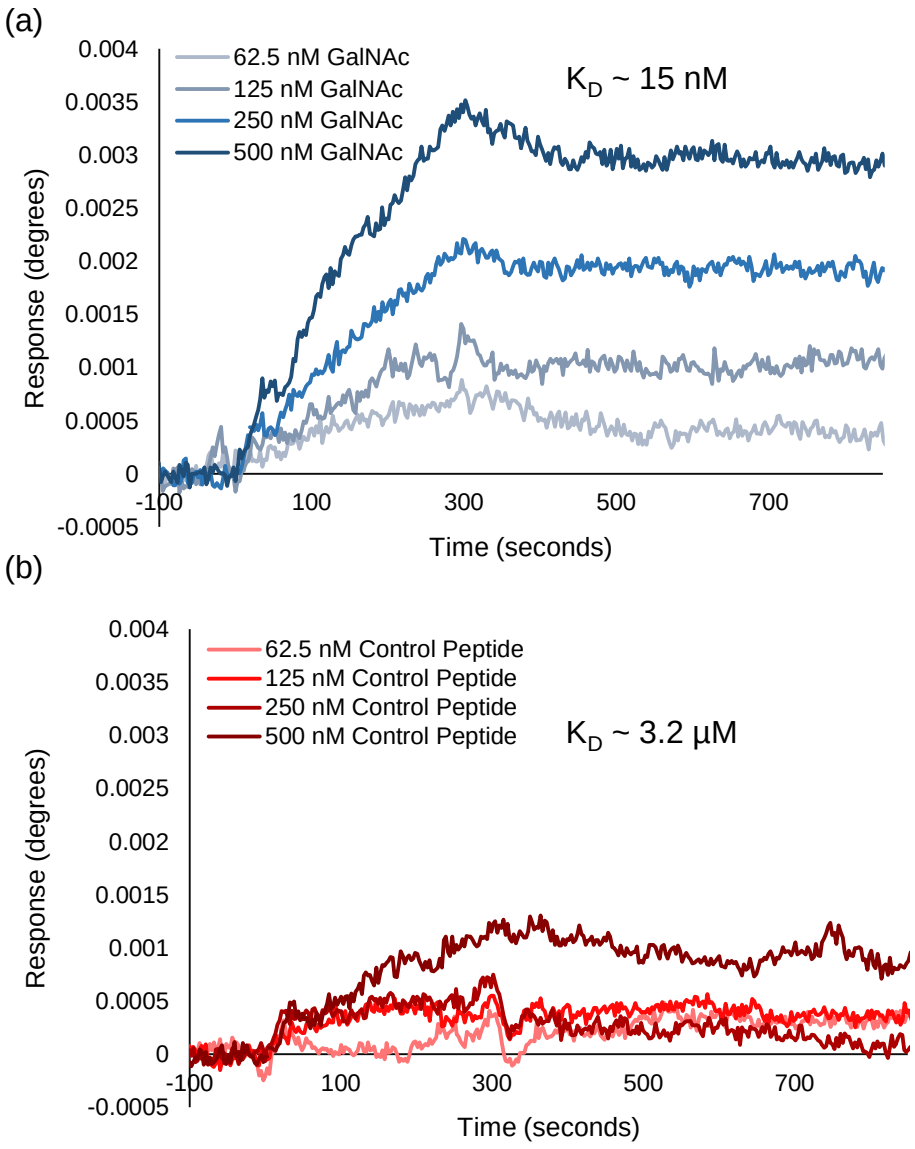

Figure 5.8: Representative SPR curve for peptide SELEX. (A) Injections of GalNAc peptide on a GalNAcS9 surface. (B) Injections of the same peptide without glycosylation over a GalNAcS9 aptamer sequence surface.

In all cases, the aptamer candidate bound with higher affinity than the control molecule. The aptamer with the highest affinity was GalNAcS4 with an affinity of 15 nM compared to an affinity of 3.2 µM

for the non-glycosylated peptide. Thus the aptamer had ~200 fold higher affinity to the control molecule over the counter target. Therefore, the device is capable of isolating aptamers with preference for a glycosylation pattern in peptide samples.

Table 5.4: Binding affinities of aptamers towards glycosylated and non-glycosylated peptides.

	GalNAcS4	GalNAcS9	GalNAcS22
Average K_D (nM) towards GalNAc Peptide	15	59	172
Average K_D (μM) towards non-GalNAc Peptide	3.2	18.5	250

5.4. Conclusion

Aptamers were isolated for four different targets, each taking approximately one day to isolate with a microfluidic approach. Aptamer candidates are affinity selected, counter selected, amplified, and conditioned back to single-stranded for further rounds of SELEX. The microfluidic device performed four rounds of SELEX for the ganglioside targets and three rounds of SELEX for the glycosylated peptide. All selection procedures used less than 500 μg of target and counter target. After isolation the aptamer candidates were characterized for their affinity and specificity. Aptamers with nanomolar affinity towards GM1, GM3 and the glycosylated peptide were isolated, while aptamers with micromolar affinity towards GD3 were isolated. It was further discovered that the format of the binding test can influence the binding affinity of the aptamer towards its target. Thus it is likely the binding affinities of the GD3 aptamers towards lyso-GD3 are much lower.

In the future, additional binding characterization will be performed on the GD3 aptamers. In particular, lyso-gangliosides will be prepared and tested on a CMD SPR sensor surface. The lyso-gangliosides can also be investigated by ITC without the concern for micelle formation. Furthermore, the ability of the aptamers to recognize targets in clinically relevant assays will be pursued. Of particular interest is the binding of GalNAc peptides in aptameric ELISA formats.

Chapter 6: Personalized Selection of Aptamers against Multiple Myeloma Proteins

6.1. Introduction

Multiple myeloma (MM) is a cancer of plasma cells primarily found in the bone marrow (BM). A common blood cancer, MM affects nearly 96,000 in the U.S.. Roughly 0.7% of men and women will be diagnosed with MM at some point during their lifetime [182]. The goal of treating MM is to achieve complete response (CR), defined as the absence of the hallmark monoclonal immunoglobulin (M-Ig) protein by immunofixation and less than 5% plasma cells in bone marrow (BM). Of patients who achieve CR, those who are negative for minimal residual disease (MRD), i.e., the presence of small numbers of myeloma cells in a patient's body [183], have better survival than those who are MRD positive [184]. Detection and monitoring of MRD is hence emerging as a cornerstone in selecting and guiding therapeutic strategies.

Sensitive detection of M-Ig in peripheral blood remains an unmet medical need. Currently available methods have a low sensitivity as they are not tumor-specific and are limited by background polyclonals and physiological variations (e.g., infections, renal impairment or recovery, and light chain ratio variability secondary to neoplasms). Serum protein electrophoresis (SPEP) and immunofixation electrophoresis (IFE) are current 'gold standards' for serum-based MM diagnosis and follow-up, but do not allow MRD detection. SPEP, which visualizes migration of monoclonal proteins in the γ, β, or α_2 region [185], has a limit of detection (LOD) of 500-2000 mg/L [186]. IFE (LOD: 100-150 mg/L [187]) allows identification of specific types of heavy (IgG, IgA, IgM, IgD, IgE) and light (λ or κ) chains, but is incapable of M-Ig quantification. Other related methods are also inadequate. For example, quantification of free light chain (FLC) ratios [188, 189] (LOD: ~1 mg/L [186]) is limited by background monoclonals, can be falsely positive due to deteriorating renal function or infection, and apply primarily to diagnosis and follow-up of light chain-producing MM (LCMM, 20% of MM [190]). Allele-specific oligonucleotide polymerase chain reaction (ASO-PCR) in peripheral blood, currently under research, has been found to be comparable to SPEP/IFE in sensitivity [191].

Affinity receptors targeting variable regions (i.e., 'idiotypes') of M-Ig would allow sensitive M-Ig detection in serum. Idiotypes are tumor-specific and unique to the patient [192]; an affinity receptor that specifically recognizes an idiotype would hence allow low concentrations of M-Ig to be detected by effectively rejecting the effects of unspecific background proteins. The clinical application requires that

idiotype-targeting aptamers be generated for each individual patient in a timely fashion. Unfortunately, this is impractical with conventional receptors such as antibodies, which are costly and time-consuming to produce and have poor batch-to-batch reproducibility. This is also impractical for aptamers which are identified with labor-intensive and time-consuming conventional SELEX platforms. Ultimately, conventional SELEX techniques involve extensive manual handling of reagents, requiring usually a month to complete just 10 cycles. Robotic automation can alleviate this issue but is cost prohibitive [129]. Alternative methods using affinity selection in solution followed by capillary electrophoresis (CE-SELEX) [100, 101] can reduce the overall processing time, but still requires tedious manual handling. Instead, rapid and efficient aptamer isolation exploiting microfluidic technology to create miniature and integrated SELEX devices at low cost, with minimized reagent consumption and in much shortened time is exploited. Such devices produce aptamers with high affinity due to intimate molecular interactions in microscale geometries

Here we apply the approach developed in Chapter 4 to rapidly isolate aptamers with high affinity and selectivity towards a myeloma patient's M-Ig. First, Rituximab, a monoclonal IgG antibody used in the treatment of cancer, is used as a model IgG monoclonal. Rituximab is chosen because of its availability to be acquired in purified form and because its immunoglobulin type (IgG) matches the most prevalent type of multiple myeloma (IgG myeloma) [193]. After isolating and characterizing aptamers with affinity towards Rituximab, we apply the protocol to isolate aptamers with affinity towards a myeloma patient's serum M-Ig (**Figure 6.1**). A multiple myeloma patient's serum sample is collected and conditioned to remove non-IgG type proteins, and bound to beads which are then directly injected into the device. Six rounds of SELEX were performed on the chip to generate high affinity aptamers without offline processes. Collected samples from each round of SELEX were comprehensively characterized through high throughput sequencing techniques. These aptamers were synthesized and screened for their binding abilities. Ultimately, an aptamer that can be used in an aptamer formatted Enzyme Linked Immunoassay (ELISA) to detect the presence of the cancer patient's M-Ig is rapidly isolated (within a day) while consuming only modest amounts of a patient's serum sample (<100 µg).

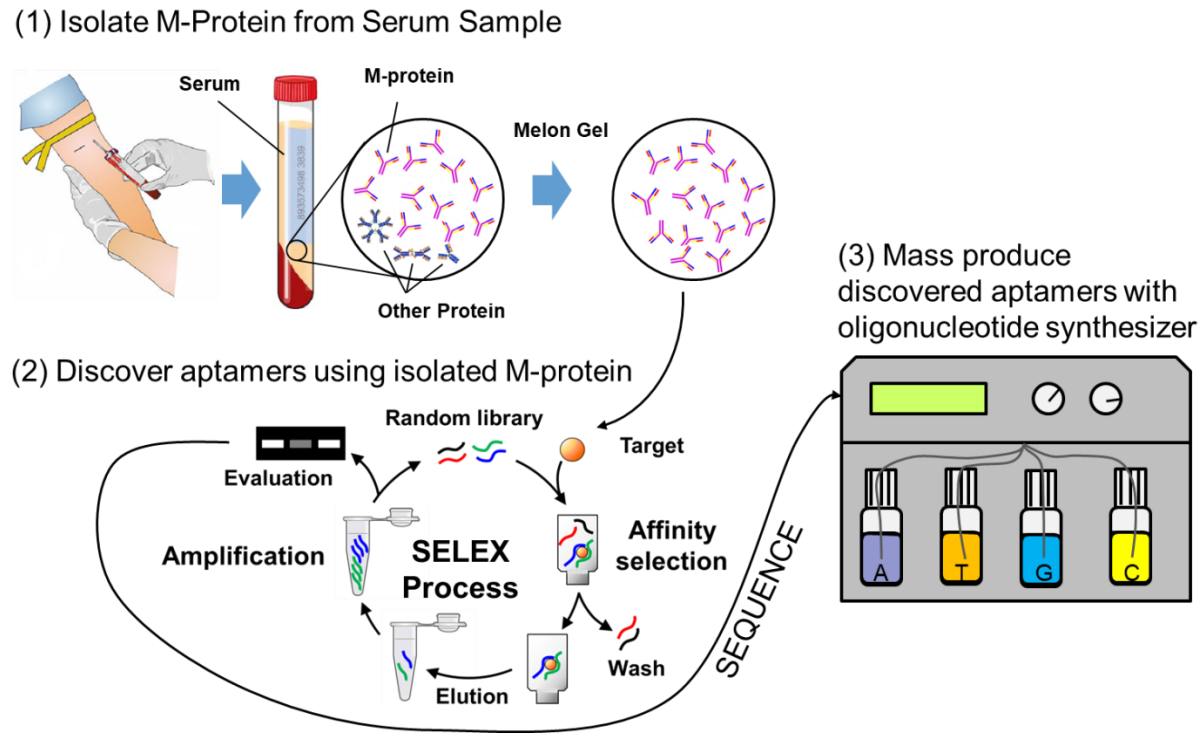

Figure 6.1: Aptamer selection process for a multiple myeloma patient. First the patient serum sample is conditioned to remove non-IgG proteins. The remaining IgG proteins are then bound to beads and used as the target in the microfluidic SELEX process. The sequences are evaluated through high throughput sequencing techniques and high potential candidates are synthesized for analysis.

6.2. Materials and Methods

6.2.1. Materials

$MgCl_2$, human polyclonal IgG and molecular biology grade water were purchased from Sigma-Aldrich (St. Louis, MO). Deoxyribonucleotide triphosphates (dNTPs) and GoTaq Flexi DNA polymerase were obtained from Promega Corp. (Madison, WI). Protein G ELISA plates, Dulbecco's phosphate buffered saline (D-PBS), Melon Gel IgG Spin Purification kits, GeneJET Purification Kits, Zeba Desaling Columns and streptavidin coupled agarose beads (Pierce Streptavidin Agarose) were purchased from ThermoFisher (Waltham, MA). Streptavidin surface plasmon resonance chips were purchased from Nicoya Lifesciences (Kitchener, ON, Canada). MiSeq 300 v2 kits and PhiX Control were purchased from Illumina (San Diego, CA). Next generation sequencing Kappa Hyper Prep Kits were purchased from Roche (Basel, Switzerland). AMPure XP magnetic purification beads were purchased from Beckman Coulter (Pasadena, CA).

Randomized oligonucleotide library (5’ – TGC CAG CAT CGT AAT AGC CTC – 40N – ACC AAG TGA ATG AGC GGT ACG– 3’) and primers (Forward Primer: 5' – TGC CAG CAT CGT AAT AGC CTC -3', and Reverse Primer: 5' – CGT ACC GCT CAT TCA CTT GGT – 3') were synthesized and purified by Integrated DNA Technologies (Coralville, IA). Rituximab was acquired from Milan Stojanovic and multiple myeloma patient serum was acquired from Tilla Worgall. Protein G beads were purchased from Santa Curz Biotechnology (Dallas, TX). Barcodes with Illumina adapters were purchased from Bioo Scientific (Austin, TX).

6.2.2. Selection of Aptamers towards Model Monoclonal

The general protocol was first implemented with Rituximab, a humanized IgG monoclonal antibody used as a pharmaceutical. Selection and counter selection beads were first prepared. Rituximab incubated for 30 minutes in Protein G beads which had previously been rinsed three times with selection buffer. The beads were then washed 5 times with selection buffer. Polyclonal IgG beads was used as the counter target and were prepared by incubating pre-rinsed polyclonal IgG with Protein G beads for 30 minutes and washing. Reverse primer beads were prepared as discussed in Chapter 4.

The general procedure followed the framework in Chapter 4 with some modifications (**Table 6.1**). The Rituximab modified beads were used for a target in affinity selection, and the polyclonal IgG beads were used as a counter target. The first rounds of SELEX consisted of selection with the Rituximab beads and then direct transfer to the amplification chamber for PCR amplification. Counter selection was not used in this first round to reduce the potential for losing sequences which present at low copy numbers early in the SELEX process. The second round of SELEX consisted of positive selection with the Rituximab beads, counter selection with bare Protein G beads, and PCR amplification. A Protein G counter was used in the second round to remove aptamer candidates which have an affinity for the matrix used to immobilize the protein. The third and fourth rounds of SELEX included positive selection with Rituximab beads, counter selection with polyclonal IgG and PCR amplification.

Table 6.1: Selection parameters for Rituximab SELEX.

Round	Wash Flow Rate	Wash Time	Counter Selection
1	20 µL/min	35 min	None
2	20 µL/min	35 min	Protein G Beads
3	20 µL/min	35 min	Polyclonal Beads
4	20 µL/min	35 min	Polyclonal Beads

6.2.3. Selection of Aptamers towards Patient M-Protein

A myeloma patient's serum sample was first prepared for the SELEX first. Patient serum was purified with Melon Gel following the manufacturer's protocol. The melon gel binds to all serum proteins except IgG allowing extraction of a patient's IgG. Because of the nature of IgG myeloma, the extracted IgG from the patient's serum will be dominated by the monoclonal IgG. The extracted IgG was suspended in selection buffer (PBS with 2 mM $MgCl_2$) and measured by UV-Vis (Implen P300, Implen GmbH, Munich, Germany). Protein G beads were rinsed three times with selection buffer and incubated with the patient IgG for 30 minutes. The beads were then washed five times with selection buffer. Extracts of this process were collected and used to verify successful conjugation by polyacrylamide gel electrophoresis (PAGE). Similarly, counter selection beads were prepared by incubating polyclonal IgG with washed protein G beads for 30 minutes and then washing the beads five times with selection buffer.

With selection beads prepared, six rounds of the SELEX process were performed as described in Chapter 4 with some modifications. First, 20 pmoles of library were used to initiate the SELEX process. A greater amount of starting library amount was used to increase the potential to isolate aptamers with very high specificity. Second, in the first round of SELEX counter selection beads were not used. This was to reduce the potential for losing high affinity sequences that are present at low abundance, as would be expected from library members. The second round used unreacted protein G beads as counter targets. Rounds three to six used polyclonal IgG beads as a counter target. Further, in the final two rounds (five and six) the washing time was increased from 35 minutes (700 µL) to 45 minutes (900 µL) to increase the selection pressure on these later rounds of the process (Table 6.2). Finally, a fraction of the eluted product of each round was collected for analysis by next generation sequencing (NGS).

Table 6.2: Selection parameters for patient monoclonal protein SELEX.

Round	Wash Flow Rate	Wash Time	Counter Selection
1	20 µL/min	35 min	None
2	20 µL/min	35 min	Protein G Beads
3	20 µL/min	35 min	Polyclonal Beads
4	20 µL/min	35 min	Polyclonal Beads
5	20 µL/min	45 min	Polyclonal Beads
6	20 µL/min	45 min	Polyclonal Beads

6.2.4. Sanger Sequencing

Aptamer candidates for the Rituximab target were identified by first subcloning the pool and then sequencing selected colonies from the subcloning using a protocol similar to the presented in Chapter 5. Briefly, aliquots from the aptamer selection process were PCR amplified and purified. The purified product was then used with a TOPO vector kit and cultured onto dishes. Colonies were then chosen from the dishes and cultured. The cultures were then purified with an E.Z.N.A. purification kit, diluted and sequenced by Genewiz (South Plainfield, NJ) through a Sanger Sequencing service.

6.2.5. Surface Plasmon Resonance (SPR)

SPR was used to discern the binding properties of the Rituximab IgG towards aptamer candidates. Biotinylated aptamers (500 nM) were injected over a streptavidin chip (Nicoya, Kitchener, ON, Canada) at a flow rate of 20 uL/min for 5 minutes. After allowing the baseline to settle, a range of concentrations of Rituximab (50 nM, 100 nM, 200 nM, 400 nM, and 800 nM) were injected. Surfaces were regenerated with 1 M sodium acetate between injections. Specificity was confirmed by injecting the polyclonal IgG over the sensor surface. Data from all injections was analyzed by 1:1 model fitting with BIAevaluate (Biacore, Slovakia).

6.2.6. High Throughput Sequencing

For the SELEX used to isolate aptamers towards the patient sample, aptamer candidates from each round were sequenced using a MiSeq platform (Illumina, San Diego, CA). First the collected products of each round were amplified off-chip by PCR and checked with a gel electropherogram. The amplified product was purified and suspended in molecular biology grade water with a GeneJet DNA clean up kit to

remove primers and the amount of DNA was quantified in the resulting solution using an Implen Spectrophotometer (Implen GmbH, Munich, Germany). 250 ng of the amplified product was used with a Kapa Hyper Prep kit and Bioo Scientific barcodes to ligate Illumina adapters. A unique barcode (6 total) was ligated to the product of each round of the SELEX allowing sequences from each round to be discernible in the NGS read file. The ligated product was verified to be of the correct length and to be of high purity by gel electrophoresis and the amount of DNA was quantified with an Implen spectrophotometer.

The barcoded samples were sequenced in two sequencing reactions. The first sequencing process sequenced rounds one to four, and a second sequencing process was used to sequence rounds five and six. Both reactions were prepared with the following procedure. A MiSeq 300 v2 cartridge was thawed to room temperature. Meanwhile, the barcoded samples were combined and diluted to create a 4 nM and 5 µL combined sample pool equally represented by each SELEX round (rounds 1-4 or rounds 5 and 6). 5 µL of 0.2 N NaOH was added to the 4 nM combined pool, mixed and left to incubate for 5 minutes at room temperature. A 1 mL and 20 pM solution was then prepared by adding 990 µL of the HT1 buffer provided by Illumina. A 600 uL and 4 pM solution was then prepared by withdrawing 120 uL from this solution and adding 480 µL of HT1 buffer. PhiX control was similarly diluted in HT1 buffer to produce a 4 pM solution of PhiX. The 4 pM PhiX (120 µL) and combined pool were mixed together to form a 600 µL solution. This solution was injected into the Illumina MiSeq cartridge and sequenced with an Illumina MiSeq instrument.

Raw data grouped by barcode was downloaded from Illumina's Basespace. Aptasuite version 0.8.9 was used to evaluate the reads. From this software the cluster, and sequence analysis modules were used to determine which sequences should be ordered for in vitro testing.

6.2.7. Enzyme-Linked Immunoassay (ELISA)

Aptamers were screened for their ability to bind to the monoclonal using an aptameric ELISA. The ELISA format consisted of monoclonal protein bound to the wells through protein G which then had a solution phase biotinylated aptamer applied. An increase in the absorbency intensity was indicative of aptamers binding to the target monoclonal protein. The wells were first washed three times with wash buffer (PBS with 2 mM MgCl2 added). Then 2.5 pmoles of target IgG or polyclonal IgG diluted in SuperBlock blocking buffer with 0.05% tween added were applied to the wells. The protein was incubated in the wells for 30 minutes at room temperature on a rotator. These wells were then washed eight times (~200 µL per

well per wash) with wash buffer. A 25 pmol solution of biotinylated aptamers in 100 µL of wash buffer were incubated in the washed wells for 60 minutes on a rotator. The wells were washed ten times (~200 µL per well per wash) with wash buffer following the aptamer incubation. Following the wash, streptavidin horseradish peroxidase was diluted according to the manufacturer's instructions in wash buffer and bovine serum albumin (BSA) and then applied to each well and allowed to incubate for 30 minutes at room temperature with an opaque cover. The wells were then washed 12 times with wash buffer. Finally freshly mixed tetramethylbenzidine and substrate (1:1) were added to each well and the absorbance was recorded by an absorbance plate reader (VersaMax, Molecular Devices, San Jose, CA). Measurements were made at 450 nm in ten minute intervals.

6.3. Results and Discussion

Aptamers were first isolated for a model IgG protein (Rituximab) which could be acquired in purified form. Aptamers were selected and characterized for this protein with results presented in this section. Then aptamers were isolated for a multiple myeloma patient's monoclonal IgG.

6.3.1. Rituximab Selection

The SELEX consisted of four rounds of selection to generate a pool of aptamer candidates. During this process, aliquots from the washing stages were collected and used to assess the success of the SELEX. During the 35 minute washing procedure, the washing fluid exiting the microfluidic device was collected into a tube. A new tube was used for every five minute interval of the washing process such that six tubes with 100 µL of wash fluid were generated. From these volumes, 2 µL were removed from the first wash of a SELEX round, the last wash of a SELEX round and the final eluted product. This aliquot was amplified by 20 cycles of PCR and imaged by gel electrophoresis techniques (**Figure 6.2**). From the gel electropherogram it can be seen that the first wash of a SELEX cycle always contained more oligonucleotides than the last wash of a selection cycle. Thus confirming the washing process removes weakly binding ssDNA. It can also be seen that the last wash of a given SELEX cycles always contains less DNA than the first wash of the next SELEX cycle. This confirms that the ssDNA is PCR amplified with the integrated PCR system in the amplification chamber. Finally the last wash of the final round of SELEX contains less DNA than the elution band confirming that ssDNA remained strongly bound to the target molecule and could be removed with a modest temperature increase.

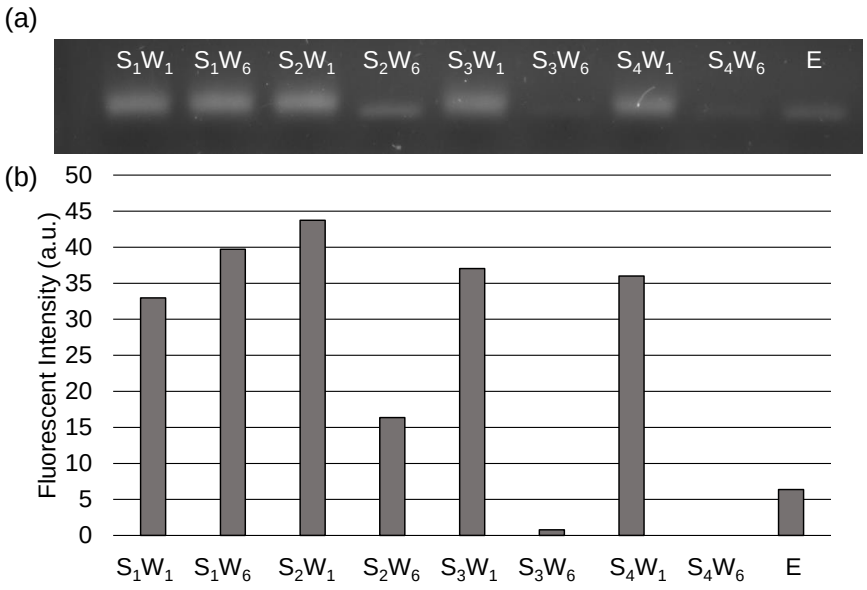

Figure 6.2: Collected eluates from the Rituximab aptamer selection process. (a) Gel electropherogram of amplified eluates and (b) bar graph depicting band intensity.S_1W_1: selection 1, wash 1; S_1W_6: selection 1, wash 6; S_2W_1: selection 2, wash 1; S_2W_6: selection 2, wash 6; S_3W_1: selection 3, wash 1; S_3W_6: selection 3, wash 6; S_4W_1: selection 4, wash 1; S_4W_6: selection 4, wash 6; E: elution.

6.3.2. Rituximab Sequencing

A sample from the eluted product was amplified by PCR and sequenced. A total of 24 colonies were selected for sequencing (**Table 6.3**). The sequences were analyzed for shared motifs and sequences with the most common regions with other sequences were synthesized and further tested.

Table 6.3: Sequences from Rituximab SELEX.

Sequence ID	Sequence
RituxS1	TTGGATTGAGAAACATCGCCGCGTTTTAGGTTCAGCGACTCACTGACACTACTCCTTGTACCTTCCTCCTGACCACATCCGAC
RituxS2	TTGGATTGAGAAACATCGCCGCTTAGACCTCGAGTGATGACCTGTGAATGCGCTACGTTGATTTCCTCCTGACCACATCCGAC
RituxS3	TTGGATTGAGAAACATCGCCGCACTAACTCTGCCTTCCGGCTTTTTATTATTTTGTGTTATTTTCCTCCTGACCACATCCGAC
RituxS4	TTGGATTGAGAAACATCGCCGCTTTGCGTAAGAACGGCTGCACCTCGGGACTATTGGTACTCTTCCTCCTGACCACATCCGAC
RituxS5	TTGGATTGAGAAACATCGCCGCTAGTTCCCTTTTATGATTTGCGATCACCCGCGGGAGTGTTTTCCTCCTGACCACATCCGAC
RituxS6	TTGGATTGAGAAACATCGCCGCATTTAATTACCTACAATCGTTCTATGTTTTTCTACACTGCTTCCTCCTGACCACATCCGAC
RituxS7	TTGGATTGAGAAACATCGCCGCGTTGGCCCAGGAGGTGCCGTGCGGTATGGGGGCCCGGGCGTTCCTCCTGACCACATCCGAC
RituxS8	TTGGATTGAGAAACATCGCCGCGCTGACGACTATTTAGTATTTTACACAGGTTCGCATTGGGTTCCTCCTGACCACATCCGAC
RituxS9	TTGGATTGAGAAACATCGCCGCGTCGGGGGGCGCGGCCGGTACGCTAGGGTTGAGTGCCTTGTTCCTCCTGACCACATCCGAC
RituxS10	TTGGATTGAGAAACATCGCCGCGGGCCCTTTTAAACGGAAGTTTCCACCGCTAGAGTGGGGTTTCCTCCTGACCACATCCGAC
RituxS11	TTGGATTGAGAAACATCGCCGCCCGTTGCTCTTTTATTTCGTGTACCACCGCTTCGGTATGATTCCTCCTGACCACATCCGAC
RituxS12	TTGGATTGAGAAACATCGCCGCGTGTTACGATGTCCAGTTAGGTCGTTGTAAAGATCTCCATTCCTCCTGACCACATCCGAC
RituxS13	TTGGATTGAGAAACATCGCCGCGGGGGCAAACTTTCCGCTGTGGGTTATACTGAACACGGACTTCCTCCTGACCACATCCGAC
RituxS14	TTGGATTGAGAAACATCGCCGCTGACTACTAAATCGGAAACGTTCCGAGAGCGGATGGTACGTTCCTCCTGACCACATCCGAC
RituxS15	TTGGATTGAGAAACATCGCCGCGCAGCGGTGCTGTCCAGCCCAGGTGGAACGCTTAGCGTTCTTCCTCCTGACCACATCCGAC
RituxS16	TTGGATTGAGAAACATCGCCGCTAACCAGGAGGGGTTGAGGCGGCAGCGGGTGAGGGGTGTGTTCCTCCTGACCACATCCGAC
RituxS17	TTGGATTGAGAAACATCGCCGCGATTTTAAGACATGATATGTCTTTCTGAGGCAGTTCGTACTTCCTCCTGACCACATCCGAC
RituxS18	TTGGATTGAGAAACATCGCCGCGAGAAAACGGAGAGGTCTGAAGCGACAAGCAGGGACGTCCTTCCTCCTGACCACATCCGAC
RituxS19	TTGGATTGAGAAACATCGCCGCTCCAGGGACGTTTCAAACTCAAAGCTATTGAGAGCATGATTTCCTCCTGACCACATCCGAC
RituxS20	TTGGATTGAGAAACATCGCCGCGTGGGCTAAACGTGGTGGTTAATGGTGAGGGGGGGTCGTCTTCCTCCTGACCACATCCGAC
RituxS21	TTGGATTGAGAAACATCGCCGCCTTTTAGTCTGGGATAGATTTCAGTGGTGCGGCGGTACAATTCCTCCTGACCACATCCGAC
RituxS22	TTGGATTGAGAAACATCGCCGCTTAAACTTTCCATATGATGCCCTAATCGATTTGGCCACTATTCCTCCTGACCACATCCGAC
RituxS23	TTGGATTGAGAAACATCGCCGCTGTTGAGAGGTGTTACGATCATTAGCGGCAGCTTAACATATTCCTCCTGACCACATCCGAC
RituxS24	TTGGATTGAGAAACATCGCCGCTGGACGCATTACGGTTATATTATTGGGAGTCGGGCGGAAGTTCCTCCTGACCACATCCGAC

6.3.3. Rituximab SPR

Aptamer candidates were evaluated for their affinity towards Rituximab by SPR. The aptamer sequence RituxS13 was found to have the highest affinity towards the target (**Figure 6.3**). A binding dissociation constant of 35.8 nM was obtained with limited binding to the polyclonal IgG. The binding of the aptamer towards Rituximab was compared to the binding towards polyclonal IgG. Rituximab and polyclonal IgG were injected at 400 nM concentration and the average response from the 200th minute to the 250th were compared. The aptamer showed much greater response towards Rituximab than towards the polyclonal IgG indicating the aptamer specifically binds to the model monoclonal protein.

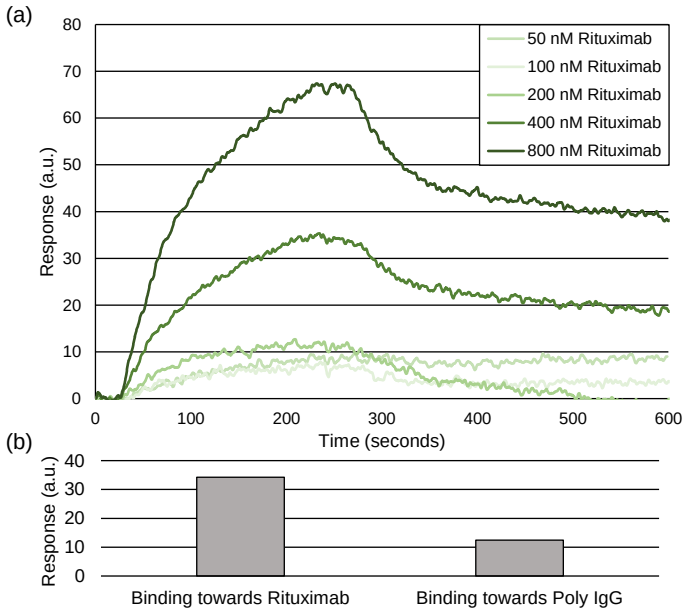

Figure 6.3: Rituximab aptamer binding characterization by SPR. (a) Aptamer RituxS13 surface with increasing concentrations of Rituximab injected. (b) Comparison of aptamer response when 400 nM of either Rituximab or polyclonal IgG are injected.

6.3.4. Rituximab ELISA

The sequence with the highest affinity from SPR (RituxS13) was further tested for its affinity in an aptamer style ELISA. Rituximab and polyclonal IgG were functionalized onto protein G wells and a biotinylated RituxS13 was incubated, washed, and exposed to biotinylated horseradish peroxidase (**Figure 6.4**). The aptamer RituxS13 was found to preferentially bind to Rituximab thus confirming the specificity of the resultant aptamer towards the target. Therefore, the microfluidic selection approach was able to isolate an aptamer towards a monoclonal protein within a day and this aptamer could be used in a clinically relevant assay.

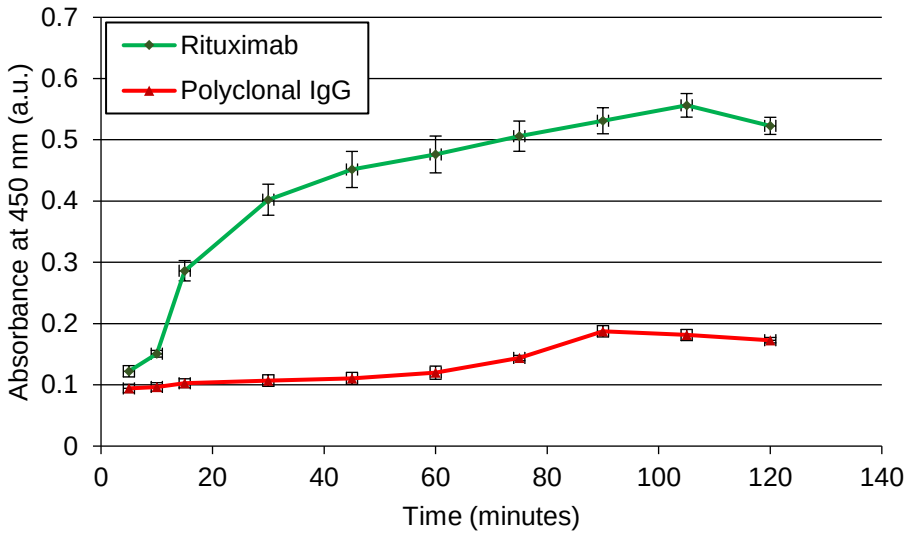

Figure 6.4: Aptamer formatted ELISA. Rituximab aptamer sequence RituxS13 was tested for its ability to bind Rituximab and the polyclonal IgG. Error bars represent standard deviations.

6.3.5. MM Patient Selection

The microfluidic approach was next used to isolate a patient specific aptamer. The success of the overall chip performance was first assessed using eluates collected during the selection process. These eluates were amplified off-chip by PCR and imaged by gel electrophoresis. As can be seen in **Figure 6.5** for every SELEX round the amount of DNA collected becomes less as the washing progresses. However, after the thermal conditions of the selection chamber are changed, a large amount of DNA that was strongly bound and eluted under the different environmental conditions could be collected. Each round of SELEX showed the monotonous decrease in the amount of DNA during washing. The first wash of the first round of selection appears to have a lower intensity but is actually artifact of having an excess of DNA in the PCR reaction. All samples were subjected to the same amount of PCR cycles (19 cycles) which proved to be excessive for that first wash. Later rounds of SELEX had more oligonucleotides in the elution compared to even the first wash indicating more of the pool was binding to the target beads than being washed away during the later rounds of SELEX.

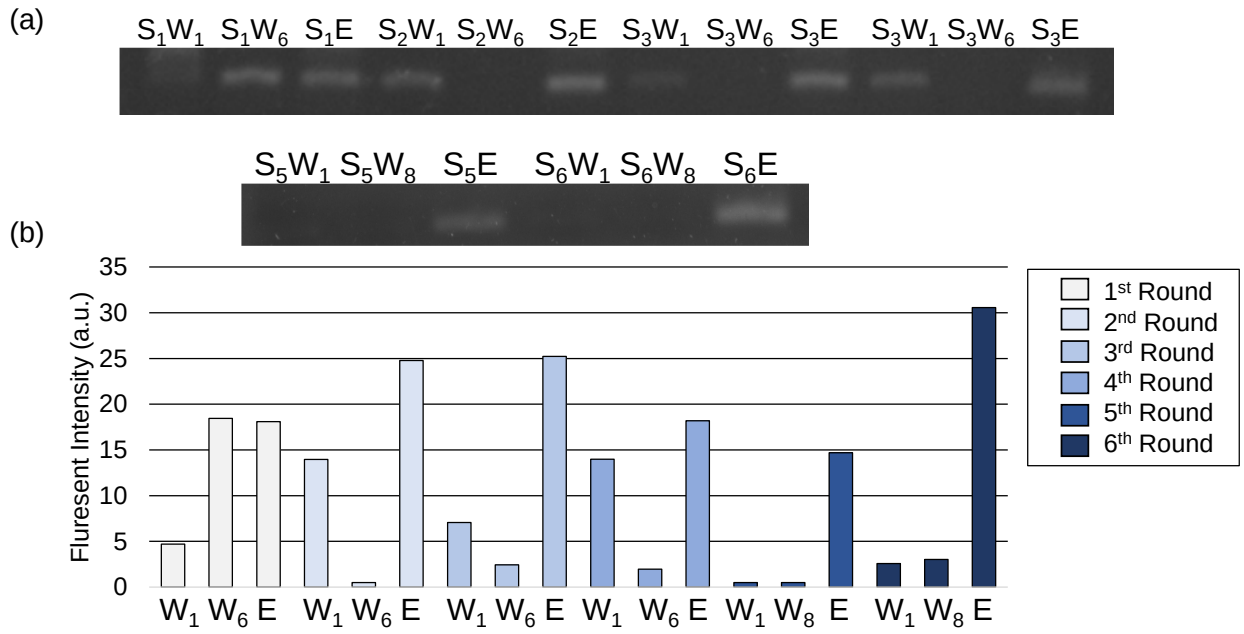

Figure 6.5: Collected eluates from the six round selection process, amplified by PCR and imaged with gel electrophoresis. (a) Gel electropherogram of amplified eluates and (b) bar graph representing electropherogram band intensity. Bar color indicates selection round. W_1 is the first wash of a selection round. W_6 is the final wash for section rounds 1-4. The final wash for rounds 5 and 6 is W_8. E is the eluted product.

6.3.6. High Throughput Sequencing

High throughput sequencing data was analyzed with the AptaSuite toolkit [194]. The toolkit fractioned the raw sequencing files into the six rounds of SELEX and accepted 3,818,436 reads as having correct forward primers and reverse primers. Of these reads, approximately all (>95%) had a randomized region size matching the starting library (40 nucleotides). The identified barcodes for each round of SELEX were approximately evenly distributed (first round: 19.1%, second round: 18.38%, third round: 17.31%, fourth round: 13.31%, fifth round: 16.12%, and sixth round: 15.57%). The amount of singletons, defined as sequences that appear with a count of one, decreased on every round of SELEX (**Figure 6.6**). Further, the amount of enriched species, defined as sequences that also appear in other rounds of SELEX increased as expected during every round of SELEX. Conversely, the unique fraction (sequences that only appear in

that SELEX round) decreases as the SELEX process progressed. It appears the singletons and enriched sequences slightly increased on the sixth round. This could indicate the process began to saturate after six rounds.

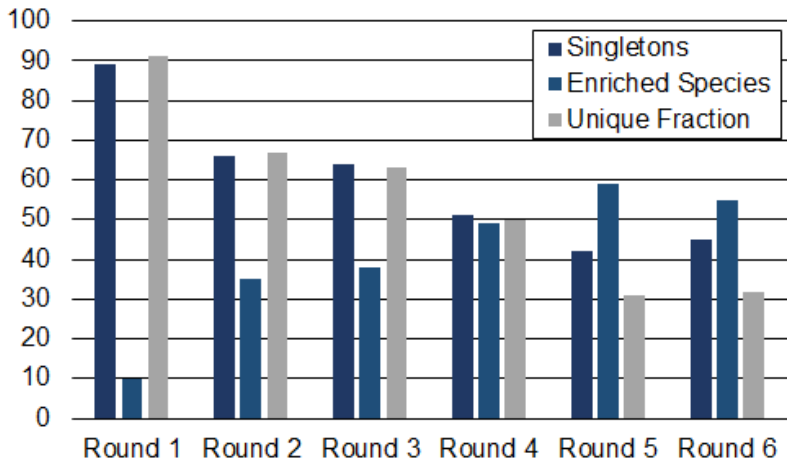

Figure 6.6: Singletons, enriched species and unique fraction of every SELEX round. Singletons are sequences that appear with a frequency of 1. Enriched species are sequences that are found in other rounds. The unique fraction are the sequences that do not appear in any other round.

A cluster program was run to group aptamer sequences by their similarities and the clusters of similar sequences. Clusters consisted of sequences that had randomized regions with only a single nucleotide allowed to mismatch. Clusters that appear at very high frequencies in the sixth round of SELEX were further evaluated for their progression through the other rounds of SELEX. A sequence of low abundancy but that is rapidly increasing in frequency in the later rounds of SELEX could suggest a potential high affinity sequence becoming enriched. The clusters were checked against the most frequent non-clustered sequences to ensure highly frequent sequences were not missed by the clustering algorithm. Sequences that contained a single nucleotide between primers were considered artifacts from the PCR processes and purification processes and discarded. The progression of the ten most abundant sequences from the sixth round are shown **Figure 6.7**.

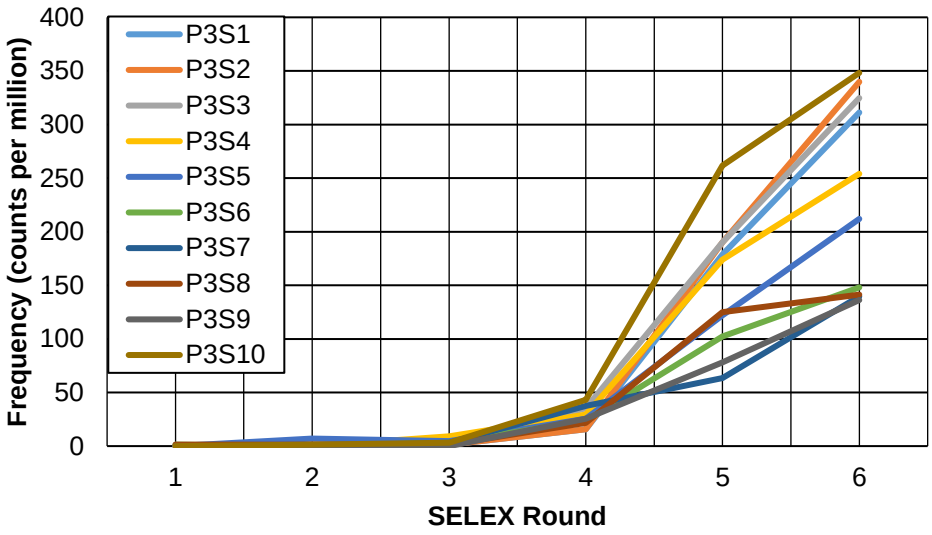

Figure 6.7: Abundance of the top 10 most frequent sequences from the sixth round of SELEX. Significant enrichment occurs from the fourth round to the fifth round.

All of the most frequent sequences increased from the fifth round to the sixth round. The most significant enrichment of the sequences occurred after the fourth round indicating that SELEX cycles beyond four could enhance the probability of identifying a high affinity aptamer. The most frequent sequences of the fourth and sixth SELEX rounds were synthesized for further in vitro testing. These sequences are tableted below (**Table 6.4**).

Table 6.4: Next generation sequencing results for each round of SELEX for the 10 most frequent sequences found in the 6th round of SELEX.

Sequence ID	Sequence	Round 1 Counts per Million	Round 2 Counts per Million	Round 3 Counts per Million	Round 4 Counts per Million	Round 5 Counts per Million	Round 6 Counts per Million
P3S1	AGAGATGGTCGGTATATATCCAATCGTGAATGCCAAGTGAA	0	1.425	1.513	15.746	190.074	339.804
P3S2	TTATTTCCTACGATCACCAAGTGAAATCCAAGTGTATGAGA	0	0	0	35.429	190.074	324.665
P3S3	GTTAATGCTAATGCCTCGTGTTTTCCAAGTGTTGAGTCGGA	0	0	9.077	29.524	173.828	254.011
P3S4	CAAGTGACATAGCAAGGGGATGAGGAAAAGAGAGTGGGCGA	0	7.123	4.539	25.588	121.842	211.957
P3S5	GGGTGTAGAATTCTCAATAACAAGTGGATGAGTTAAGCGGA	1.356	0	3.026	23.619	102.348	148.032
P3S6	CGATAGCGAGATGTAGTCGCATTAGGAAAAGTGTGAGCGGA	0	0	3.026	37.397	63.358	139.622
P3S7	AAAGCAATACAAAGAGACAGCAACCAAGTACGAATGGGCGA	1.356	1.425	1.513	21.651	125.091	141.304
P3S8	AACCATGCCAAGTGATTAAGGTATAAATACCAAGTGAAGTA	0	2.849	9.077	23.619	77.979	137.941
P3S9	TTACGTTGATTGTGGTCCATGTGCATGAGGGAAGGAGCGGA	0	0	0	25.588	77.979	136.258
P3S10	AGTAAACCAAGTAAAGAGTGTACCAGTTCTAAGTGAATG	0	1.425	3.026	43.302	261.554	348.218

6.3.7. Aptameric ELISA

The ability of the aptamers to bind to the target myeloma patient M-Ig could be demonstrated by aptameric ELISA (**Figure 6.8**). Conceivable, ELISA could be a test used to track patient M-Ig during disease progression. Thus, ELISA was not only used to demonstrate aptamer binding but to illustrate the potential of the aptamers in a clinical test. Ten sequences identified from the high throughput sequencing were screened with the aptameric ELISA. From these clones, the observed binding was higher towards the M-Ig than towards polyclonal IgG for sequences P3S1, P3S3, P3S5, P3S6, P3S9 and P3S10. Of these, it was determined P3S10 and P3S5 had the greatest difference in binding towards the M-Ig than the polyclonal.

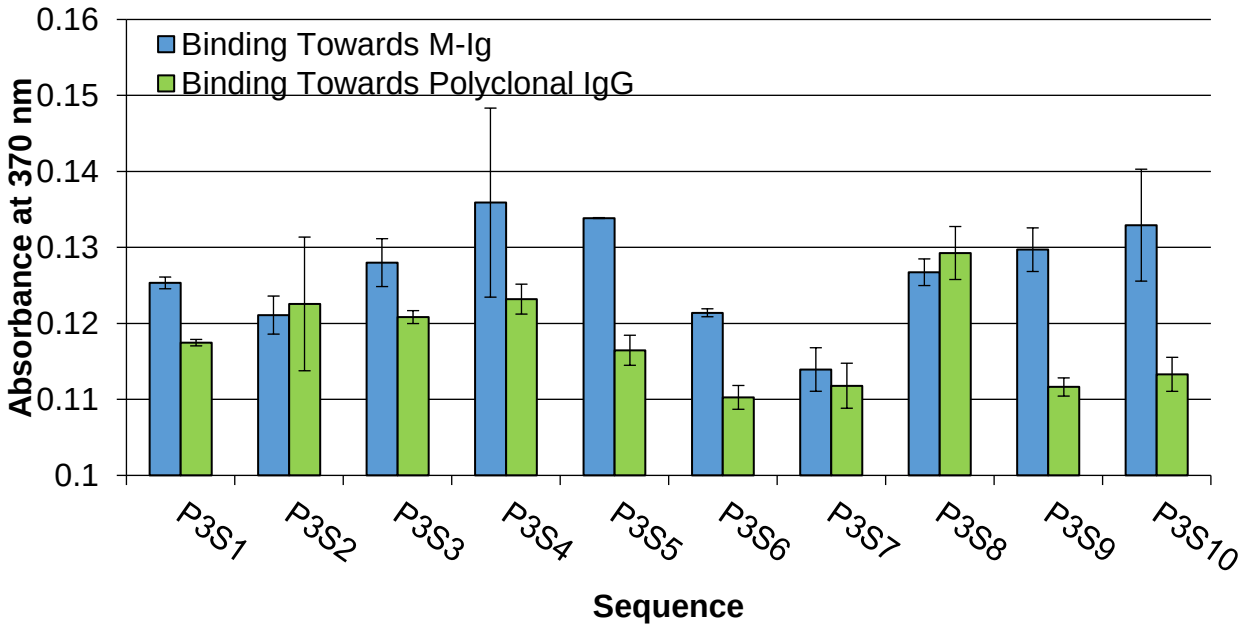

Figure 6.8: Aptameric ELISA results of a patient monoclonal IgG bound to the well surface through protein G and solution phase aptamer. Absorbance was measured at 370 nm in 10 minute intervals. Measurement shown is after 75 minutes. Error bars represented standard deviations from triplicate measurements.

These results can be compared to their enrichment found through NGS where sequence 10 was the most prevalent sequence for the fourth, fifth, and sixth SELEX round. While it was the most prevalent for the sequences tested, there were other sequences at the fourth round which were more frequent than P3S10 but these sequences became less frequent in the fifth and sixth round.

6.3.8. SPR Analysis

The aptamer with greatest binding from the ELISA (P3S10) was further analyzed by SPR. A biotinylated version of the aptamer was bound to one of the sensing surfaces while a scrambled control was bound to the other. SPR measurements were taken from the difference of these two channels such that only the specific binding of the aptamer to the injected molecule was considered. Patient serum purified for IgG by Melon Gel was injected into the SPR instrument in various concentrations. The aptamer and scrambled sequence were then regenerated and human polyclonal IgG was then injected at the same concentrations and compared to the patient injections (**Figure 6.9**). These experiments were performed in triplicate for both the M-Ig and polyclonal IgG.

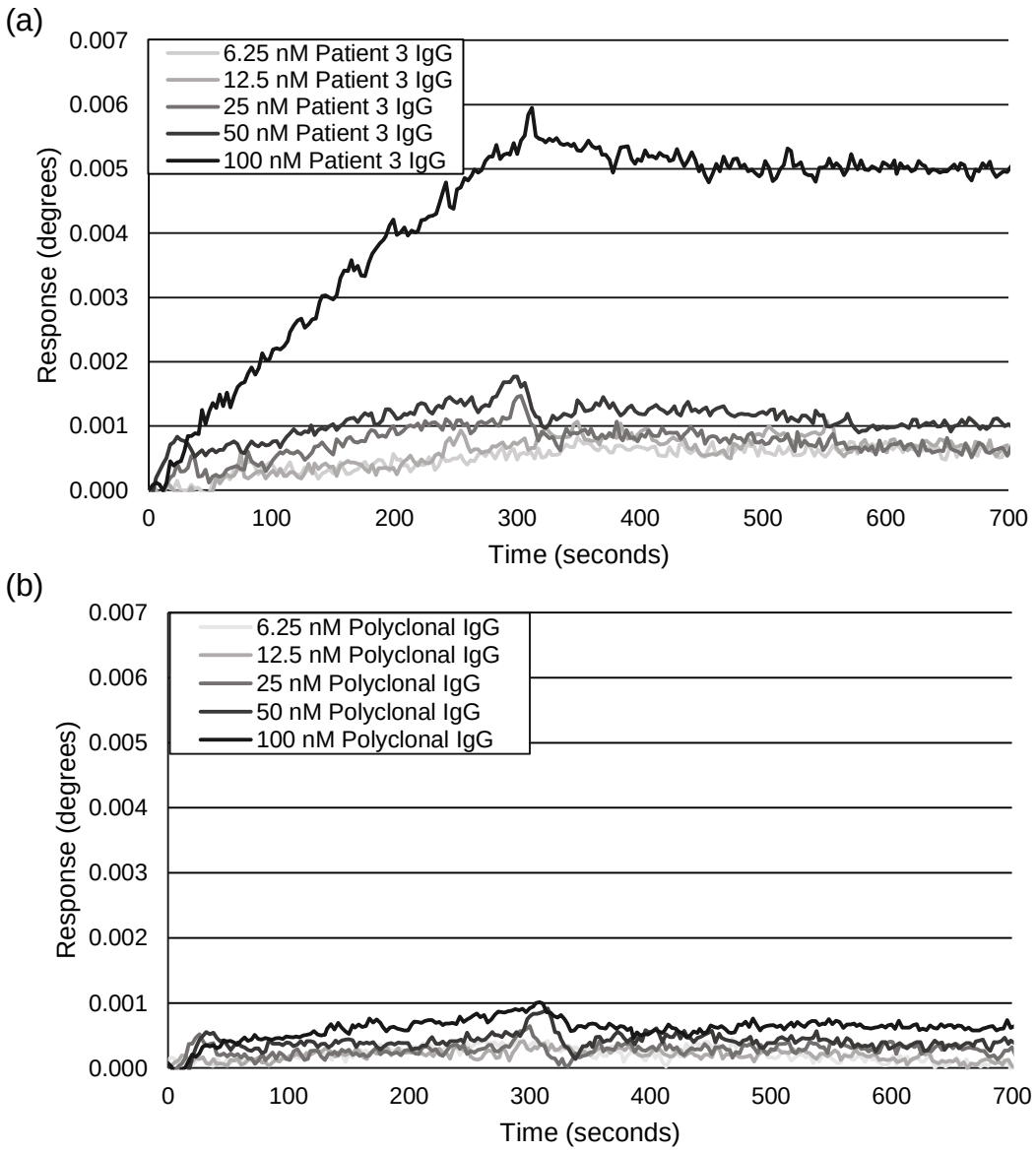

Figure 6.9: Representative SPR response curves for aptamer P3S10 from triplicate experiments. (a) Aptamer response towards patient 3 IgG and (b) aptamer response to a polyclonal IgG used as a control.

From the SPR responses it can be observed that significant binding was found to the patient IgG protein while negligible binding was found when the polyclonal human IgG was injected. By applying a 1:1 fitting model to the M-Ig binding curves, a binding dissociation constant of (K_D) of ~27.7 nM is obtained. Therefore, a patient M-Ig specific aptamer has been isolated. The concentrations of protein used in these SPR plots

are orders of magnitude lower than the limit of detection for conventional MM diagnostics, though it must be noted the SPR proteins were diluted in buffer.

6.4. Conclusion

The microfluidic approach was used to perform SELEX on a model monoclonal protein, Rituximab. An aptamer was identified with a binding dissociation constant of 35 nM and the aptamer could be further used in an aptamer formatted ELISA. With this insight, the approach was applied to the isolation of a patient derived monoclonal protein. This protein was first isolated from serum and then put onto selection beads which were injected into the microfluidic device. High throughput sequencing was used to analyze the resulting aptamer pools and to select sequences to be further analyzed. These sequences were analyzed by an aptameric ELISA and sequences P3S10 was found to have higher binding to the patient M-Ig than to the polyclonal control. P3S10 was further analyzed by SPR and found to have a specific response to the patient IgG and negligible response to a polyclonal IgG pool. The rapid isolation time of these aptamers (<12 hours) could allow the development of personalized probes for MRD diagnostics for a cohort of patients.

The application of this aptamer for minimal residual disease needs further exploration. ELISA studies in physiological media, such as serum, would help determine its clinical applicability. Also, finding the limit of detection in buffer and in serum through a titration from a higher concentration would provide this information. As this is the first isolation of an aptamer towards a myeloma patient M-Ig, it would be beneficial to investigate it further before isolating additional aptamers for other patients. Binding studies to determine the generalized binding dissociation constant would be illustrative for future selections though for an aptamer to work in ELISA it generally needs dissociation constants in the nanomolar range. Additional purification of the patient IgG sample would allow curve fitting from the SPR results. The study would also benefit from fragment screening or crystallography studies to determine where exactly the aptamer binds to the patient protein and if it is indeed targeting the protein idiotype. Finally, additional selections of aptamers towards other IgG myeloma patients and myeloma patients of other immunoglobulin subtypes would demonstrate the robustness of the approach.

Chapter 7: Concluding Remarks

7.1. Thesis Summary

Precision medicine is in need of tools that can detect expressed biomarkers. Mass spectrometry techniques lack the required sensitivity needed for many applications, and monoclonal antibodies, while they can act as sensitive probes, have a prohibitively expensive development process making them poor candidates as probes for the thousands of relevant biomarkers. Aptamers are capable diagnostic probes but the development of aptamers towards new biomarkers also suffers from time, and resource consumptive processes.

In this thesis, the aptamer development process is integrated into a microfluidic device which results in a reduction in the amount of time and reagents needed to isolate aptamers of high affinity. This reduction in time is the result of the larger surface area to volume ratios afforded in microscale geometries and the high degree of integration which enables seamless transition from one step of SELEX to the next. As such, the aptamer development time can be completed within a day thereby allowing the selection of aptamers towards precision medicine probes at a realistic scale. The first part of this thesis involves the development of microfluidic SELEX techniques for rapid aptamer isolation while the second part applies this technology to a few examples within precision medicine. A series of aptamers are generated to several targets including a small molecule glycan, a glycosylated peptide, and an IgG protein.

Specific results of this thesis include:

7.1.1. Hybrid SELEX Approach

A microfluidic approach for aptamer isolation is explored which uses electrophoretic locomotion to transport ssDNA from the selection chamber to the amplification chamber and then pressure driven flow to transport PCR amplified ssDNA back to the selection chamber for further rounds of SELEX. Thus the chip leveraged the simplified work flow of previously reported electrokinetic SELEX devices, while also preventing the exposure of the target molecule to potentially deleterious electric field effects. The device was fully capable of performing 4 rounds of SELEX on a single chip without the need for off-line processes. Using IgE as a model target, an aptamer pool with an equilibrium dissociation constant (K_D) of approximately 12 nM and limited cross-reactivity towards IgA.

7.1.2. Electrokinetic SELEX Approach

A second microfluidic SELEX approach which used purely electrokinetics to transport ssDNA between various SELEX stages was developed. The approach simplifies the device fabrication and design while integrating the affinity selection and amplification stages of SELEX with free solution electrokinetic oligonucleotide transfer. As such, the SELEX process can be completed without the need for flow control components or gel components. The approach was realized in a microfluidic chip consisting of two microchambers separated by a long, torturous, serpentine channel of high flow resistance. While this channel would prevent diffusion and flow under normal operating conditions, with the application of an electric field between the two microchambers, oligonucleotides could be transferred between the two microchambers, allowing oligonucleotides to be transferred from the affinity selection microchamber to the PCR amplification microchamber. Thus the approach is capable of multi-round enrichment of oligonucleotides using simple transfer processes while maintaining a high level of device integration, as demonstrated by the isolation of an aptamer pool against a protein target (IgA) with significantly higher binding affinity than the starting library in approximately 4 hours of processing time.

7.1.3. Three Chamber Approach

A third microfluidic approach was developed which featured a selection chamber, a counter selection chamber, and amplification chamber connected by microchannels to form an integrated SELEX capable loop. The approach affinity selected aptamers in one channel, then transferred selected aptamers through a counter selection chamber until finally reaching a PCR amplification chamber. Therefore, for every round of SELEX aptamer candidates are affinity selected, counter selected and PCR amplified. The amplified PCR product would then be thermally eluted and transferred back to the selection chamber for further rounds of SELEX. The device used to realize the approach employed integrated microvalves to control the fluid motion, and thus oligonucleotides, within the device. Gel electropherograms confirmed the device was capable of performing selection and amplification stages of SELEX. Furthermore, the approach could be used for many rounds of SELEX without degrading. It was concluded in this chapter that a device with sufficient reliability and robustness to pursue precision medicine applications had been developed.

7.1.4. Glycan Binding Aptamer Isolation

The three chamber approach was employed to select aptamers towards glycan molecules. Gangliosides GM1, GM3, and GD3 were chosen as targets for aptamer development. Aptamers were isolated with 4 rounds of SELEX for each of these targets and characterized by SPR and ITC techniques. These aptamers displayed binding dissociation constants, K_D, of 49.6 nM towards GM1, 43.59 nM towards GM3, and 2.48 µM towards GD3. It was also observed the binding test format had a large influence on the binding behavior of the aptamer candidates. These glycan approaches were extended to the isolation of aptamers with affinity towards a glycosylated peptide. A synthesized glycosylated peptide was used as a target for SELEX while its non-glycosylated version was used as a counter target. After 3 rounds of SELEX, aptamers were isolated with binding affinities (K_D) as low as 15 nM towards the glycosylated peptide and 3.2 µM towards the non-glycosylated version.

7.1.5. Monoclonal Protein Aptamer Isolation

Multiple myeloma is a cancer of the plasma cell for which sensitive methods to track disease progression remain scarce. The hallmark of the disease is a monoclonal protein that is unique for every patient. Targeting this monoclonal protein would allow sensitive monitoring of disease progression for these patients but doing so would require a unique probe for each myeloma patient. The three chamber approach is used to first isolate an aptamer towards a model monoclonal protein (Rituximab) of the same class as the most frequent cases of multiple myeloma. An aptamer with an affinity (K_D) of 32 nM is isolated for Rituximab. A myeloma patient serum sample is then used in the device to obtain patient specific aptamers. The cancer related protein is purified from the patient serum sample and used within the microfluidic device. Resulting aptamer pools were sequenced using next generation techniques and screened in an aptamer formatted ELISA resulting in the discovery of an aptamer which non-specifically responds to the patient cancer protein. The aptamer was also tested with SPR and was shown to only bind to the patient associated monoclonal protein.

7.2. Future Work

The devices demonstrated in this work were proofs-of-concept and have opportunity for further improvement.

7.2.1. On-chip Aptamer Development Tracking

The devices presented are effective at performing the stages of SELEX and generating a pool of aptamer candidates which can then be characterized; however, they do not offer information of the selection process while it is occurring. The amount of selection cycles to perform is based on experience and must be determined before the SELEX begins, as are the amount of PCR cycles performed for the amplification stage. If the device included features which could assess the amount of ssDNA binding during the selection stage of SELEX then the device operator could determine the point at which the SELEX should be concluded. Timely termination could prevent wasted time on characterization of aptamer candidates from a pool that is not sufficiently enriched, or conversely the loss of aptamer candidates from too many SELEX cycles to PCR preferential sequences which do not have an affinity towards the target molecule.

Incorporating qPCR into the amplification stage could allow monitoring of the SELEX process. By employing qPCR the amplification process can be monitored and terminated at the same amplification level for every round of SELEX. The advantages of this are two-fold. First selection cycles are normalized between rounds with equal starting material. Second, the amount of cycles needed to reach the specified amount of DNA can be used as an indicator for the amount of ssDNA that bound to the target during the selection phase. Thus, the success of the selection stage can be monitored with a single qPCR stage.

Preliminary results indicate this is possible by including a SYBR fluorescent dye in the PCR reagents (**Figure 7.1**). SYBR dye is frequently used to assess the amount of dsDNA in qPCR. Three rounds of SELEX were performed with this dye in the amplification buffer. Images were taken for every PCR cycle with an epifluorescent microscope. As the SELEX process proceeded, increasing amounts of dsDNA were generated for each SELEX cycle. While this demonstrated the potential for qPCR to be used in SELEX it had some limitations. First, a system to control the amplification in automated fashion needs to be developed. The qPCR plots could only be generated retrospectively and a set number of PCR cycles were used during the amplification process. Second, passivation techniques which prevent the absorption of the fluorescent dye into the PDMS microchip architecture need to be further explored. It was observed that the amplification curves for the later SELEX rounds were influenced by the residual dye in the PDMS microchamber walls which could not be removed by washing. However, there are a multitude of solutions to overcome these limitations [195-198].

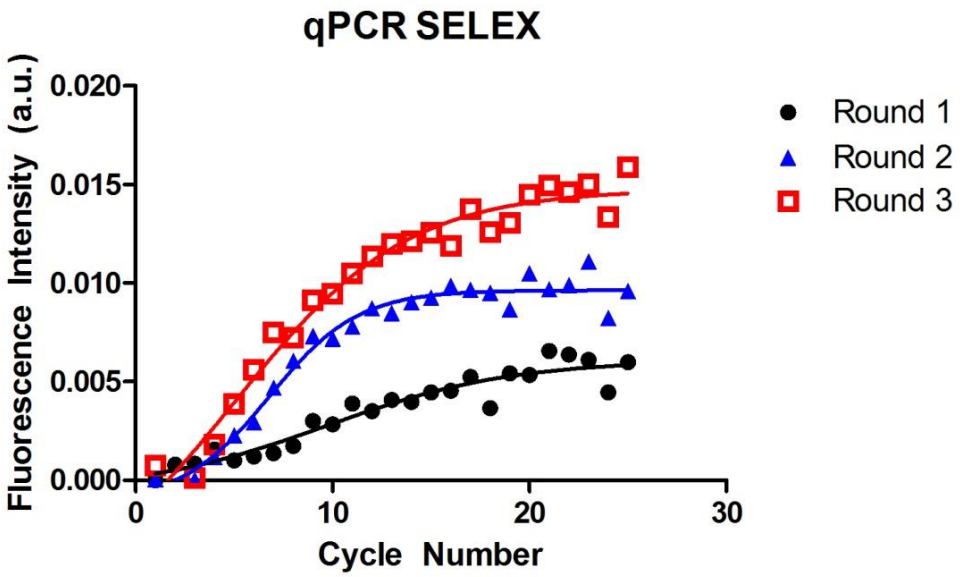

Figure 7.1: Amplification curves for 4 rounds of SELEX. SYBR green dye was included with the PCR reagents to allow fluorescent imaging of the amplification process.

7.2.2. Selection as a Diagnostic

Extensive research has focused on employing microfluidics for sensors, including sensors which use aptamers as a readout. It is envisioned that microfluidic sensing technology could be combined with SELEX into a microfluidic platform where sensing and aptamer development occur simultaneously, thereby eliminating the need for time consuming aptamer characterization assays. The selection stage of SELEX process is similar to many affinity assays - a ligand is immobilized and an analyte is introduced and washed away. If aptamer tracking can be successfully implemented into a SELEX device then a baseline can be created for a specific amount of target and aptamer. Once this is established a target sample of unknown concentration could be introduced and the amount of binding aptamer could be measured to determine if the target sample contains more or less than the baseline. In this simplified example, the characterization of the aptamers occurs during the selection process thus eliminating off-chip characterization. Furthermore, it is often observed aptamer candidates prefer target molecules in the selection format and sometimes will

not bind in other formats. This issue is obviated if the ultimate aptamer diagnostic assay directly mimics the selection condition.

7.2.3. Automation of Devices

The devices presented were developed such that they could be fully automated with proper supporting equipment. However, for the proof-of-principle demonstrations the aptamer selection process relied on semi-automated syringe pumps and the pipetting of beads and reagents into the functional microchambers. These processes could be replaced with the integration of a computer controlled valving and pumping manifold as recently presented by the Fordyce Lab [199]. Such a setup would allow aptamer isolation without the presence of an operator. This could allow high throughput aptamer selections which not only could generate aptamers for many different targets, but would also create opportunities to further optimize the SELEX process. It is envisioned an aptamer library could be created with standardized selection procedures and information on targets and selection conditions.

Characterization and Applications of Glycan Binding Aptamers

The glycan binding aptamers all showed affinity to their targets but the affinity was dependent on the format of the binding test. Lyso-gangliosides were used for the selection of the aptamers but only the GM1 and GM3 aptamers were tested for affinity with the lyso-ganglioside, and unsurprisingly, they showed high affinity to the target in that format. Binding characterization studies still need to be performed on the lyso-GD3 gangliosides and it is expected the aptamers will show higher affinity to the lyso-targets than they did for the intact ganglioside. Dissociation constants were found for these aptamers because they can provide a generalized measure of binding ability which a glycoscientist would be able build an assay around. It would be further illustrative of the aptamers potential to also apply the aptamers to commonly used assays within the glycan research field. For example, the aptamers could be used in a glycan microarray or in a flow cytometry example case.

Furthermore, glycans used in these proof-of-principle studies were chosen to demonstrate the ability of the approach to isolate aptamers that could distinguish similar glycan molecules. There are still more than 60 known gangliosides for which it would be useful to have affinity probes. It is expected additional modifications to the SELEX procedure will be needed to get the desired specificity, but one potential approach to overcome specificity shortcomings could rely on building a library of aptamers and

then using this library to block shared features between glycan molecules. For example, an aptamer that is isolated and found to bind to GD3 could be used in the selection of GD1 aptamers to block the shared structures between the two gangliosides.

Most proteins are glycosylated and aberrant glycosylation patterns have been implicated in many diseases. Aptamers for these aberrant glycosylation patterns could prove to be important diagnostic probes. This thesis demonstrated the feasibility of isolating such probes but did not examine a specific disease. Future work will focus on the isolation of aptamer candidates towards a well characterized disease.

7.2.4. Application of Aptamers to Histological Patient Serum

The aptamers isolated in Chapter 6 had affinity towards the patient specific monoclonal protein and could potentially be used to monitor this patient's disease state. Further studies on the aptamer's binding ability in pure serum need investigation. These studies could be done in the aptamer formatted ELISA or other clinically relevant assay. Limits of detection and limits of quantification would illustrate the usefulness of these aptamers in tracking a patient's cancer, especially for cases where the patient has minimal residual disease. With a sufficiently sensitive aptamer, studies using histological serum samples could be conducted with potential to change the diagnostic procedures used in multiple myeloma treatment. Isolation of aptamers to additional patients could also assess the widespread applicability of the approach to multiple myeloma patients. Aptamers for a group of patients could provide information on the similarities and differences between patients within multiple myeloma. A database of aptamers and myeloma patients could be created to allow further separation of myeloma patients into smaller population groups for more tailored treatment.

References

[1] R. Mirnezami, J. Nicholson, and A. Darzi, "Preparing for precision medicine," *New England Journal of Medicine,* vol. 366, no. 6, pp. 489-491, 2012.

[2] E. A. Ashley, "The precision medicine initiative: a new national effort," *Jama,* vol. 313, no. 21, pp. 2119-2120, 2015.

[3] R. Chen and M. Snyder, "Promise of personalized omics to precision medicine," *Wiley Interdisciplinary Reviews: Systems Biology and Medicine,* vol. 5, no. 1, pp. 73-82, 2013.

[4] F. S. Collins and H. Varmus, "A new initiative on precision medicine," *New England Journal of Medicine,* vol. 372, no. 9, pp. 793-795, 2015.

[5] R. Moeini, Z. Memariani, P. Pasalar, and N. Gorji, "Historical root of precision medicine: an ancient concept concordant with the modern pharmacotherapy," *DARU Journal of Pharmaceutical Sciences,* vol. 25, no. 1, p. 7, 2017.

[6] S. Hawgood, I. G. Hook-Barnard, T. C. O'brien, and K. R. Yamamoto, "Precision medicine: beyond the inflection point," *Science translational medicine,* vol. 7, no. 300, pp. 300ps17-300ps17, 2015.

[7] A. Almeida and D. Kolarich, "The promise of protein glycosylation for personalised medicine," *Biochimica et Biophysica Acta (BBA)-General Subjects,* vol. 1860, no. 8, pp. 1583-1595, 2016.

[8] S. J. Aronson and H. L. Rehm, "Building the foundation for genomics in precision medicine," *Nature,* vol. 526, no. 7573, p. 336, 2015.

[9] S. L. Martiniano, S. D. Sagel, and E. T. Zemanick, "Cystic fibrosis: a model system for precision medicine," *Current opinion in pediatrics,* vol. 28, no. 3, p. 312, 2016.

[10] P. R. Sosnay, K. R. Siklosi, F. Van Goor, K. Kaniecki, H. Yu, N. Sharma, A. S. Ramalho, M. D. Amaral, R. Dorfman, and J. Zielenski, "Defining the disease liability of variants in the cystic fibrosis transmembrane conductance regulator gene," *Nature genetics,* vol. 45, no. 10, p. 1160, 2013.

[11] C. G. A. R. Network, "Comprehensive molecular profiling of lung adenocarcinoma," *Nature,* vol. 511, no. 7511, p. 543, 2014.

[12] G. J. Korpanty, D. M. Graham, M. D. Vincent, and N. B. Leighl, "Biomarkers that currently affect clinical practice in lung cancer: EGFR, ALK, MET, ROS-1, and KRAS," *Frontiers in oncology,* vol. 4, p. 204, 2014.

[13] M. Kumar, V. Ernani, and T. K. Owonikoko, "Biomarkers and targeted systemic therapies in advanced non-small cell lung cancer," *Molecular aspects of medicine,* vol. 45, pp. 55-66, 2015.

[14] A. J. Vargas and C. C. Harris, "Biomarker development in the precision medicine era: lung cancer as a case study," *Nature Reviews Cancer,* vol. 16, no. 8, p. 525, 2016.

[15] G. Lauc, "Precision medicine that transcends genomics: Glycans as integrators of genes and environment," *BBA-General Subjects,* vol. 8, no. 1860, pp. 1571-1573, 2016.

[16] M. Novokmet, E. Lukić, F. Vučković, T. Keser, K. Rajšl, D. Remondini, G. Castellani, H. Gašparović, O. Gornik, and G. Lauc, "Changes in IgG and total plasma protein glycomes in acute systemic inflammation," *Scientific reports,* vol. 4, p. 4347, 2014.

[17] R. Parekh, R. Dwek, B. Sutton, D. Fernandes, A. Leung, D. Stanworth, T. Rademacher, T. Mizuochi, T. Taniguchi, and K. Matsuta, "Association of rheumatoid arthritis and primary osteoarthritis with changes in the glycosylation pattern of total serum IgG," *Nature,* vol. 316, no. 6027, p. 452, 1985.

[18] F. E. van de Geijn, M. Wuhrer, M. H. Selman, S. P. Willemsen, Y. A. de Man, A. M. Deelder, J. M. Hazes, and R. J. Dolhain, "Immunoglobulin G galactosylation and sialylation are associated with pregnancy-induced improvement of rheumatoid arthritis and the postpartum flare: results from a large prospective cohort study," *Arthritis research & therapy,* vol. 11, no. 6, p. R193, 2009.

[19] M. Wuhrer, J. C. Stam, F. E. van de Geijn, C. A. Koeleman, C. T. Verrips, R. J. Dolhain, C. H. Hokke, and A. M. Deelder, "Glycosylation profiling of immunoglobulin G (IgG) subclasses from human serum," *Proteomics,* vol. 7, no. 22, pp. 4070-4081, 2007.

[20] S. Goodwin, J. D. McPherson, and W. R. McCombie, "Coming of age: ten years of next-generation sequencing technologies," *Nature Reviews Genetics,* vol. 17, no. 6, p. 333, 2016.

[21] P. Muir, S. Li, S. Lou, D. Wang, D. J. Spakowicz, L. Salichos, J. Zhang, G. M. Weinstock, F. Isaacs, and J. Rozowsky, "The real cost of sequencing: scaling computation to keep pace with data generation," *Genome biology,* vol. 17, no. 1, p. 53, 2016.

[22] J. L. Jameson and D. L. Longo, "Precision medicine—personalized, problematic, and promising," *Obstetrical & Gynecological Survey,* vol. 70, no. 10, pp. 612-614, 2015.

[23] R. Collins, "What makes UK Biobank special?," *The Lancet,* vol. 379, no. 9822, pp. 1173-1174, 2012.
[24] M. Anbalagan, B. Huderson, L. Murphy, and B. G. Rowan, "Post-translational modifications of nuclear receptors and human disease," *Nuclear receptor signaling,* vol. 10, 2012.
[25] A. M. Bode and Z. Dong, "Post-translational modification of p53 in tumorigenesis," *Nature Reviews Cancer,* vol. 4, no. 10, p. 793, 2004.
[26] M. Pertea, G. M. Pertea, C. M. Antonescu, T.-C. Chang, J. T. Mendell, and S. L. Salzberg, "StringTie enables improved reconstruction of a transcriptome from RNA-seq reads," *Nature biotechnology,* vol. 33, no. 3, p. 290, 2015.
[27] C. Vogel and E. M. Marcotte, "Insights into the regulation of protein abundance from proteomic and transcriptomic analyses," *Nature Reviews Genetics,* vol. 13, no. 4, p. 227, 2012.
[28] Z. Wang, M. Gerstein, and M. Snyder, "RNA-Seq: a revolutionary tool for transcriptomics," *Nature reviews genetics,* vol. 10, no. 1, p. 57, 2009.
[29] N. L. Anderson and N. G. Anderson, "The human plasma proteome history, character, and diagnostic prospects," *Molecular & cellular proteomics,* vol. 1, no. 11, pp. 845-867, 2002.
[30] R. Apweiler, H. Hermjakob, and N. Sharon, "On the frequency of protein glycosylation, as deduced from analysis of the SWISS-PROT database1," *Biochimica et Biophysica Acta (BBA)-General Subjects,* vol. 1473, no. 1, pp. 4-8, 1999.
[31] C. L. Sawyers, "The cancer biomarker problem," *Nature,* vol. 452, no. 7187, p. 548, 2008.
[32] S. Sharma, H. Byrne, and R. J. O'Kennedy, "Antibodies and antibody-derived analytical biosensors," *Essays in biochemistry,* vol. 60, no. 1, pp. 9-18, 2016.
[33] B. Lu, M. R. Smyth, and R. O'Kennedy, "Tutorial review. Oriented immobilization of antibodies and its applications in immunoassays and immunosensors," *Analyst,* vol. 121, no. 3, pp. 29R-32R, 1996.
[34] R. S. Yalow and S. A. Berson, "Immunoassay of endogenous plasma insulin in man," *The Journal of clinical investigation,* vol. 39, no. 7, pp. 1157-1175, 1960.
[35] E. Engvall and P. Perlmann, "Enzyme-linked immunosorbent assay (ELISA) quantitative assay of immunoglobulin G," *Immunochemistry,* vol. 8, no. 9, pp. 871-874, 1971.
[36] J. A. DiMasi, H. G. Grabowski, and R. W. Hansen, "Innovation in the pharmaceutical industry: new estimates of R&D costs," *Journal of health economics,* vol. 47, pp. 20-33, 2016.
[37] N. L. Anderson, "The clinical plasma proteome: a survey of clinical assays for proteins in plasma and serum," *Clinical chemistry,* vol. 56, no. 2, pp. 177-185, 2010.
[38] J. Li and Z. Zhu, "Research and development of next generation of antibody-based therapeutics," *Acta Pharmacologica Sinica,* vol. 31, no. 9, p. 1198, 2010.
[39] C. Sturgeon, R. Hill, G. L. Hortin, and D. Thompson, "Taking a new biomarker into routine use–a perspective from the routine clinical biochemistry laboratory," *PROTEOMICS–Clinical Applications,* vol. 4, no. 12, pp. 892-903, 2010.
[40] S. Rogstad, A. Faustino, A. Ruth, D. Keire, M. Boyne, and J. Park, "A retrospective evaluation of the use of mass spectrometry in FDA biologics license applications," *Journal of The American Society for Mass Spectrometry,* vol. 28, no. 5, pp. 786-794, 2017.
[41] R. J. Cotter, "Laser mass spectrometry: an overview of techniques, instruments and applications," *Analytica chimica acta,* vol. 195, pp. 45-59, 1987.
[42] E. De Hoffmann, "Mass spectrometry," *Kirk-Othmer Encyclopedia of Chemical Technology,* 2000.
[43] P. Kebarle, "A brief overview of the present status of the mechanisms involved in electrospray mass spectrometry," *Journal of mass spectrometry,* vol. 35, no. 7, pp. 804-817, 2000.
[44] R. González-Domínguez, T. García-Barrera, and J. L. Gómez-Ariza, "Metabolomic study of lipids in serum for biomarker discovery in Alzheimer's disease using direct infusion mass spectrometry," *Journal of pharmaceutical and biomedical analysis,* vol. 98, pp. 321-326, 2014.
[45] H. Keshishian, T. Addona, M. Burgess, D. Mani, X. Shi, E. Kuhn, M. S. Sabatine, R. E. Gerszten, and S. A. Carr, "Quantification of cardiovascular biomarkers in patient plasma by targeted mass spectrometry and stable isotope dilution," *Molecular & cellular proteomics,* vol. 8, no. 10, pp. 2339-2349, 2009.
[46] M.-S. Kim, S. M. Pinto, D. Getnet, R. S. Nirujogi, S. S. Manda, R. Chaerkady, A. K. Madugundu, D. S. Kelkar, R. Isserlin, and S. Jain, "A draft map of the human proteome," *Nature,* vol. 509, no. 7502, p. 575, 2014.

[47] Y. J. Kim, K. Sertamo, M.-A. Pierrard, C. d. Mesmin, S. Y. Kim, M. Schlesser, G. Berchem, and B. Domon, "Verification of the biomarker candidates for non-small-cell lung cancer using a targeted proteomics approach," *Journal of proteome research,* vol. 14, no. 3, pp. 1412-1419, 2015.

[48] W. Kolch, C. Neusüß, M. Pelzing, and H. Mischak, "Capillary electrophoresis–mass spectrometry as a powerful tool in clinical diagnosis and biomarker discovery," *Mass Spectrometry Reviews,* vol. 24, no. 6, pp. 959-977, 2005.

[49] H. Liao, J. Wu, E. Kuhn, W. Chin, B. Chang, M. D. Jones, S. O'neil, K. R. Clauser, J. Karl, and F. Hasler, "Use of mass spectrometry to identify protein biomarkers of disease severity in the synovial fluid and serum of patients with rheumatoid arthritis," *Arthritis & Rheumatism,* vol. 50, no. 12, pp. 3792-3803, 2004.

[50] H. Mischak, T. Kaiser, M. Walden, M. Hillmann, S. Wittke, A. Herrmann, S. Knueppel, H. Haller, and D. Fliser, "Proteomic analysis for the assessment of diabetic renal damage in humans," *Clinical Science,* vol. 107, no. 5, pp. 485-495, 2004.

[51] M. Uhlén, L. Fagerberg, B. M. Hallström, C. Lindskog, P. Oksvold, A. Mardinoglu, Å. Sivertsson, C. Kampf, E. Sjöstedt, and A. Asplund, "Tissue-based map of the human proteome," *Science,* vol. 347, no. 6220, p. 1260419, 2015.

[52] E. M. Weissinger, S. Wittke, T. Kaiser, H. Haller, S. Bartel, R. Krebs, I. Golovko, H. D. Rupprecht, M. Haubitz, and H. Hecker, "Proteomic patterns established with capillary electrophoresis and mass spectrometry for diagnostic purposes," *Kidney international,* vol. 65, no. 6, pp. 2426-2434, 2004.

[53] M. Wilhelm, J. Schlegl, H. Hahne, A. M. Gholami, M. Lieberenz, M. M. Savitski, E. Ziegler, L. Butzmann, S. Gessulat, and H. Marx, "Mass-spectrometry-based draft of the human proteome," *Nature,* vol. 509, no. 7502, p. 582, 2014.

[54] S. Wittke, H. Mischak, M. Walden, W. Kolch, T. Rädler, and K. Wiedemann, "Discovery of biomarkers in human urine and cerebrospinal fluid by capillary electrophoresis coupled to mass spectrometry: towards new diagnostic and therapeutic approaches," *Electrophoresis,* vol. 26, no. 7-8, pp. 1476-1487, 2005.

[55] B. Wu, T. Abbott, D. Fishman, W. McMurray, G. Mor, K. Stone, D. Ward, K. Williams, and H. Zhao, "Comparison of statistical methods for classification of ovarian cancer using mass spectrometry data," *Bioinformatics,* vol. 19, no. 13, pp. 1636-1643, 2003.

[56] K. Yanagisawa, Y. Shyr, B. J. Xu, P. P. Massion, P. H. Larsen, B. C. White, J. R. Roberts, M. Edgerton, A. Gonzalez, and S. Nadaf, "Proteomic patterns of tumour subsets in non-small-cell lung cancer," *The Lancet,* vol. 362, no. 9382, pp. 433-439, 2003.

[57] T. A. Zhukov, R. A. Johanson, A. B. Cantor, R. A. Clark, and M. S. Tockman, "Discovery of distinct protein profiles specific for lung tumors and pre-malignant lung lesions by SELDI mass spectrometry," *Lung cancer,* vol. 40, no. 3, pp. 267-279, 2003.

[58] K. L. Lynch, "CLSI C62-A: a new standard for clinical mass spectrometry," *Clinical chemistry,* vol. 62, no. 1, pp. 24-29, 2016.

[59] T. A. Addona, S. E. Abbatiello, B. Schilling, S. J. Skates, D. Mani, D. M. Bunk, C. H. Spiegelman, L. J. Zimmerman, A.-J. L. Ham, and H. Keshishian, "Multi-site assessment of the precision and reproducibility of multiple reaction monitoring–based measurements of proteins in plasma," *Nature biotechnology,* vol. 27, no. 7, p. 633, 2009.

[60] G. Candiano, L. Musante, M. Bruschi, A. Petretto, L. Santucci, P. Del Boccio, B. Pavone, F. Perfumo, A. Urbani, and F. Scolari, "Repetitive fragmentation products of albumin and α1-antitrypsin in glomerular diseases associated with nephrotic syndrome," *Journal of the American society of nephrology,* vol. 17, no. 11, pp. 3139-3148, 2006.

[61] S. Schaub, J. A. Wilkins, M. Antonovici, O. Krokhin, T. Weiler, D. Rush, and P. Nickerson, "Proteomic-based identification of cleaved urinary β2-microglobulin as a potential marker for acute tubular injury in renal allografts," *American Journal of Transplantation,* vol. 5, no. 4, pp. 729-738, 2005.

[62] B. Sabbagh, S. Mindt, M. Neumaier, and P. Findeisen, "Clinical applications of MS-based protein quantification," *PROTEOMICS–Clinical Applications,* vol. 10, no. 4, pp. 323-345, 2016.

[63] J. Dittrich, S. Becker, M. Hecht, and U. Ceglarek, "Sample preparation strategies for targeted proteomics via proteotypic peptides in human blood using liquid chromatography tandem mass spectrometry," *PROTEOMICS–Clinical Applications,* vol. 9, no. 1-2, pp. 5-16, 2015.

[64] G. L. Wright Jr, "SELDI proteinchip MS: a platform for biomarker discovery and cancer diagnosis," *Expert review of molecular diagnostics,* vol. 2, no. 6, pp. 549-563, 2002.
[65] E. T. Fung, "A recipe for proteomics diagnostic test development: the OVA1 test, from biomarker discovery to FDA clearance," *Clinical chemistry,* vol. 56, no. 2, pp. 327-329, 2010.
[66] J. T. Lathrop, D. A. Jeffery, Y. R. Shea, P. F. Scholl, and M. M. Chan, "US Food and Drug Administration perspectives on clinical mass spectrometry," *Clinical chemistry,* p. clinchem. 2015.244731, 2015.
[67] A. D. Ellington and J. W. Szostak, "In vitro selection of RNA molecules that bind specific ligands," *nature,* vol. 346, no. 6287, p. 818, 1990.
[68] C. Tuerk and L. Gold, "Systematic evolution of ligands by exponential enrichment: RNA ligands to bacteriophage T4 DNA polymerase," *Science,* vol. 249, no. 4968, pp. 505-510, 1990.
[69] L. Gold, "SELEX: how it happened and where it will go," *Journal of molecular evolution,* vol. 81, no. 5-6, pp. 140-143, 2015.
[70] C. Mannironi, A. Di Nardo, P. Fruscoloni, and G. Tocchini-Valentini, "In vitro selection of dopamine RNA ligands," *Biochemistry,* vol. 36, no. 32, pp. 9726-9734, 1997.
[71] D. Nieuwlandt, M. Wecker, and L. Gold, "In vitro selection of RNA ligands to substance P," *Biochemistry,* vol. 34, no. 16, pp. 5651-5659, 1995.
[72] A. Geiger, P. Burgstaller, H. von der Eltz, A. Roeder, and M. Famulok, "RNA aptamers that bind L-arginine with sub-micromolar dissociation constants and high enantioselectivity," *Nucleic Acids Research,* vol. 24, no. 6, pp. 1029-1036, 1996.
[73] K. Harada and A. D. Frankel, "Identification of two novel arginine binding DNAs," *The EMBO Journal,* vol. 14, no. 23, p. 5798, 1995.
[74] S. E. Lupold, B. J. Hicke, Y. Lin, and D. S. Coffey, "Identification and characterization of nuclease-stabilized RNA molecules that bind human prostate cancer cells via the prostate-specific membrane antigen," *Cancer Research,* vol. 62, no. 14, pp. 4029-4033, 2002.
[75] T. W. Wiegand, P. B. Williams, S. C. Dreskin, M.-H. Jouvin, J.-P. Kinet, and D. Tasset, "High-affinity oligonucleotide ligands to human IgE inhibit binding to Fc epsilon receptor I," *The Journal of Immunology,* vol. 157, no. 1, pp. 221-230, 1996.
[76] J. K. Herr, J. E. Smith, C. D. Medley, D. Shangguan, and W. Tan, "Aptamer-conjugated nanoparticles for selective collection and detection of cancer cells," *Analytical Chemistry,* vol. 78, no. 9, pp. 2918-2924, 2006.
[77] D. Shangguan, Y. Li, Z. Tang, Z. C. Cao, H. W. Chen, P. Mallikaratchy, K. Sefah, C. J. Yang, and W. Tan, "Aptamers evolved from live cells as effective molecular probes for cancer study," *Proceedings of the National Academy of Sciences,* vol. 103, no. 32, pp. 11838-11843, 2006.
[78] S. C. B. Gopinath, "Methods developed for SELEX," *Analytical and Bioanalytical Chemistry,* vol. 387, no. 1, pp. 171-182, 2007.
[79] W. James, "Aptamers in the virologists' toolkit," *Journal of General Virology,* vol. 88, no. 2, pp. 351-364, 2007.
[80] H.-P. Hofmann, S. Limmer, V. Hornung, and M. Sprinzl, "Ni2+-binding RNA motifs with an asymmetric purine-rich internal loop and a GA base pair," *Rna,* vol. 3, no. 11, pp. 1289-1300, 1997.
[81] J. Ciesiolka, J. Gorski, and M. Yarus, "Selection of an RNA domain that binds Zn2+," *Rna,* vol. 1, no. 5, pp. 538-550, 1995.
[82] Z. Tang, D. Shangguan, K. Wang, H. Shi, K. Sefah, P. Mallikratchy, H. W. Chen, Y. Li, and W. Tan, "Selection of aptamers for molecular recognition and characterization of cancer cells," *Analytical Chemistry,* vol. 79, no. 13, pp. 4900-4907, 2007.
[83] D. H. Bunka and P. G. Stockley, "Aptamers come of age–at last," *Nature Reviews Microbiology,* vol. 4, no. 8, pp. 588-596, 2006.
[84] T. Fitzwater and B. Polisky, "[17] A SELEX primer," *Methods in enzymology,* vol. 267, pp. 275-301, 1996.
[85] C. L. Hamula, J. W. Guthrie, H. Zhang, X.-F. Li, and X. C. Le, "Selection and analytical applications of aptamers," *TrAC Trends in Analytical Chemistry,* vol. 25, no. 7, pp. 681-691, 2006.
[86] S. D. Jayasena, "Aptamers: an emerging class of molecules that rival antibodies in diagnostics," *Clinical Chemistry,* vol. 45, no. 9, pp. 1628-1650, 1999.
[87] R. Stoltenburg, C. Reinemann, and B. Strehlitz, "SELEX—a (r) evolutionary method to generate high-affinity nucleic acid ligands," *Biomolecular engineering,* vol. 24, no. 4, pp. 381-403, 2007.

[88] K.-M. Song, S. Lee, and C. Ban, "Aptamers and their biological applications," *Sensors,* vol. 12, no. 1, pp. 612-631, 2012.
[89] J. G. Bruno, "Predicting the uncertain future of aptamer-based diagnostics and therapeutics," *Molecules,* vol. 20, no. 4, pp. 6866-6887, 2015.
[90] A. D. Ellington and J. W. Szostak, "Selection in vitro of single-stranded DNA molecules that fold into specific ligand-binding structures," *Nature,* vol. 355, no. 6363, p. 850, 1992.
[91] A. D. Ellington and J. W. Szostak, "In vitro selection of RNA molecules that bind specific ligands," *Nature,* vol. 346, no. 6287, pp. 818-822, 1990.
[92] S. M. Shamah, J. M. Healy, and S. T. Cload, "Complex Target SELEX," *Accounts of Chemical Research,* vol. 41, no. 1, pp. 130-138, 2008.
[93] M. Svobodová, A. Pinto, P. Nadal, and C. O'Sullivan, "Comparison of different methods for generation of single-stranded DNA for SELEX processes," *Analytical and bioanalytical chemistry,* vol. 404, no. 3, pp. 835-842, 2012.
[94] M. Darmostuk, S. Rimpelova, H. Gbelcova, and T. Ruml, "Current approaches in SELEX: An update to aptamer selection technology," *Biotechnology advances,* vol. 33, no. 6, pp. 1141-1161, 2015.
[95] S. K. Dembowski and M. T. Bowser, "Microfluidic methods for aptamer selection and characterization," *Analyst,* vol. 143, no. 1, pp. 21-32, 2018.
[96] G. M. Whitesides, "The origins and the future of microfluidics," *Nature,* vol. 442, no. 7101, p. 368, 2006.
[97] P. Kim, K. W. Kwon, M. C. Park, S. H. Lee, S. M. Kim, and K. Y. Suh, "Soft lithography for microfluidics: a review," 2008.
[98] S. Bhattacharya, A. Datta, J. M. Berg, and S. Gangopadhyay, "Studies on surface wettability of poly (dimethyl) siloxane (PDMS) and glass under oxygen-plasma treatment and correlation with bond strength," *Journal of microelectromechanical systems,* vol. 14, no. 3, pp. 590-597, 2005.
[99] A. Mata, A. J. Fleischman, and S. Roy, "Characterization of polydimethylsiloxane (PDMS) properties for biomedical micro/nanosystems," *Biomedical microdevices,* vol. 7, no. 4, pp. 281-293, 2005.
[100] S. D. Mendonsa and M. T. Bowser, "In vitro evolution of functional DNA using capillary electrophoresis," *Journal of the American Chemical Society,* vol. 126, no. 1, pp. 20-21, 2004.
[101] R. K. Mosing, S. D. Mendonsa, and M. T. Bowser, "Capillary electrophoresis-SELEX selection of aptamers with affinity for HIV-1 reverse transcriptase," *Analytical Chemistry,* vol. 77, no. 19, pp. 6107-6112, 2005.
[102] M. Jing and M. T. Bowser, "Tracking the emergence of high affinity aptamers for rhVEGF165 during CE-SELEX using high throughput sequencing," *Analytical chemistry,* vol. 85, no. 22, p. 10761, 2013.
[103] L. Dong, Q. Tan, W. Ye, D. Liu, H. Chen, H. Hu, D. Wen, Y. Liu, Y. Cao, and J. Kang, "Screening and identifying a novel ssDNA aptamer against alpha-fetoprotein using CE-SELEX," *Scientific reports,* vol. 5, p. 15552, 2015.
[104] R. M. Eaton, J. A. Shallcross, L. E. Mael, K. S. Mears, L. Minkoff, D. J. Scoville, and R. J. Whelan, "Selection of DNA aptamers for ovarian cancer biomarker HE4 using CE-SELEX and high-throughput sequencing," *Analytical and bioanalytical chemistry,* vol. 407, no. 23, pp. 6965-6973, 2015.
[105] S. N. Krylov, "Nonequilibrium capillary electrophoresis of equilibrium mixtures (NECEEM): A novel method for biomolecular screening," *Journal of biomolecular screening,* vol. 11, no. 2, pp. 115-122, 2006.
[106] J. Qian, X. Lou, Y. Zhang, Y. Xiao, and H. T. Soh, "Generation of highly specific aptamers via micromagnetic selection," *Analytical Chemistry,* vol. 81, no. 13, pp. 5490-5495, 2009.
[107] M. Cho, Y. Xiao, J. Nie, R. Stewart, A. T. Csordas, S. S. Oh, J. A. Thomson, and H. T. Soh, "Quantitative selection of DNA aptamers through microfluidic selection and high-throughput sequencing," *Proceedings of the National Academy of Sciences,* vol. 107, no. 35, pp. 15373-15378, 2010.
[108] X. Lou, J. Qian, Y. Xiao, L. Viel, A. E. Gerdon, E. T. Lagally, P. Atzberger, T. M. Tarasow, A. J. Heeger, and H. T. Soh, "Micromagnetic selection of aptamers in microfluidic channels," *Proceedings of the National Academy of Sciences,* vol. 106, no. 9, pp. 2989-2994, 2009.
[109] K. M. Ahmad, S. S. Oh, S. Kim, F. M. McClellen, Y. Xiao, and H. T. Soh, "Probing the limits of aptamer affinity with a microfluidic SELEX platform," *PloS one,* vol. 6, no. 11, p. e27051, 2011.

[110] Q. Wang, W. Liu, Y. Xing, X. Yang, K. Wang, R. Jiang, P. Wang, and Q. Zhao, "Screening of DNA aptamers against myoglobin using a positive and negative selection units integrated microfluidic chip and its biosensing application," *Analytical chemistry,* vol. 86, no. 13, pp. 6572-6579, 2014.
[111] X. Liu, H. Li, W. Jia, Z. Chen, and D. Xu, "Selection of aptamers based on a protein microarray integrated with a microfluidic chip," *Lab on a Chip,* vol. 17, no. 1, pp. 178-185, 2017.
[112] C. M. Birch, H. W. Hou, J. Han, and J. C. Niles, "Identification of malaria parasite-infected red blood cell surface aptamers by inertial microfluidic SELEX (I-SELEX)," *Scientific reports,* vol. 5, p. 11347, 2015.
[113] S. Lee, J. Kang, S. Ren, T. Laurell, S. Kim, and O. C. Jeong, "A cross-contamination-free SELEX platform for a multi-target selection strategy," *BioChip Journal,* vol. 7, no. 1, pp. 38-45, 2013.
[114] J.-Y. Ahn, S. Lee, M. Jo, J. Kang, E. Kim, O. C. Jeong, T. Laurell, and S. Kim, "Sol–Gel Derived Nanoporous Compositions for Entrapping Small Molecules and Their Outlook toward Aptamer Screening," *Analytical Chemistry,* vol. 84, no. 6, pp. 2647-2653, 2012.
[115] S.-M. Park, J.-Y. Ahn, M. Jo, D.-k. Lee, J. T. Lis, H. G. Craighead, and S. Kim, "Selection and elution of aptamers using nanoporous sol-gel arrays with integrated microheaters," *Lab on a Chip,* vol. 9, no. 9, pp. 1206-1212, 2009.
[116] J.-Y. Ahn, M. Jo, P. Dua, D.-k. Lee, and S. Kim, "A sol–gel-based microfluidics system enhances the efficiency of RNA aptamer selection," *Oligonucleotides,* vol. 21, no. 2, pp. 93-100, 2011.
[117] G. Hybarger, J. Bynum, R. F. Williams, J. J. Valdes, and J. P. Chambers, "A microfluidic SELEX prototype," *Analytical and Bioanalytical Chemistry,* vol. 384, no. 1, pp. 191-198, 2006.
[118] C.-H. Weng, C.-J. Huang, and G.-B. Lee, "Screening of aptamers on microfluidic systems for clinical applications," *Sensors,* vol. 12, no. 7, pp. 9514-9529, 2012.
[119] J. Kim, T. R. Olsen, J. Zhu, J. P. Hilton, K.-A. Yang, R. Pei, M. N. Stojanovic, and Q. Lin, "Integrated Microfluidic Isolation of Aptamers Using Electrophoretic Oligonucleotide Manipulation," *Scientific Reports,* vol. 6, p. 26139, 2016.
[120] J. P. Hilton, T. Olsen, J. Kim, J. Zhu, T. Nguyen, M. Barbu, R. Pei, M. Stojanovic, and Q. Lin, "Isolation of thermally sensitive protein-binding oligonucleotides on a microchip," *Microfluidics and Nanofluidics,* vol. 19, no. 4, pp. 795-804, 2015.
[121] T. C. Chu, K. Y. Twu, A. D. Ellington, and M. Levy, "Aptamer mediated siRNA delivery," *Nucleic Acids Research,* vol. 34, no. 10, pp. e73-e73, 2006.
[122] J. O. McNamara, D. Kolonias, F. Pastor, R. S. Mittler, L. Chen, P. H. Giangrande, B. Sullenger, and E. Gilboa, "Multivalent 4-1BB binding aptamers costimulate CD8+ T cells and inhibit tumor growth in mice," *Journal of Clinical Investigation,* vol. 118, no. 1, pp. 376-386, 2008.
[123] E. Gilboa, J. McNamara, and F. Pastor, "Use of oligonucleotide aptamer ligands to modulate the function of immune receptors," *Clinical Cancer Research,* vol. 19, no. 5, pp. 1054-1062, 2013.
[124] O. C. Farokhzad, J. Cheng, B. A. Teply, I. Sherifi, S. Jon, P. W. Kantoff, J. P. Richie, and R. Langer, "Targeted nanoparticle-aptamer bioconjugates for cancer chemotherapy in vivo," *Proceedings of the National Academy of Sciences,* vol. 103, no. 16, pp. 6315-6320, 2006.
[125] E. N. Brody, M. C. Willis, J. D. Smith, S. Jayasena, D. Zichi, and L. Gold, "The use of aptamers in large arrays for molecular diagnostics," *Molecular Diagnosis,* vol. 4, no. 4, pp. 381-388, 1999.
[126] C. Ravelet, C. Grosset, and E. Peyrin, "Liquid chromatography, electrochromatography and capillary electrophoresis applications of DNA and RNA aptamers," *Journal of Chromatography A,* vol. 1117, no. 1, pp. 1-10, 2006.
[127] D. Proske, M. Blank, R. Buhmann, and A. Resch, "Aptamers—basic research, drug development, and clinical applications," *Applied Microbiology and Biotechnology,* vol. 69, no. 4, pp. 367-374, 2005.
[128] S. M. Nimjee, C. P. Rusconi, and B. A. Sullenger, "Aptamers: an emerging class of therapeutics," *Annu. Rev. Med.,* vol. 56, pp. 555-583, 2005.
[129] J. C. Cox and A. D. Ellington, "Automated selection of anti-protein aptamers," *Bioorganic & Medicinal Chemistry,* vol. 9, no. 10, pp. 2525-2531, 2001.
[130] H. Lin, W. Zhang, S. Jia, Z. Guan, C. J. Yang, and Z. Zhu, "Microfluidic approaches to rapid and efficient aptamer selection," *Biomicrofluidics,* vol. 8, no. 4, p. 041501, 2014.
[131] C.-H. Weng, I.-S. Hsieh, L.-Y. Hung, H.-I. Lin, S.-C. Shiesh, Y.-L. Chen, and G.-B. Lee, "An automatic microfluidic system for rapid screening of cancer stem-like cell-specific aptamers," *Microfluidics and Nanofluidics,* vol. 14, pp. 753-765, 2013.

[132] C.-H. Weng, K.-Y. Lien, S.-Y. Yang, and G.-B. Lee, "A suction-type, pneumatic microfluidic device for liquid transport and mixing," *Microfluidics and Nanofluidics,* vol. 10, no. 2, pp. 301-310, 2011.
[133] C. M. Birch, H. W. Hou, J. Han, and J. C. Niles, "Identification of malaria parasite-infected red blood cell surface aptamers by inertial microfluidic SELEX (I-SELEX)," *Scientific Reports,* vol. 5, 2015, Art. no. 11347.
[134] H. Stoll, H. Kiessling, M. Stelzle, H. P. Wendel, J. Schütte, B. Hagmeyer, and M. Avci-Adali, "Microfluidic chip system for the selection and enrichment of cell binding aptamers," *Biomicrofluidics,* vol. 9, no. 3, p. 034111, 2015.
[135] H.-C. Lai, C.-H. Wang, T.-M. Liou, and G.-B. Lee, "Influenza A virus-specific aptamers screened by using an integrated microfluidic system," *Lab on a Chip,* vol. 14, no. 12, pp. 2002-2013, 2014.
[136] L.-Y. Hung, C.-H. Wang, K.-F. Hsu, C.-Y. Chou, and G.-B. Lee, "An on-chip Cell-SELEX process for automatic selection of high-affinity aptamers specific to different histologically classified ovarian cancer cells," *Lab on a Chip,* vol. 14, no. 20, pp. 4017-4028, 2014.
[137] L.-Y. Hung, C.-H. Wang, Y.-J. Che, C.-Y. Fu, H.-Y. Chang, K. Wang, and G.-B. Lee, "Screening of aptamers specific to colorectal cancer cells and stem cells by utilizing On-chip Cell-SELEX," *Scientific Reports,* vol. 5, 2015, Art. no. 10326.
[138] H.-I. Lin, C.-C. Wu, C.-H. Yang, K.-W. Chang, G.-B. Lee, and S.-C. Shiesh, "Selection of aptamers specific for glycated hemoglobin and total hemoglobin using on-chip SELEX," *Lab on a Chip,* vol. 15, no. 2, pp. 486-494, 2014.
[139] C.-J. Huang, H.-I. Lin, S.-C. Shiesh, and G.-B. Lee, "An integrated microfluidic system for rapid screening of alpha-fetoprotein-specific aptamers," *Biosensors and Bioelectronics,* vol. 35, no. 1, pp. 50-55, 2012.
[140] J. P. Hilton, T. Olsen, J. Kim, J. Zhu, T. Nguyen, M. Barbu, R. Pei, M. Stojanovic, and Q. Lin, "Isolation of thermally sensitive protein-binding oligonucleotides on a microchip," *Microfluidics and Nanofluidics,* 2015.
[141] M. A. Unger, H.-P. Chou, T. Thorsen, A. Scherer, and S. R. Quake, "Monolithic microfabricated valves and pumps by multilayer soft lithography," *Science,* vol. 288, no. 5463, pp. 113-116, 2000.
[142] T. Hianik, V. Ostatná, M. Sonlajtnerova, and I. Grman, "Influence of ionic strength, pH and aptamer configuration for binding affinity to thrombin," *Bioelectrochemistry,* vol. 70, no. 1, pp. 127-133, 2007.
[143] L. Huang, X. Yang, C. Qi, X. Niu, C. Zhao, X. Zhao, D. Shangguan, and Y. Yang, "A label-free electrochemical biosensor based on a DNA aptamer against codeine," *Analytica Chimica Acta,* vol. 787, pp. 203-210, 2013.
[144] J. G. Wetmur and N. Davidson, "Kinetics of renaturation of DNA," *Journal of Molecular Biology,* vol. 31, no. 3, pp. 349-370, 1968.
[145] T. Olsen, J. Zhu, J. Kim, R. Pei, M. N. Stojanovic, and Q. Lin, "An Integrated Microfluidic SELEX Approach Using Combined Electrokinetic and Hydrodynamic Manipulation," *Journal of Laboratory Automation,* p. 2211068216659255, 2016.
[146] H.-B. Liu, H.-Q. Gong, N. Ramalingam, Y. Jiang, C.-C. Dai, and K. M. Hui, "Micro air bubble formation and its control during polymerase chain reaction (PCR) in polydimethylsiloxane (PDMS) microreactors," *Journal of Micromechanics and Microengineering,* vol. 17, no. 10, p. 2055, 2007.
[147] X. Ren, M. Bachman, C. Sims, G. Li, and N. Allbritton, "Electroosmotic properties of microfluidic channels composed of poly (dimethylsiloxane)," *Journal of Chromatography B: Biomedical Sciences and Applications,* vol. 762, no. 2, pp. 117-125, 2001.
[148] A. M. Spehar, S. Koster, V. Linder, S. Kulmala, N. F. de Rooij, E. Verpoorte, H. Sigrist, and W. Thormann, "Electrokinetic characterization of poly (dimethylsiloxane) microchannels," *Electrophoresis,* vol. 24, no. 21, pp. 3674-3678, 2003.
[149] Y. Liu, J. C. Fanguy, J. M. Bledsoe, and C. S. Henry, "Dynamic coating using polyelectrolyte multilayers for chemical control of electroosmotic flow in capillary electrophoresis microchips," *Analytical chemistry,* vol. 72, no. 24, pp. 5939-5944, 2000.
[150] J. D. Marth, "A unified vision of the building blocks of life," *Nature cell biology,* vol. 10, no. 9, p. 1015, 2008.
[151] A. Varki, "Biological roles of glycans," *Glycobiology,* vol. 27, no. 1, pp. 3-49, 2017.
[152] M. J. Kailemia, D. Park, and C. B. Lebrilla, "Glycans and glycoproteins as specific biomarkers for cancer," *Analytical and bioanalytical chemistry,* vol. 409, no. 2, pp. 395-410, 2017.
[153] D. H. Dube and C. R. Bertozzi, "Glycans in cancer and inflammation—potential for therapeutics and diagnostics," *Nature reviews Drug discovery,* vol. 4, no. 6, p. 477, 2005.

[154] H. J. An, S. R. Kronewitter, M. L. A. de Leoz, and C. B. Lebrilla, "Glycomics and disease markers," *Current opinion in chemical biology,* vol. 13, no. 5-6, pp. 601-607, 2009.
[155] C. B. Lebrilla and H. J. An, "The prospects of glycan biomarkers for the diagnosis of diseases," *Molecular bioSystems,* vol. 5, no. 1, pp. 17-20, 2009.
[156] J. F. Rakus and L. K. Mahal, "New technologies for glycomic analysis: toward a systematic understanding of the glycome," *Annual review of analytical chemistry,* vol. 4, pp. 367-392, 2011.
[157] S. A. Svarovsky and L. Joshi, "Cancer glycan biomarkers and their detection–past, present and future," *Analytical Methods,* vol. 6, no. 12, pp. 3918-3936, 2014.
[158] S. Di Palma, M. L. Hennrich, A. J. Heck, and S. Mohammed, "Recent advances in peptide separation by multidimensional liquid chromatography for proteome analysis," *Journal of proteomics,* vol. 75, no. 13, pp. 3791-3813, 2012.
[159] J. Hirabayashi, "Concept, strategy and realization of lectin-based glycan profiling," *Journal of biochemistry,* vol. 144, no. 2, pp. 139-147, 2008.
[160] J. Katrlík, J. Švitel, P. Gemeiner, T. Kožár, and J. Tkac, "Glycan and lectin microarrays for glycomics and medicinal applications," *Medicinal research reviews,* vol. 30, no. 2, pp. 394-418, 2010.
[161] A. Kuno, N. Uchiyama, S. Koseki-Kuno, Y. Ebe, S. Takashima, M. Yamada, and J. Hirabayashi, "Evanescent-field fluorescence-assisted lectin microarray: a new strategy for glycan profiling," *Nature methods,* vol. 2, no. 11, p. 851, 2005.
[162] N. Sharon, "Lectins: carbohydrate-specific reagents and biological recognition molecules," *Journal of Biological Chemistry,* 2006.
[163] J. Hirabayashi, "Lectin-based structural glycomics: glycoproteomics and glycan profiling," *Glycoconjugate journal,* vol. 21, no. 1-2, pp. 35-40, 2004.
[164] O. Haji-Ghassemi, R. J. Blackler, N. Martin Young, and S. V. Evans, "Antibody recognition of carbohydrate epitopes," *Glycobiology,* vol. 25, no. 9, pp. 920-952, 2015.
[165] E. J. Cho, J.-W. Lee, and A. D. Ellington, "Applications of aptamers as sensors," *Annual Review of Analytical Chemistry,* vol. 2, pp. 241-264, 2009.
[166] A. D. Keefe, S. Pai, and A. Ellington, "Aptamers as therapeutics," *Nature Reviews Drug Discovery,* vol. 9, no. 7, pp. 537-550, 2010.
[167] A. Ozer, J. M. Pagano, and J. T. Lis, "New technologies provide quantum changes in the scale, speed, and success of SELEX methods and aptamer characterization," *Molecular Therapy-Nucleic Acids,* vol. 3, 2014.
[168] B. Boese, K. Corbino, and R. Breaker, "In vitro selection and characterization of cellulose-binding RNA aptamers using isothermal amplification," *Nucleosides, Nucleotides and Nucleic Acids,* vol. 27, no. 8, pp. 949-966, 2008.
[169] B. J. Boese and R. R. Breaker, "In vitro selection and characterization of cellulose-binding DNA aptamers," *Nucleic acids research,* vol. 35, no. 19, pp. 6378-6388, 2007.
[170] S. Jeong, T.-Y. Eom, S.-J. Kim, S.-W. Lee, and J. Yu, "< i> In Vitro</i> Selection of the RNA Aptamer against the Sialyl Lewis X and Its Inhibition of the Cell Adhesion," *Biochemical and biophysical research communications,* vol. 281, no. 1, pp. 237-243, 2001.
[171] J. Kawakami, Y. Kawase, and N. Sugimoto, "In vitro selection of aptamers that recognize a monosaccharide," *Analytica chimica acta,* vol. 365, no. 1, pp. 95-100, 1998.
[172] S.-E. Kim, W. Su, M. Cho, Y. Lee, and W.-S. Choe, "Harnessing aptamers for electrochemical detection of endotoxin," *Analytical biochemistry,* vol. 424, no. 1, pp. 12-20, 2012.
[173] M. Li, N. Lin, Z. Huang, L. Du, C. Altier, H. Fang, and B. Wang, "Selecting aptamers for a glycoprotein through the incorporation of the boronic acid moiety," *Journal of the American Chemical Society,* vol. 130, no. 38, pp. 12636-12638, 2008.
[174] S. Y. Low, J. E. Hill, and J. Peccia, "DNA aptamers bind specifically and selectively to (1→ 3)-β-d-glucans," *Biochemical and biophysical research communications,* vol. 378, no. 4, pp. 701-705, 2009.
[175] M. Mehedi Masud, M. Kuwahara, H. Ozaki, and H. Sawai, "Sialyllactose-binding modified DNA aptamer bearing additional functionality by SELEX," *Bioorganic & medicinal chemistry,* vol. 12, no. 5, pp. 1111-1120, 2004.
[176] M. Sprinzl, M. Milovnikova, and C. Voertler, "RNA aptamers directed against oligosaccharides," in *RNA Towards Medicine*: Springer, 2006, pp. 327-340.

[177] C. Srisawat, I. J. Goldstein, and D. R. Engelke, "Sephadex-binding RNA ligands: rapid affinity purification of RNA from complex RNA mixtures," *Nucleic acids research,* vol. 29, no. 2, pp. e4-e4, 2001.
[178] Y. Wang, J. Killian, K. Hamasaki, and R. R. Rando, "RNA molecules that specifically and stoichiometrically bind aminoglycoside antibiotics with high affinities," *Biochemistry,* vol. 35, no. 38, pp. 12338-12346, 1996.
[179] Q. Yang, I. J. Goldstein, H.-Y. Mei, and D. R. Engelke, "DNA ligands that bind tightly and selectively to cellobiose," *Proceedings of the National Academy of Sciences,* vol. 95, no. 10, pp. 5462-5467, 1998.
[180] K.-A. Yang, R. Pei, D. Stefanovic, and M. N. Stojanovic, "Optimizing Cross-reactivity with Evolutionary Search for Sensors," *Journal of the American Chemical Society,* vol. 134, no. 3, pp. 1642-1647, 2012.
[181] M. Ollmann, G. Schwarzmann, K. Sandhoff, and H. J. Galla, "Pyrene-labeled gangliosides: micelle formation in aqueous solution, lateral diffusion, and thermotropic behavior in phosphatidylcholine bilayers," *Biochemistry,* vol. 26, no. 18, pp. 5943-5952, 1987.
[182] N. Howlader, A. Noone, M. Krapcho, J. Garshell, N. Neyman, S. Altekruse, C. Kosary, M. Yu, J. Ruhl, and Z. Tatalovich, "SEER Cancer Statistics Review, 1975–2012, National Cancer Institute; 2015," ed, 2016.
[183] J. Martinez-Lopez, J. J. Lahuerta, F. Pepin, M. González, S. Barrio, R. Ayala, N. Puig, M. A. Montalban, B. Paiva, and L. Weng, "Prognostic value of deep sequencing method for minimal residual disease detection in multiple myeloma," *Blood,* vol. 123, no. 20, pp. 3073-3079, 2014.
[184] A. C. Rawstron, J. A. Child, R. M. de Tute, F. E. Davies, W. M. Gregory, S. E. Bell, A. J. Szubert, N. Navarro-Coy, M. T. Drayson, and S. Feyler, "Minimal residual disease assessed by multiparameter flow cytometry in multiple myeloma: impact on outcome in the Medical Research Council Myeloma IX Study," *Journal of Clinical Oncology,* vol. 31, no. 20, pp. 2540-2547, 2013.
[185] R. A. Kyle, "The monoclonal gammopathies," *Clinical chemistry,* vol. 40, no. 11, pp. 2154-2161, 1994.
[186] J. Tate, S. Bazeley, S. Sykes, and P. Mollee, "Quantitative serum free light chain assay–analytical issues," *The Clinical Biochemist Reviews,* vol. 30, no. 3, p. 131, 2009.
[187] H. Ludwig, D. Milosavljevic, N. Zojer, J. Faint, A. Bradwell, W. Hübl, and S. Harding, "Immunoglobulin heavy/light chain ratios improve paraprotein detection and monitoring, identify residual disease and correlate with survival in multiple myeloma patients," *Leukemia,* vol. 27, no. 1, pp. 213-219, 2012.
[188] N. A. Bakshi, R. Gulbranson, D. Garstka, A. R. Bradwell, and D. F. Keren, "Serum free light chain (FLC) measurement can aid capillary zone electrophoresis in detecting subtle FLC-producing M proteins," *American journal of clinical pathology,* vol. 124, no. 2, pp. 214-218, 2005.
[189] P. G. Hill, J. M. Forsyth, B. Rai, and S. Mayne, "Serum free light chains: an alternative to the urine Bence Jones proteins screening test for monoclonal gammopathies," *Clinical chemistry,* vol. 52, no. 9, pp. 1743-1748, 2006.
[190] R. S. Abraham, R. J. Clark, S. C. Bryant, J. F. Lymp, T. Larson, R. A. Kyle, and J. A. Katzmann, "Correlation of serum immunoglobulin free light chain quantification with urinary Bence Jones protein in light chain myeloma," *Clinical chemistry,* vol. 48, no. 4, pp. 655-657, 2002.
[191] R. Vij, A. Mazumder, M. Klinger, D. O'Dea, J. Paasch, T. Martin, L. Weng, J. Park, M. Fiala, M. Faham, and J. Wolf, "Deep Sequencing Reveals Myeloma Cells in Peripheral Blood in Majority of Multiple Myeloma Patients," *Clinical Lymphoma Myeloma and Leukemia,* vol. 14, no. 2, pp. 131-139.e1, 2014.
[192] P. J. Delves, S. J. Martin, D. R. Burton, and I. M. Roitt, *Roitt's essential immunology*. John Wiley & Sons, 2011.
[193] R. A. Kyle, M. A. Gertz, T. E. Witzig, J. A. Lust, M. Q. Lacy, A. Dispenzieri, R. Fonseca, S. V. Rajkumar, J. R. Offord, and D. R. Larson, "Review of 1027 patients with newly diagnosed multiple myeloma," in *Mayo Clinic Proceedings*, 2003, vol. 78, no. 1, pp. 21-33: Elsevier.
[194] J. Hoinka, R. Backofen, and T. M. Przytycka, "AptaSUITE: A Full-Featured Bioinformatics Framework for the Comprehensive Analysis of Aptamers from HT-SELEX Experiments," *Molecular Therapy-Nucleic Acids,* vol. 11, pp. 515-517, 2018.

[195] T. Glawdel, Z. Almutairi, S. Wang, and C. Ren, "Photobleaching absorbed Rhodamine B to improve temperature measurements in PDMS microchannels," *Lab on a Chip,* vol. 9, no. 1, pp. 171-174, 2009.
[196] H. Sasaki, H. Onoe, T. Osaki, R. Kawano, and S. Takeuchi, "Parylene-coating in PDMS microfluidic channels prevents the absorption of fluorescent dyes," *Sensors and Actuators B: Chemical,* vol. 150, no. 1, pp. 478-482, 2010.
[197] M. W. Toepke and D. J. Beebe, "PDMS absorption of small molecules and consequences in microfluidic applications," *Lab on a Chip,* vol. 6, no. 12, pp. 1484-1486, 2006.
[198] J. D. Wang, N. J. Douville, S. Takayama, and M. ElSayed, "Quantitative analysis of molecular absorption into PDMS microfluidic channels," *Annals of biomedical engineering,* vol. 40, no. 9, pp. 1862-1873, 2012.
[199] K. Brower, R. R. Puccinelli, C. J. Markin, T. C. Shimko, S. A. Longwell, B. Cruz, R. Gomez-Sjoberg, and P. M. Fordyce, "An open-source, programmable pneumatic setup for operation and automated control of single-and multi-layer microfluidic devices," *HardwareX,* vol. 3, pp. 117-134, 2018.